

Part I

A strongly consistent geometrical scheme for the Affine Scale Space

Chapter 2

The Affine Scale Space

2.1 Image analysis and scale spaces

When devising an algorithm to analyze images, a major question must be raised : what kind of information are we looking for, and how can we extract it from the image ? In particular, it is clear that what we can see on an image depends on the focalization of the look we take at it : we cannot at the same time examine small details and recognize large structures. Hence, there is a natural *scale* parameter that cannot be eluded in the analysis process. This suggests that an image should be represented in a multiscale way, the smallest details being described at small scales and the largest ones at large scales. Such a multiscale representation of an image is called a **scale-space** : to a raw image u_0 we associate a continuous collection of images $(u(t))_{t>0}$ that are obtained from u_0 by a simplification process which “eliminates” details as the scale increases. The collection of operators (T_t) that define $u(t)$ from u_0 is called a **multiscale analysis** of images.

From a mathematical point of view, an image shall be regarded in the following as a map $u_0 : \mathbb{R}^2 \rightarrow \mathbb{R}$, the value $u(\mathbf{x})$ corresponding to the grey-level¹ (the luminance) at point $\mathbf{x} = (x, y)$ of the plane². Then, a scale space is represented by a map $u : \mathbb{R}^2 \times [0, +\infty[\rightarrow \mathbb{R}$, the third coordinate being the scale t . A simple example of a linear scale space can be defined by the heat equation

$$\begin{cases} \frac{\partial u}{\partial t} = \Delta u \\ u(\cdot, 0) = u_0(\cdot), \end{cases} \quad (2.1)$$

where $\Delta = \frac{\partial^2}{\partial x^2} + \frac{\partial^2}{\partial y^2}$ is the two-dimensional Laplacian operator. The simplification process induced by Equation 2.1 is an isotropic diffusion that can also be described by the convolution of u_0 with a two-dimensional Gaussian kernel. Although Equation 2.1 satisfies the required properties to define an interesting scale space, as we shall see later, it is not well adapted to

¹We do not consider the case of color images.

²In practice, a grey-level image is represented by computers as a finite two-dimensional array of integer values.

image analysis due to its linear nature. The main reason is that the image formation process results from a superimposition of objects rather than from a linear combination of them.

2.2 Definition

The affine scale space has been discovered a few years ago in its image and geometrical formulation (see [4] and [68]).

2.2.1 Image formulation

Let us first express it in terms of image processing. The affine morphological scale space (shortly written AMSS) is defined by the degenerated parabolic evolution equation

$$\begin{cases} \frac{\partial u}{\partial t} = |Du| \operatorname{curv}(u)^{\frac{1}{3}} \\ u(\cdot, 0) = u_0(\cdot). \end{cases} \quad (2.2)$$

The term $Du = (u_x, u_y)$ represents the spatial gradient of u , u_x and u_y being short notations for the partial derivatives $\frac{\partial u}{\partial x}$ and $\frac{\partial u}{\partial y}$. The second order operator

$$\operatorname{curv}(u) = \operatorname{div} \left(\frac{Du}{|Du|} \right) = \frac{(u_x)^2 u_{yy} - 2u_x u_y u_{xy} + (u_y)^2 u_{xx}}{|Du|^3}$$

can be viewed as the curvature at point \mathbf{x} of the level line³ of u going through \mathbf{x} . In the following, we take the convention that $r^{\frac{1}{3}}$ means $-|r|^{\frac{1}{3}}$ when r is negative. When $Du = 0$, $\operatorname{curv}(u)$ is not defined, but

$$|Du| \operatorname{curv}(u)^{\frac{1}{3}} = \left[(u_x)^2 u_{yy} - 2u_x u_y u_{xy} + (u_y)^2 u_{xx} \right]^{\frac{1}{3}}$$

is naturally equal to zero, so that Equation 2.2 remains defined. Hence, from now on we assume that $|Du| \operatorname{curv}(u)^{\frac{1}{3}}$ is defined and equal to 0 when $Du = 0$.

In fact, Equation 2.2 is a parabolic PDE of the kind

$$\frac{\partial u}{\partial t} = F(D^2 u, Du),$$

where $F : \mathcal{S}(\mathbb{R}^2) \times \mathbb{R}^2 \rightarrow \mathbb{R}$ is a continuous function, nondecreasing with respect to its first argument (for the usual order defined on $\mathcal{S}(\mathbb{R}^2)$, the set of symmetric 2×2 real matrices). For this kind of evolution equations, weak solutions —only continuous— have been defined, and are called for historical reasons *viscosity solutions*. We shall be more precise in Chapter 5, but one may refer to [10] or [27] for further details. The reason why Equation 2.2 is called Affine Morphological Scale Space comes from important properties of the associated multiscale analysis $(T_t)_{t \geq 0}$, defined by

$$(T_t u_0)(\mathbf{x}) = u(\mathbf{x}, t).$$

³Of course, this makes sense only at points where the equation $u = cte$ defines locally a smooth curve.

First, the nature of Equation 2.2 concedes a semi-group structure to this family of operators, inasmuch as

$$T_{t+s} = T_t \circ T_s.$$

Secondly, these operators are morphological, that is, they satisfy the property

[Morphological Invariance] : For any nondecreasing (or nonincreasing) continuous function $g : \mathbb{R} \rightarrow \mathbb{R}$,

$$\forall u, \forall t, \quad T_t(g \circ u) = g \circ T_t(u).$$

The fact that T_t commutes with any contrast change g implies that it operates on the level lines of u ; we shall give a geometric interpretation of this later. The word “affine” comes from an interesting geometrical invariance :

[Affine invariance] : For any bijective affine map ϕ ,

$$\forall t, \exists t', \forall u, \quad T_t(u \circ \phi) = T_{t'}(u) \circ \phi.$$

By affine map, we mean any linear operator on \mathbb{R}^2 . If ϕ belongs to the special linear group — i.e. $\det \phi = 1$ —, we have $T_t(u \circ \phi) = T_t(u) \circ \phi$. Another relevant property of the semi-group (T_t) is the maximum principle, which gives sense to viscosity solutions for (2.2). This principle can be expressed by

[Comparison Principle] : $\forall u, v, \quad u \leq v \Rightarrow \forall t > 0, \quad T_t u \leq T_t v.$

A local version of this principle (called Local Comparison Principle) is also satisfied (see Chapter 5). These principles are very important, and they guarantee that Equation 2.2 “simplifies” the initial image u_0 as the scale t increases. They also ensure numerical stability to associated algorithms.

We shall come back to these fundamental properties, but it is interesting to mention that the AMSS is the only regular multiscale analysis which satisfies them. This was proved by L.Alvarez, F.Guichard, P.-L.Lions and J.-M.Morel in [4]. As regards the linear scale space we defined in introduction by Equation 2.1, it also satisfies the semi-group property and the comparison principle, but it is neither affine invariant nor morphological. Figure 2.1 compares this scale space with the AMSS for an image of a cheetah.



Figure 2.1: Two scale spaces of a cheetah image.

The two images of first column are the same original image of a cheetah head. This image is analyzed with two different scale spaces : the affine morphological scale space (row 1) and the linear scale space (row 2). Column 2 corresponds to a medium scale of analysis and column 3 to a larger scale. Notice how the affine morphological scale space preserves geometrical structures, whereas the linear scale space performs mainly a global blur.

2.2.2 Geometric formulation

We now come to the geometric formulation of the affine scale space. Because of the morphological invariance, the evolution of u_0 according to Equation 2.2 is formally equivalent to the evolution of its level curves. This curve evolution was discovered by G.Sapiro and A.Tannenbaum : it is the affine analog of the Euclidean shortening flow studied by M.Gage and R.S.Hamilton in [36] and M.A.Grayson in [39]. An initial curve $p \mapsto \mathbf{C}_0(p) = \mathbf{C}(p, 0)$ evolves according to the equation

$$\frac{\partial \mathbf{C}}{\partial t}(p, t) = \gamma(p, t)^{\frac{1}{3}} \mathbf{N}(p, t), \quad (2.3)$$

where $\gamma(p, t)$ and $\mathbf{N}(p, t)$ are respectively the curvature and the normal vector of the curve $\mathbf{C}(\cdot, t)$ in $\mathbf{C}(p, t)$. Replacing p with an affine arclength parameter s satisfying the constant determinant relation

$$\left[\frac{\partial \mathbf{C}}{\partial s}, \frac{\partial^2 \mathbf{C}}{\partial s^2} \right] = 1,$$

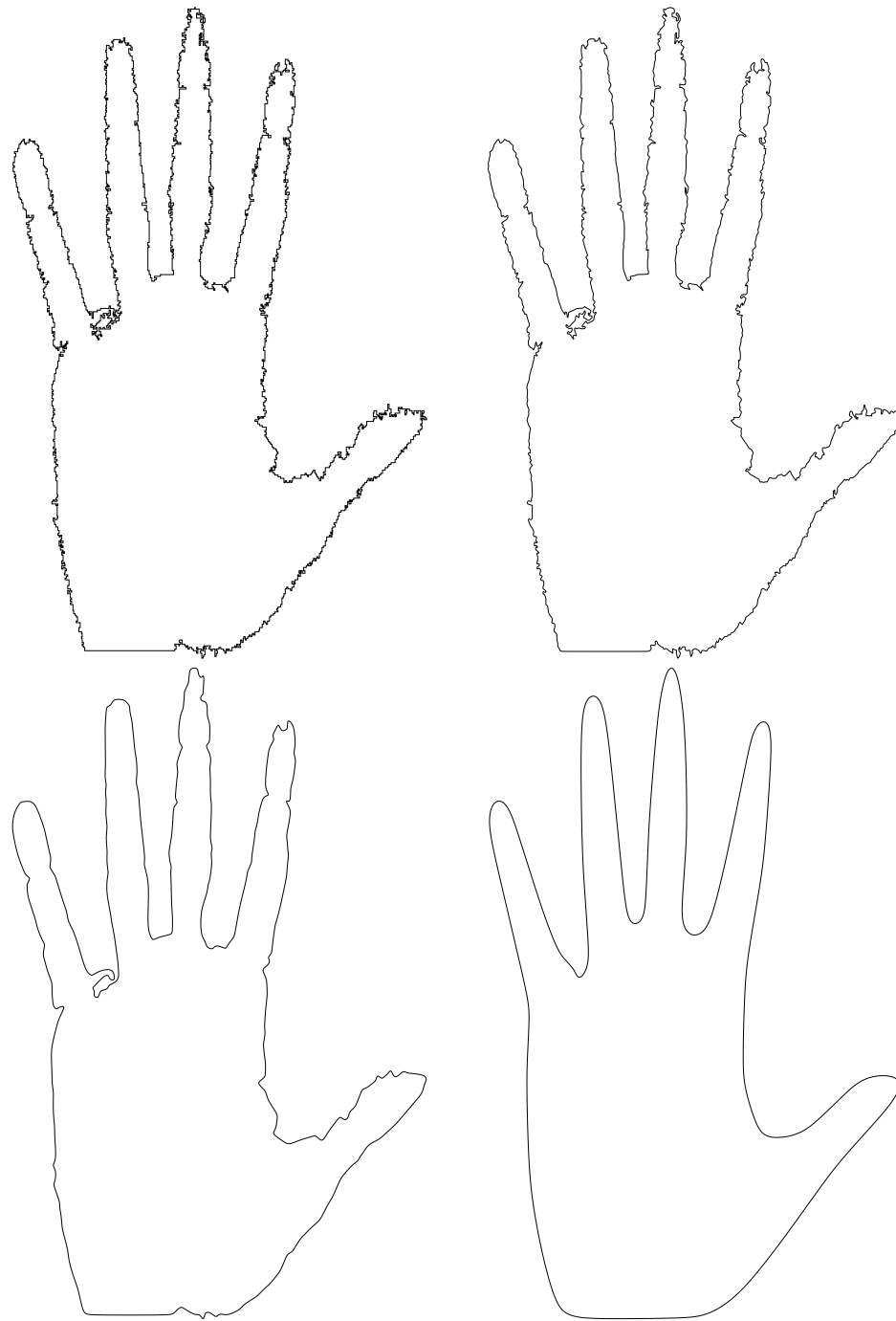


Figure 2.2: Affine Scale Space of a “hand” curve.

The scale of analysis is, from left to right, and then top to bottom : 0 (original curve), 1, 8, 200. It is clear that the original curve (top-left) cannot be directly analyzed by a shape recognition device due to its very noisy aspect. This is the reason why we need to simplify it in the most natural possible way, which has been theoretically proven to be the affine scale space. To ensure good performances of the shape recognition process, a high accuracy is needed in the computation of the scale space, even for large scales.

Equation 2.3 reduces to a nonlinear intrinsic heat equation

$$\frac{\partial \mathbf{C}}{\partial t} = \frac{\partial^2 \mathbf{C}}{\partial s^2}.$$

As for the image formulation, the collection of curves $(\mathbf{C}(\cdot, t))_{t \geq 0}$ is called Affine Scale Space.

We must mention the fact that the existence and uniqueness of a solution of (2.3) for an initial non-convex curve has not been proved so far (whereas it has been proved in [36], [39] in the Euclidean case). Hence, although the image and the geometrical formulations of the affine scale space are formally equivalent, we shall rather use the first one to establish precise results.

Figure 2.2 shows the geometrical affine scale space of a “real-world” curve that was obtained from the photograph of a hand.

2.2.3 Applications

By now, the main application of the affine scale space is probably shape analysis. It was used by T.Cohignac in [26] to perform an affine invariant shape recognition algorithm for partially occluded shapes. In this case, classical methods based on a global affine normalization cannot be used anymore, and one needs to characterize a shape locally by affine invariant descriptors. This was done by T.Cohignac by means of a technique which is directly related to the affine scale space (see Figure 2.3). To perform an efficient shape recognition, an accurate implementation of the affine scale space is required, both for small and for large scales.

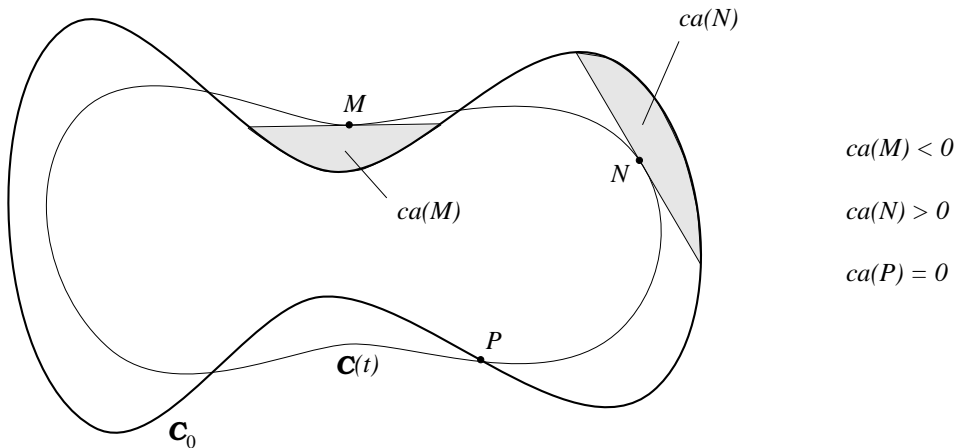


Figure 2.3: Characteristic area as defined by T.Cohignac.

The original curve \mathbf{C}_0 is smoothed by the affine scale space at scale t into a new curve $\mathbf{C}(t)$. Then, to each point M of $\mathbf{C}(t)$ we associate the (algebraic) area $ca(M)$ of the domain bounded by \mathbf{C}_0 and the tangent to $\mathbf{C}(t)$ in M . The characteristic points are defined on $\mathbf{C}(t)$ as the points M where the characteristic area $ca(M)$ attains an extremum. A local affine invariant shape recognition device is obtained by identifying these characteristic points in all intrinsic affine bases (see [26] for more details).

The AMSS model can also be viewed, when applied at small scales, as an affine invariant denoising process, very efficient —like the median filter— in the case of non-additive noises (impulse noise⁴ for example). This property is illustrated on Figure 2.4.



Figure 2.4: Denoising effects of scale spaces.

Top-Left : original Lena image,
Top-Right : Lena image corrupted with 30% impulse noise ,
Bottom-Left : Top-Right image smoothed by the linear scale space,
Bottom-Right : Top-Right image smoothed by the AMSS

Due to its morphological nature, the Affine Morphological Scale Space (AMSS) performs a much better noise removal than any linear process, especially in the case of a non-additive noise.

⁴Corrupting an image with a 10% impulse noise means that random, independent and uniformly distributed values are attributed to a uncorrelated random 10% amount of the image pixels.

2.3 Numerical schemes for the Affine Scale Space

2.3.1 Definitions

Consider a numerical scheme for the AMSS, described by the iteration of an operator T depending on a scale step Δt and a space step $\Delta \mathbf{x}$. As in [40], we shall say that T is **consistent** with the AMSS if

$$\frac{Tu - u}{\Delta t} \rightarrow |Du| \operatorname{curv}(u)^{\frac{1}{3}}$$

when the steps $\Delta \mathbf{x}$ and Δt tend to 0 in a suitable way. The scheme is **convergent** if the iterated filter $T^n = T \circ T \circ \dots \circ T$ converges⁵ towards the AMSS at scale t when Δt and $\Delta \mathbf{x}$ tend to 0 in a suitable way, and $n\Delta t \rightarrow t$.

2.3.2 The Osher-Sethian's method

Since the image formulation of the affine scale space (Equation 2.2) and the geometrical formulation (Equation 2.3) are equivalent, a numerical scheme for a formulation can be transposed into a numerical scheme for the other one. S.Osher and J.A.Sethian successfully used an image formulation to compute the affine scale space of a planar set (see [65], [71]). They also applied to several other evolution equations the general idea of viewing a hypersurface as the level set of a scalar function. The great advantage of this method is that the topological changes on the evolving set (e.g. loss of connectedness) are automatically handled by the function ; this approach permits complicated curve evolutions, but it inherits the drawbacks of the numerical scheme used for the associated scalar function. Moreover, it is likely — though not proven by now — that no topological change can occur in the special case of the planar affine scale space (that is, a Jordan curve remains a Jordan curve), so that such an image formulation is not absolutely required to compute the affine scale space of a curve.

2.3.3 State of the art

The Bence-Merriman-Osher Algorithm for Mean Curvature Motion

In [12], J.Bence, B.Merriman and S.Osher proposed a very simple algorithm for computing the mean curvature flow. The mean curvature scale space is defined by

$$\begin{cases} \frac{\partial u}{\partial t} = |Du| \operatorname{curv}(u) \\ u(\cdot, 0) = u_0(\cdot). \end{cases} \quad (2.4)$$

It is quite similar to the AMSS, except that it is not affine invariant. The Bence-Merriman-Osher scheme seems difficult to extend to the affine case, but we would still like to mention it. The idea is to compute the evolution of a set by applying the heat equation to its characteristic

⁵We shall be more precise later about the kind of convergence we mean (simple, uniform, ...).

function, the result being thresholded after each iteration. In other words, the evolution of a set S_0 is obtained by iterating the kernel

$$\mathcal{H}(t) = Q \circ G_t \circ \chi,$$

where

$$Q(u) = \left\{ \mathbf{x} \in \mathbb{R}^n, u(\mathbf{x}, t) \geq \frac{1}{2} \right\}, \quad \chi(S)(x) = \begin{cases} 1 & \text{if } \mathbf{x} \in S, \\ 0 & \text{otherwise,} \end{cases}$$

and G_t is the Gaussian convolution kernel solving the heat equation

$$\frac{\partial u}{\partial t} = \Delta u.$$

As $n \rightarrow \infty$, $\mathcal{H}(t/m)^m S_0$ tends towards the mean curvature flow of S_0 at scale t , at least in the viscosity sense for the associated characteristic function. This convergence property has been proved by G.Barles and C.Georgelin in [9], and by L.C.Evans in [30]. H.Ishii also proposed a generalization in [45]. However, such a scheme does not remain consistent in its discrete implementation, as F.Guichard remarked in [40].

A quasilinear scheme

An efficient quasilinear finite difference scheme was proposed in 1993 by L.Alvarez and F.Guichard (see [40] for example). The idea is to iterate the discrete evolution

$$u_{n+1}(\mathbf{x}) = u_n(\mathbf{x}) + \Delta t \cdot A(u_n)(\mathbf{x}),$$

where $A(u)(\mathbf{x})$ is a discrete approximation at point \mathbf{x} of $|Du|\text{curv}(u)^{\frac{1}{3}}$ using the 9 values of u on a 3x3 neighborhood of \mathbf{x} . They proved that one can choose $A(u)$ in order that the approximation $A(u) \simeq |Du|\text{curv}(u)^{\frac{1}{3}}$ is exact for any polynomial u of degree 3. The resulting scheme is neither morphological nor monotone, but is experimentally stable. Of course, such a local scheme cannot be really affine invariant, because the neighborhood size is fixed in advance.

Inf-Sup operators

In [41], F.Guichard and J.-M.Morel showed that appropriate iterated inf-sup operators converge towards the affine morphological scale space. We shall describe these operators more precisely in Chapter 5. The Euclidean case had been treated before by F. Catté and F. Dibos in [22]. However, because of the spatial quantization and the morphological invariance (no new grey-level is created on the image), the discrete alternate iterated inf-sup operator gets “stuck” after several iterations (that is, no evolution occurs any longer). Indeed, on a spatial grid, a level curve is constrained to move at entire speeds : at each step, either it does not move, or it jumps over one pixel at least (see [26]).

A multiscale spline representation

In [17], G.Sapiro, A.Cohen and A.M.Bruckstein described a multiscale representation of planar shapes using B-splines. This representation is affine invariant, but it cannot be described by an evolution equation, and in particular it does not satisfy the inclusion principle (analog for sets to the comparison principle for images) :

$$A \subset B \quad \Rightarrow \quad \forall t \geq 0, \quad T_t(A) \subset T_t(B). \quad (2.5)$$

For that reason, it is not well adapted to image analysis and has little to do with the affine morphological scale space.

The Osher-Sethian algorithm

As we described in Introduction, one can apply a numerical scheme for the AMSS to a set S by considering its signed distance image $u(x) = \varepsilon(x)\text{dist}(x, S)$, where $\varepsilon(x) = -1$ if $x \in S$, 1 otherwise. With this method, S.Osher and J.A.Sethian transposed the difficult problem of a geometric curve evolution into the implementation of the AMSS. However, the major drawback is that the full affine invariance is impossible to obtain with such a method, since no image representation can be affine invariant. In addition, the large image size required to achieve a reasonable precision in the curve evolution makes the process rather slow.

2.3.4 Point evolution schemes

For the affine scale space of curves, all geometrical schemes that have been proposed so far suffer from the space quantization of the curves (see [40]), which prevents the inclusion principle (2.5) from being satisfied. The main difficulty comes from the fact that there is no a priori relation between the number of vertices of a polygon and the number of the vertices needed to represent its affine shortening⁶ (this number increases drastically for a triangle, but decreases as much for a very irregular curve). Thus, any algorithm based on a point-by-point evolution cannot implement the affine scale space successfully.

However, it is likely that the most accurate implementation of the Affine Scale Space is a curve evolution one, because it seems impossible to achieve precise evolutions and to guarantee a full affine invariance in any image evolution algorithm.

2.4 A fully consistent scheme

How can we implement the affine scale space with a geometrical algorithm ? Since no point evolution scheme can be efficient, we have to consider the problem globally, that is, to find an

⁶i.e. its affine scale space at a given scale.

operator T acting on curves and consistent with the affine scale space : this way, we can hope to build a numerical scheme for the affine scale space by iterating T . Moreover, we would like this operator to be affine invariant, monotone (i.e. preserving global inclusion), and easy to compute on a general kind of discrete curves (on polygons for example).

We shall propose such an operator and call it *affine erosion*. It is more or less a continuous generalization of a discrete operator briefly described in [40]. It is also somewhat related to the notion of characteristic area introduced by T.Cohignac (see [26]) : indeed, the following study proves that as the scale t tends towards 0, the characteristic area of all non-inflexion points of the curve is equivalent to $\pm c.t^\alpha$, c and α being universal constants. This can suggest our definition of the affine erosion.

In Chapter 3, we define precisely the affine erosion for a certain kind of curves and sets. We investigate some properties of this operator, and point out an important characterization for convex curves. We also prove that the number of inflexion points (in a generalized sense) cannot increase when this operator is applied to a non-convex curve. Last, we establish the geometrical consistency of the affine erosion with respect to the geometrical affine scale space.

In Chapter 4, we compare the Affine Scale Space and the affine erosion on a few examples, namely conics. We compute explicitly the action of these operators, and show that the affine erosion remains a good approximation of the affine scale space not only for small scales. This suggests that the affine erosion can be iterated using rather large scale steps to approximate the affine scale space efficiently.

We extend the affine erosion to grey-level images in Chapter 5, by applying the geometrical affine erosion to the level sets of an image. The resulting operator is fully consistent, inasmuch as it satisfies the most important properties of the affine scale space (the affine and morphological invariances and the comparison principle), except —naturally— the semi-group property (this is why we need to iterate the affine erosion). We also make a comparison with the inf-sup operators studied in [41], and in particular we prove that for C^1 curves, a classical affine invariant inf-sup operator acts exactly like the affine erosion for small scales. Then, we establish precise consistency and convergence properties for the alternated iterated scheme associated with the affine erosion. We link these results with Matheron's Theorem and techniques used in [41].

Chapter 6 is devoted to the numerical scheme. We prove that the affine erosion of a polygon is made of the concatenation of hyperbola pieces and segments. We present an algorithm to compute exactly the affine erosion of a polygon, and show that the resulting curve can be quantized in an affine invariant way. We compare the space and scale discretizations, and show that our algorithm has little to do with classical finite element methods. Then we present an approximate algorithm, which is very close to the first one, much faster, and which also gives accurate results.

Last, we present in Chapter 7 several experiments. Affine erosions and scale spaces are computed for simple polygons and more complicated curves, including “real-world” curves given by level curves of digitized photographs.

We conclude in Chapter 8 on the possible application of such a global technique to other evolution equations, and we indicate further axes of development.

Chapter 3

Affine erosion of curves and sets

3.1 Preliminaries

In order to define what we shall call the affine erosion of a curve or a set, we first need to make clear what kind of curves and sets we are going to consider, since it is impossible to dissociate the relation between a set and its boundary in the definition. We first restrain our study to sets whose boundaries can be described by piecewise convex curves, for which the definition and the basic properties of the affine erosion are natural. In a further chapter, we shall extend the affine erosion to any set of the plane and to grey-level images.

Let us begin with some notations and definitions. We write $\text{dist}(A, B)$ for the Euclidean distance between two points A and B of the plane, AB for the vector $B - A$, $|AB| = \text{dist}(A, B)$ for the Euclidean norm of AB and $[AB]$ (resp. $]AB[$) for the closed (resp. open) segment with endpoints A and B . The determinant of two vectors \mathbf{v}_1 and \mathbf{v}_2 will be noted $[\mathbf{v}_1, \mathbf{v}_2]$, and if they are both nonzero we note $\angle(\mathbf{v}_1, \mathbf{v}_2) \in S^1 = \mathbb{R}/_{2\pi}\mathbb{Z}$ the angle from \mathbf{v}_1 to \mathbf{v}_2 .

When s and t belong to the circle S^1 , $[s, t]$ means the class of the interval $[s', t']$ where s' and t' are real number such that $s' = s$ and $t' = t$ modulo 2π and $s' \leq t' < s' + 2\pi$. As well, the inequality $a_1 \leq a_2 \leq \dots \leq a_n$ on S^1 means that we can find some real numbers a'_1, a'_2, \dots, a'_n equal to a_1, a_2, \dots, a_n modulo 2π such that $a'_1 \leq a'_2 \leq \dots \leq a'_n < a'_1 + 2\pi$ (which makes sense for $n \geq 3$).

We choose to call a **simple curve** any subset of \mathbb{R}^2 homeomorphic to the circle S^1 (**closed curve**) or \mathbb{R} (**non closed curve**). We shall often refer to a simple curve using the notation $C(I)$, which means implicitly that $C : I \rightarrow C(I)$ is a parameterization of the curve ; unless additional specification is given, we shall suppose in general that $I = \mathbb{R}$ or $I = S^1$. Among all possible parameterizations of a curve, two classes can be distinguished according to the set $\{C([s, t]); s, t \in I\}$. Choosing a class of parameterization defines an orientation of the curve. As usual, a curve \mathcal{C} is of class C^1 if it admits a parameterization $C : I \rightarrow \mathcal{C}$ of class C^1 such that C' never vanishes (such a parameterization is called **regular**). A curve is of class C^n ($n > 1$) if it admits a regular parameterization of class C^n .

We define a **semi-closed curve** as an oriented simple curve \mathcal{C} such that $\mathbb{R}^2 - \mathcal{C}$ has exactly two connected components, called the inside part and the outside part of \mathcal{C} according to the orientation of \mathcal{C} (with the classical convention that the inside part of \mathcal{C} , noted $\mathcal{I}(\mathcal{C})$, is “on the left” when one runs positively on \mathcal{C}). A semi-closed curve can also be viewed as a simple oriented closed curve defined on the Alexandroff compactification of the plane $\mathbb{R}^2 \cup \{\infty\}$; in particular, a closed curve is semi-closed.

Let $C(I)$ be a simple curve. Then, $(s, t) \in I^2$ is a **chord** of C if and only if the piece of curve $C(]s, t])$ and the open segment $]C(s)C(t)[$ are disjoint or equal. The connected closed set enclosed by $C(]s, t])$ and the chord segment $]C(s)C(t)[$ is a **chord set** of C , written $C_{s,t}$ (see Figure 3.1). If $\text{area}(C_{s,t}) = \sigma$, then (s, t) is called a σ -chord and $C_{s,t}$ a σ -chord set of C .

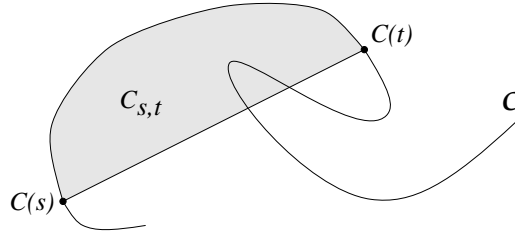


Figure 3.1: A chord set of a simple curve.

Notice that the chord segment $]C(s)C(t)[$ can intersect $\mathcal{C} \setminus C(]s, t])$.

Following this idea, if $C(]a, b])$ is a semi-closed curve ($\{a, b\} \subset \overline{\mathbb{R}}$), we say that (s, b) is an **infinite σ -chord** of C if there exists a half line D with start-point $C(s)$ such that $C(]s, b]) \cap D = \emptyset$ and the chord set $C_{s,b}$ enclosed by D and $C(]s, b])$ is of finite area σ . The case of the infinite chord (a, s) is symmetric. Last, (a, b) is an infinite σ -chord of C if there exists a line D such that $C(]a, b]) \cap D = \emptyset$ and the chord set $C_{a,b}$ enclosed by D and $C(]s, b])$ is of finite area σ . For example, if we consider the curve $C(\mathbb{R})$ defined by $C(x) = (x, e^{-x^2})$ in an orthonormal basis of the plane, then the line $\{y = 0\}$ is an infinite chord segment associated to the $\sqrt{\pi}$ -chord set $C_{-\infty, +\infty}$ (from now on, we assume that a “chord segment” can be finite or infinite, i.e. either a true segment, a half line, or a line).

If \mathcal{C} is oriented and $\text{area}(C_{s,t}) \neq 0$, the orientation induced by C on the boundary of $C_{s,t}$ tells whether (s, t) is a positive or a negative chord. We take the convention that a 0-chord set is both positive and negative. The collection of all positive (resp. negative) σ -chord sets of C will be written $\mathcal{K}_\sigma^+(C)$ (resp. $\mathcal{K}_\sigma^-(C)$). Since the previous definition of a chord set does not depend on the parameterization of the curve, it makes sense to write $\mathcal{K}_\sigma^+(\mathcal{C})$ (resp. $\mathcal{K}_\sigma^-(\mathcal{C})$) for the collection of all positive (resp. negative) σ -chord sets of an oriented curve \mathcal{C} .

Now we give a definition of convex curves which makes also sense in the case of non semi-closed curves.

Definition 1 An oriented simple curve $C(I)$ is

- **locally convex** in $C(s)$ if for $\varepsilon > 0$ small enough,

$$[C(s - \varepsilon)C(s), C(s)C(s + \varepsilon)] \geq 0.$$

- **locally concave** in $C(s)$ if for $\varepsilon > 0$ small enough,

$$[C(s - \varepsilon)C(s), C(s)C(s + \varepsilon)] \leq 0.$$

- **convex** (resp. **concave**) if it is locally convex (resp. concave) everywhere.

A (non oriented) simple curve is convex if it is convex for a certain orientation.

We may use the term “strictly convex” (resp. strictly concave) for an oriented curve which is convex and nowhere locally concave (resp. concave and nowhere locally convex). In other words, a curve is strictly convex if it is convex and does not contain any segment of nonzero length.

For a convex curve, it is not true in general that any chord set is convex (see Figure 3.2). However, if the curve is convex and semi-closed, then its inside part is convex and any couple $(s, t) \in I^2$ (with $s \leq t$ if $I \subset \mathbb{R}$) defines a convex chord set. Conversely, any convex subset of the plane is the inside part of a semi-closed convex curve.

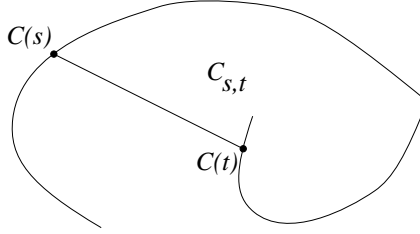


Figure 3.2: A non convex chord-set of a convex curve.

We recall that if \mathcal{C} is a convex curve, one can find a regular parameterization C admitting everywhere a non-vanishing left and right derivative C'_- and C'_+ (which can differ at most on a countable number of points). Given a point A of an oriented convex curve \mathcal{C} , we note \mathbf{T}_A^- (resp. \mathbf{T}_A^+) the unitary left-tangent (resp. right-tangent) of \mathcal{C} in A . Thus, if $\mathcal{C} = C(I)$ and $A = C(s)$, we have $C'_+(s) = |C'_+(s)| \mathbf{T}_A^+$ and $C'_-(s) = |C'_-(s)| \mathbf{T}_A^-$.

Definition 2 A **piecewise convex curve** is a simple curve $C(I)$ for which there exists a finite subdivision (s_1, s_2, \dots, s_n) of I such that each sub-curve $C(]s_i, s_{i+1}[)$ is convex.

In general, we shall suppose that the subdivision (s_i) is optimal, i.e. that n is minimal. However, even with this constraint the decomposition is not necessarily unique (consider the case of a polygonal curve for example). We shall see later that there exists a canonical decomposition.

Definition 3 An open subset S of the plane \mathbb{R}^2 is a **C-set** if

- (i) it has a finite number of connected components
- (ii) the boundary of any connected component is a finite disjoint union of semi-closed piecewise convex curves.

These oriented curves enclosing the connected components of S are called the **components of ∂S** .

Remark : One should be careful not to mix up the connected components of a C-set S with the components of ∂S . In particular, the components of ∂S are not necessarily disjoint : if S is the inside of a “8”, the boundary of S is connected but has two components. On Figure 3.3 for example, the initial C-set S has 3 connected components and ∂S has 4 components.

The previous definition of a C-set is a compromise between regularity (the boundary of a C-set admits a tangent almost everywhere) and generality (any finite union of convex sets is a C-set, as well as the inside part of any polygon).

Definition 4 A C-set is *simple* if its boundary has only one component.

A simple C-set S shall often be written $\mathcal{I}(\mathcal{C})$, which means that \mathcal{C} is a semi-closed piecewise convex curve whose inside part is S . Notice that a C-set S can always be written

$$S = \bigsqcup_i \left(S_i \setminus \overline{\bigsqcup_j T_{i,j}} \right),$$

where the S_i and $T_{i,j}$ are finite collections of simple C-sets and the symbols \sqcup and \overline{A} mean respectively a disjoint union of sets and the topological closure of a set A .

3.2 Affine erosion of sets

In this section, we define the affine erosion of a C-set, and we establish some basic properties of this operator.

3.2.1 Definition

Definition 5 The **σ -affine erosion** of a C-set S is the set of the points of S which cannot be enclosed in any positive chord set with area less than σ of a component of ∂S .

$$E_\sigma(S) = S \setminus \bigcup_{\substack{\sigma' \leq \sigma \\ K \in \mathcal{K}_{\sigma'}^+(\partial S)}} K.$$

Here, $\mathcal{K}_\sigma^+(\partial S)$ means all the σ '-chord sets of all components of ∂S . Figure 3.3 represents an intricate C-set and its affine erosion (only the oriented boundaries of the sets have been drawn for a better understanding).

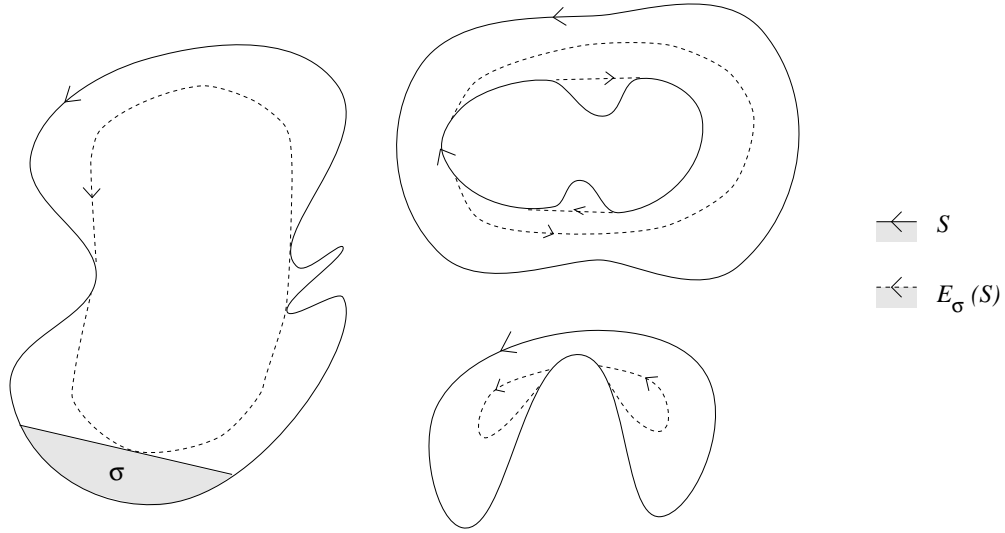


Figure 3.3: Affine erosion of an intricate C-set

3.2.2 Example

Before we go further, let us compute explicitly the affine erosion of a “corner”. This computation has strong consequences on the numerical scheme we present later. Other exact computations can be found in the next chapter.

Proposition 1 *The σ -affine erosion of the “corner”*

$$W = \{O + x \mathbf{v}_1 + y \mathbf{v}_2; x > 0, y > 0\}$$

is the inside (convex) part of a hyperbola, given in the affine basis $(O, \mathbf{v}_1, \mathbf{v}_2)$ by the equation

$$x \cdot y > \frac{\sigma}{2 [\mathbf{v}_1, \mathbf{v}_2]}, \quad x > 0, y > 0. \quad (3.1)$$

In what follows, σ will be called the **apparent area** of the hyperbola defined by Equation 3.1.

Proof :

First, we notice that only the positive chord sets with area σ are significant to define the affine erosion of W because W is convex (a positive chord set with area less than σ can always be enclosed in a positive σ -chord set).

Now, any positive σ -chord segment of W is supported by a line with equation $x/a + y/b = 1$ (see Figure 3.4) submitted to the area constraint $2\sigma = ab [\mathbf{v}_1, \mathbf{v}_2]$. Consequently, the boundary

of $E_\sigma(W)$ is obtained by the envelope of these lines, given by the system

$$\begin{cases} D_a : \frac{x}{a} + \frac{a[\mathbf{v}_1, \mathbf{v}_2]y}{2\sigma} = 1 \\ D'_a : \frac{-x}{a^2} + \frac{[\mathbf{v}_1, \mathbf{v}_2]y}{2\sigma} = 0. \end{cases}$$

Then, eliminating a yields

$$xy = \frac{\sigma}{2[\mathbf{v}_1, \mathbf{v}_2]}.$$

□

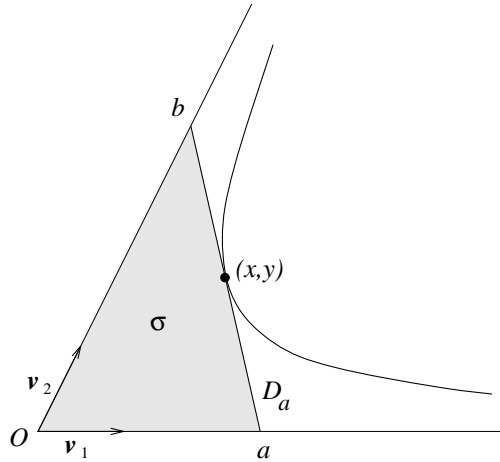


Figure 3.4: Affine erosion of a “corner”

3.2.3 Topological structure

We now establish a useful property of the affine erosion : if S is a C-set, each point of the boundary of $E_\sigma(S)$ lies on a chord segment of S .

Definition 6 Let S be a C-set and $C(I)$ a component of ∂S , then a σ' -chord (s, t) of C is σ -**limit chord** if $\sigma' \leq \sigma$ and C has no chord (s', t') of area lower than σ including strictly (s, t) (i.e. such that $s' < s \leq t \leq t'$ or $s' \leq s \leq t < t'$ in \bar{I}).

Lemma 1 For any C-set S , the boundary of $E_\sigma(S)$ is included in the union of the positive σ -limit chord segments of S .

Proof :

1. First, we prove that any $M \in \partial E_\sigma(S)$ belongs to a positive σ' -chord segment of a component of ∂S , where $\sigma' \leq \sigma$.

$M \in \partial E_\sigma(S)$ means that we can find a sequence (A_n, B_n) of finite and positive chords with area less than σ and such that $\text{dist}(M, [A_n B_n]) \rightarrow 0$ as $n \rightarrow \infty$. Since S has a finite number of

components, necessarily one component \mathcal{C} of ∂S contains a infinite number of chords (A_n, B_n) . Thus, we can extract from the sequence (A_n, B_n) a subsequence $(A_{\varphi(n)}, B_{\varphi(n)})$ of σ_n chords of \mathcal{C} , and we can suppose that $\sigma_n \rightarrow \sigma' \leq \sigma$ either (up to another subsequence extraction).

1.a. If $(A_{\varphi(n)})$ and $(B_{\varphi(n)})$ are bounded, we can extract from $(A_{\varphi(n)}, B_{\varphi(n)})$ a convergent subsequence in \mathcal{C}^2 . The limit (A, B) satisfies $d(M, [AB]) = 0$, which means that $M \in [AB]$, and a part of $[AB]$ — or $[AB]$ itself — defines a σ' -chord segment of S containing M (with $\sigma' \leq \sigma$).

1.b. If $(A_{\varphi(n)})$ is bounded and $(B_{\varphi(n)})$ is not, we can extract from $(A_{\varphi(n)})$ a subsequence that converges towards $A \in \mathcal{C}$. If $A = M$, then M belongs to the chord $[A, A]$ of \mathcal{C} and we have finished. If $A \neq M$, then a part of the half line $[AM)$ defines a positive chord segment of \mathcal{C} (finite or infinite) containing M . The case $(B_{\varphi(n)})$ bounded and $(A_{\varphi(n)})$ not bounded is symmetric.

1.c. If both $(A_{\varphi(n)})$ and $(B_{\varphi(n)})$ are not bounded, then up to a subsequence extraction we can find a nonzero vector \mathbf{v} such that $\angle(\mathbf{v}, A_{\varphi(n)}B_{\varphi(n)})$ is defined and converges towards zero. Then, the line (M, \mathbf{v}) defines a σ' -chord segment of S (finite or infinite) containing M (with $\sigma' \leq \sigma$).

2. Last, we note that only the σ -limits chord sets are significant to define $E_\sigma(S)$, because if a chord (A, B) is not σ -limit we can find a σ -limit chord set which contains strictly the chord set associated to (A, B) . \square

Corollary 1 *The affine erosion of a C-set is an open subset of the plane.*

Proof :

From Lemma 1 we know that if S is a C-set, the boundary of $E_\sigma(S)$ is part of

$$A = \bigcup_{\substack{\sigma' \leq \sigma \\ K \in \mathcal{K}_{\sigma'}^+(\partial S)}} K.$$

Therefore, ${}^c E_\sigma(S) = A \cup {}^c S$ is closed (because it contains its boundary) and $E_\sigma(S)$ is open (${}^c S$ denotes the complementary set of S , i.e. ${}^c S = \mathbb{R}^2 \setminus S$). \square

Remark : Lemma 1 highlights the necessity of considering infinite chords for non-bounded curves. Look at the previous example of the C-set S defined in an orthonormal basis of the plane by the equation $y < e^{-x^2}$: if we had not allowed infinite chords in the affine erosion of S , then the σ -affine erosion of S would have been the *closed* half plane $\{y \leq 0\}$ for any $\sigma \geq \sqrt{\pi}$ (instead of the open half plane $\{y < 0\}$), and Corollary 1 would not have been satisfied any more.

However, infinite chord are rather rare, because :

- a bounded C-set has no infinite chord,
- if a non-bounded C-set S admits an infinite chord, then it contains a half line which is an asymptote to a component of ∂S .

We could have restrained our definition of the affine erosion to less general sets (to bounded sets, for example) in order to avoid the case of infinite chords ; however, in the next chapter we shall be interested in non-bounded conics like hyperbolae and parabolae. Moreover, it is more satisfactory to define the affine erosion of any convex set (bounded or not).

3.2.4 Affine dilation

We can define in two equivalent ways the dual operator to affine erosion, that we shall call affine dilation. The first one is to reverse the orientation of the curves, the second one is to consider the open complementary of each set (for which the orientation of the boundary is reversed).

Definition 7 *The σ -affine dilation of a C-set S is defined by*

$$D_\sigma(S) = E_\sigma({}^c\overline{S}).$$

Proposition 2 *The closure of the σ -affine dilation of a C-set S is the union of S and all negative chord-sets with area less than σ of the components of ∂S .*

$$\overline{D_\sigma(S)} = S \cup \bigcup_{\substack{\sigma' \leq \sigma \\ K \in \mathcal{K}_{\sigma'}^-(\partial S)}} K.$$

Proof :

This is a simple consequence of the identity $\mathcal{K}_\sigma^-(S) = \mathcal{K}_\sigma^+({}^c\overline{S})$.

3.2.5 Basic properties of the affine erosion

Lemma 2 *$E_\sigma(S)$ is nonincreasing with respect to σ , i.e.*

$$\sigma_1 \leq \sigma_2 \Rightarrow E_{\sigma_2}(S) \subset E_{\sigma_1}(S).$$

Proof :

We just need to notice that if $\sigma_1 \leq \sigma_2$ then

$$\bigcup_{\substack{\sigma' \leq \sigma_1 \\ K \in \mathcal{K}_{\sigma'}^+(\partial S)}} K \subset \bigcup_{\substack{\sigma' \leq \sigma_2 \\ K \in \mathcal{K}_{\sigma'}^+(\partial S)}} K,$$

and consequently $E_{\sigma_2}(S) \subset E_{\sigma_1}(S)$. □

Definition 8 We call *extinction scale* of a C-set S and we note $\sigma_e(S)$ the lower bound of the scales σ for which $E_\sigma(S) = \emptyset$.

Proposition 3 If S is a simple bounded C-set, then $\sigma_e(S) \leq \frac{1}{2} \text{area}(S)$.

Proof :

Let us prove that for any simple bounded C-set S of area 2σ , $E_\sigma(S) = \emptyset$. Consider M a point of S : there exist two points A and B lying on ∂S such that the open segment $]AB[$ is included in S and contains M . This segment defines two positive chord-sets of S of area σ_1 and σ_2 such that $\sigma_1 + \sigma_2 = \text{area}(S)$. Necessarily, $\sigma_1 \leq \sigma$ or $\sigma_2 \leq \sigma$, which means that M belongs to a positive chord set of area not larger than σ , i.e. $M \notin E_\sigma(S)$. \square

One could think that the extinction scale of a simple bounded C-set is exactly half of its area. Although this is true for convex C-sets symmetric with respect to a point, this result is generally false for other simple C-sets, even convex. In the next chapter, we show that the extinction area of a triangle is $\frac{4}{9}$ of its area.

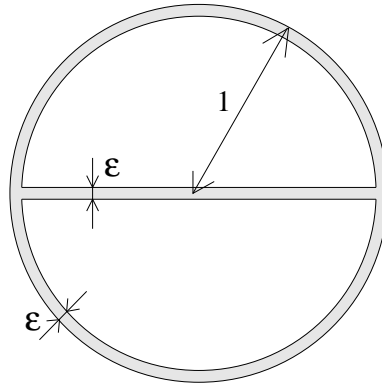


Figure 3.5: A C-set with small area and large extinction area

Proposition 3 is not true for a non simple bounded C-set. In fact, it is possible to build a C-set of area as small as we want comparatively to its extinction area. The shaded part of Figure 3.5 defines a C-set of area less than $2\varepsilon(\pi + 1)$, whereas its extinction scale is exactly $\pi/2$, i.e. half of the area of the enclosing disk. Indeed, we can deduce from Proposition 3 that the extinction area of any bounded C-set is less than half the external area of its largest connected component (the external area of a connected C-set is the area enclosed by its external boundary, i.e. including the area of its “holes”).

Proposition 4 $E_\sigma(S)$ is nondecreasing with respect to S , i.e.

$$S_1 \subset S_2 \quad \Rightarrow \quad E_\sigma(S_1) \subset E_\sigma(S_2).$$

Proof :

Let S_1 and S_2 be two C-sets such that $S_1 \subset S_2$, and consider M a point of S_2 . If M does not belong to $E_\sigma(S_2)$, there exists a positive σ' -chord segment D (finite or infinite) of a component of ∂S_2 such that $\sigma' \leq \sigma$ and M belongs to the associated chord set.

1. If $M \notin S_1$, then $E_\sigma(S_1) \subset S_1$ yields $M \notin E_\sigma(S_1)$.

2. If $M \in S_1$, consider the connected component A of S_1 containing M .

2.a. If $A \cap D = \emptyset$, then the external boundary of A encloses a subset of area less than σ' , so that from Proposition 3 we get $M \notin E_\sigma(S_1)$.

2.b. If $A \cap D \neq \emptyset$, then $A \cap D$ is a disjoint union of chord segments of S_1 (finite or infinite), and one of these chord segments defines a σ'' -chord set of S_1 containing M (see Figure 3.6). But since $S_1 \subset S_2$, we have $\sigma'' \leq \sigma'$, so that $M \notin E_\sigma(S_1)$.

Thus, $M \notin E_\sigma(S_2) \Rightarrow M \notin E_\sigma(S_1)$, which means that $E_\sigma(S_1) \subset E_\sigma(S_2)$. \square

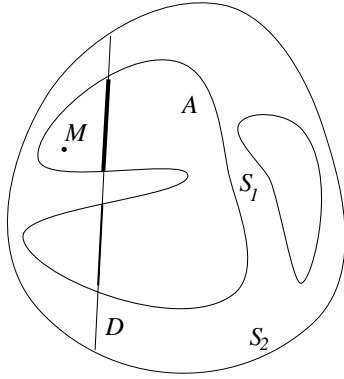


Figure 3.6: E_σ is monotone

Proposition 5 *The affine erosion is covariant with respect to the affine transformations of the plane, i.e for any affine map ϕ ,*

$$\phi(E_\sigma(S)) = E_{\sigma \cdot |\det \phi|}(\phi(S)),$$

det ϕ being the determinant of the linear part of ϕ , i.e. $\det \phi = \det A$ where $\phi(M) = AM + B$ and $(A, B) \in L(\mathbb{R}^2) \times \mathbb{R}^2$.

Proof :

This elementary result simply arises from the fact that for a C-set S , we have

$$\phi[\mathcal{K}_\sigma^+(\partial S)] = \{\phi(K); K \in \mathcal{K}_\sigma^+(\partial S)\} = \mathcal{K}_{\sigma \cdot |\det \phi|}^+(\partial \phi(S)).$$

\square

3.3 Affine erosion of convex curves

Let us first consider two particular kinds of convex C-sets : half planes, and strips (i.e. sets enclosed by two parallel straight lines). These C-sets (to which we shall refer as *trivial* C-sets) are invariant under affine erosion, because they only have 0-chord sets. One easily checks that they are the only simple C-sets which satisfy this property. So, since they would not satisfy most of the statements which follow, we shall exclude them most of the time. Another reason is that any nontrivial convex C-set is simple.

3.3.1 Basic statements

Proposition 6 *The affine erosion of a convex C-set is a convex C-set.*

Proof :

If S is a convex C-set, then $S - K$ is also convex for any positive σ -chord set K of ∂S . It follows that

$$E_\sigma(S) = \bigcap_{\substack{\sigma' \leq \sigma \\ K \in \mathcal{K}_\sigma^+(S)}} (S - K)$$

is convex as an intersection of convex sets. \square

A consequence of this proposition is that we can define the affine erosion for convex curves. According to the previous remark, we call *trivial* any convex semi-closed curve made of a straight line. From now on, we also suppose that a convex semi-closed curve is naturally oriented in such a way that its inside is convex. Hence, nontrivial convex semi-closed curves and nontrivial convex C-sets are equivalent since the map $\mathcal{C} \mapsto \mathcal{I}(\mathcal{C})$ establishes a bijective correspondence between them. Notice incidentally that any chord set of a convex set is positive and finite (i.e. bounded).

Definition 9 *The σ -affine erosion of a convex semi-closed curve \mathcal{C} is the convex semi-closed curve*

$$E_\sigma(\mathcal{C}) = \partial E_\sigma(\mathcal{I}(\mathcal{C})).$$

Of course, the notation $E_\sigma(\mathcal{C})$ is abusive, but more simple. We shall always avoid any possibility of confusion between the affine erosion of a set and the affine erosion of a curve anyway.

Proposition 7 *If S is a non-trivial convex C-set, then for any $\sigma \leq \sigma_e(S)$, only the σ -chord sets matter in the definition of the σ -affine erosion of S , i.e.*

$$E_\sigma(S) = S - \bigcup_{K \in \mathcal{K}_\sigma^+(\partial S)} K.$$

Proof :

Let $C(I)$ be the boundary of S : since S is convex, any couple $(s, t) \in I^2$ is a chord of C , and the map $t \mapsto \text{area}(C_{s,t})$ is continuous and increasing from 0 towards $\text{area}(S)$ (which may be infinite) unless S is trivial, which is not the case here. Consequently, if (s, t) is a σ' -chord of S with $\sigma' < \sigma \leq \sigma_\varepsilon(S) \leq \text{area}(S)$, then $(s, t + \varepsilon)$ is a σ -chord of S for a judicious choice of ε , and $C_{s,t} \subset C_{s,t+\varepsilon}$, which means that (s, t) is not a σ -limit chord of C . In other words, all σ -limit chords of S are σ -chords of S and Lemma 1 achieves the proof. \square

3.3.2 The middle point property

We now establish an interesting property of convex semi-closed curves : their σ -affine erosion is always included in the set of the middle points of their σ -chord segments, and the equality holds beyond a limit scale of erosion (which is nonzero for most of the curves). The reason is roughly explained on Figure 3.7 : given a curve $\mathcal{C} = C(I)$ and σ -chord segment $[C(s)C(t)]$, another σ -chord segment of \mathcal{C} intersects $[C(s)C(t)]$ in $I(\theta)$, and as $\theta \rightarrow 0$, the area equality forces

$$\frac{1}{2}r_1^2(\theta) \cdot \theta = \frac{1}{2}r_2^2(\theta) \cdot \theta + o(\theta),$$

so that $r_1(\theta) - r_2(\theta) \rightarrow 0$ and $I(\theta)$ converges towards the middle of $[C(s)C(t)]$. This means that the envelope of the σ -chord segments of \mathcal{C} is made of the middle points of these segments. Under additional conditions, we shall prove that this envelope is exactly the σ -affine erosion of \mathcal{C} .

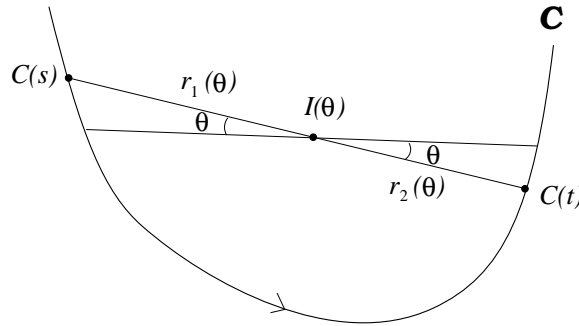


Figure 3.7: The middle point property

We begin with a useful geometric lemma.

Lemma 3 Consider A, B, A', B' four distinct points of the plane such that

$$[AB] \cap [A'B'] = \{M\}$$

and

$$\text{area}(MAA') = \text{area}(MBB').$$

Then,

$$\frac{\text{dist}(A, B)}{\text{dist}(A, M)} = 2 - \frac{[AA', BB']}{[AB, BB']}.$$

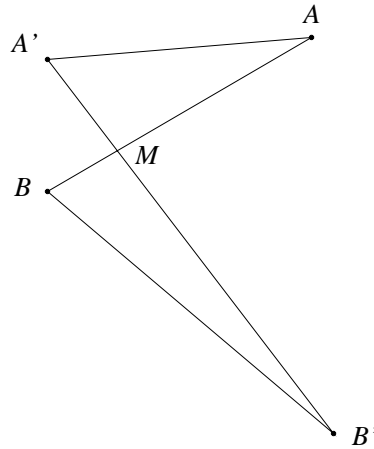


Figure 3.8: 4 points Lemma

Proof :

Let us first define λ with $AM = \lambda AB$, which implies $MB = (1 - \lambda)AB$. Since the area of the triangles MAA' and MBB' are equal, we have

$$[AA', AM] = [BB', BM],$$

which gives

$$\lambda [AA', AB] = (1 - \lambda) [AB, BB']. \quad (3.2)$$

Moreover, as M also lies on the segment $[A'B']$, we can write

$$[MA', MB'] = 0 = [MA + AA', MB + BB'] = [-\lambda AB + AA', (1 - \lambda)AB + BB'],$$

so that

$$-\lambda [AB, BB'] + (1 - \lambda) [AA', AB] + [AA', BB'] = 0. \quad (3.3)$$

Now, multiplying Equation 3.3 by λ and replacing the second term from Equation 3.2, we obtain

$$-\lambda^2 [AB, BB'] + (1 - \lambda)^2 [AB, BB'] + \lambda [AA', BB'] = 0,$$

and the terms in λ^2 cancel so that

$$\lambda (2 [AB, BB'] - [AA', BB']) = [AB, BB'].$$

Finally, we obtain as announced

$$\frac{1}{\lambda} = \frac{\text{dist}(A, B)}{\text{dist}(A, M)} = 2 - \frac{[AA', BB']}{[AB, BB']}.$$

□

which proves that $\lambda \leq \frac{1}{2}$ according to Step 2.

4. A symmetrical reasoning proves that $\lambda \geq \frac{1}{2}$ as well, and consequently $\lambda = \frac{1}{2}$, i.e. I is the middle of the segment associated to the σ -chord (s, t) . \square

From this result, it is natural to wonder whether there is an exact correspondence between the σ -affine erosion of a non-trivial convex semi-closed curve and the set of the middle points of its σ -chord segments. We are going to prove that the answer is positive for a large class of curves, including C^1 curves and many polygons, provided that σ is small enough. For that purpose, we introduce the following definitions of regular chord and regular scale.

Definition 10 *Let \mathcal{C} be a convex semi-closed curve, then a chord (A, B) of \mathcal{C} is **regular** if $\angle(\mathbf{T}_A^-, \mathbf{T}_B^+) \in [0, \pi[$.*

Definition 11 *Let \mathcal{C} be a non-trivial convex semi-closed curve. A real $\sigma \geq 0$ is a **regular scale** for \mathcal{C} if any σ -chord of \mathcal{C} is regular. We note $\sigma_r(\mathcal{C})$ the upper bound of the regular scales of \mathcal{C} .*

Theorem 1 (middle point property) *Let \mathcal{C} be a non-trivial convex semi-closed curve, and σ a regular scale of \mathcal{C} . Then $E_\sigma(\mathcal{C})$ is exactly the set of the middle points of the σ -chord segments of \mathcal{C} , and there is a natural homeomorphism between \mathcal{C} and $E_\sigma(\mathcal{C})$.*

Proof :

According to Proposition 8, we only have to prove that the middle point of any σ -chord belongs to $E_\sigma(\mathcal{C})$. Consider C a regular parameterization of \mathcal{C} , let (s, t) be a σ -chord of \mathcal{C} , and define α the smallest positive number x such that $(s - x, s)$ is a σ -chord of \mathcal{C} . Finally, let $\mathcal{D}^+ =] - \alpha, 0[$ and $\mathcal{D}^- =]0, t - s[$ (if \mathcal{C} is closed, then these intervals must be considered in S^1). For any $a \in \mathcal{D}^- \cup \mathcal{D}^+$, we call $I(a)$ the intersection between $[C(s)C(t)]$ and the chord segment associated to the σ -chord of origin $s + a$, and define $\lambda(a)$ by $C(s)I(a) = \lambda(a)C(s)C(t)$.

Notice that if a σ -chord of \mathcal{C} intersects $]C(s)C(t)[$ then its origin can be taken in $\mathcal{D}^- \cup \{0\} \cup \mathcal{D}^+$. Hence, to prove that no σ -chord set of \mathcal{C} contains I , the middle of $[C(s)C(t)]$, it is sufficient to prove that $\lambda > \frac{1}{2}$ on \mathcal{D}^+ as well as $\lambda < \frac{1}{2}$ on \mathcal{D}^- .

1. We first establish that for $\varepsilon > 0$ small enough, $\lambda(-\varepsilon) < \frac{1}{2} < \lambda(\varepsilon)$.

Consider $\varepsilon, \varepsilon'$ such that $s < s + \varepsilon < t < t + \varepsilon'$ and $(s + \varepsilon, t + \varepsilon')$ is another σ -chord of \mathcal{C} (implicitly, ε' depends on s, t and ε). Now define $k(\varepsilon)$ such that $C(t), C(t + \varepsilon'), C(s)$ and $A^\varepsilon = C(s) + k(\varepsilon)C'_+(s)$ are four points satisfying the equi-area hypothesis of Lemma 3. Necessarily, $M_\varepsilon = [C(t)C(s)] \cap [C(t + \varepsilon')A^\varepsilon]$ belongs to $[I(\varepsilon)C(s)]$, so that $\lambda(\varepsilon) \geq \lambda'(\varepsilon)$ where $\lambda'(\varepsilon)$ is defined by $C(s)M_\varepsilon = \lambda'(\varepsilon)C(s)C(t)$. Moreover, from Lemma 3 we get

$$\begin{aligned} \frac{1}{1 - \lambda'(\varepsilon)} &= 2 - \frac{[C(t)C(t + \varepsilon'), k(\varepsilon)C'_+(s)]}{[C(t)C(s), k(\varepsilon)C'_+(s)]} \\ &= 2 + \frac{[C'_+(s), C(t)C(t + \varepsilon')]}{[C'_+(s), C(s)C(t)]}. \end{aligned}$$

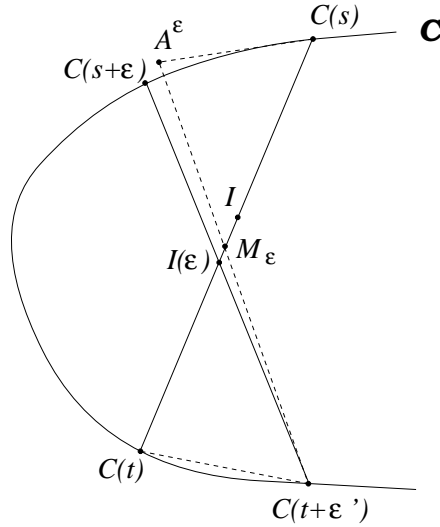


Figure 3.10: The middle point property (2)

Since \mathcal{C} is convex, $[C'_+(s), C(s)C(t)] > 0$, and as (s, t) is a regular chord of C , we have as well, for $\varepsilon > 0$ small enough, $[C'_+(s), C(t)C(t + \varepsilon')] > 0$. Consequently, $\lambda(\varepsilon) \geq \lambda'(\varepsilon) > \frac{1}{2}$ for $\varepsilon > 0$ small enough, and a symmetric proof would establish $\lambda(-\varepsilon) < \frac{1}{2}$ for $\varepsilon > 0$ small enough.

2. Let us check that λ is continuous. Given $a \in \mathcal{D}^- \cup \mathcal{D}^+$, there exists a unique $b(a)$ such that $(s + a, t + b(a))$ is a σ -chord of \mathcal{C} . Since the map $(s, t) \mapsto \text{area}(C_{s,t})$ is continuous, so is the map $a \mapsto b(a)$. Now, as $I(a) = [C(s)C(t)] \cap [C(s + a)C(t + b(a))]$, a simple computation gives

$$\lambda(a) = \frac{[C(s + a)C(t + b(a)), C(s)C(t + b(a))]}{[C(s + a)C(t + b(a)), C(s)C(t)]},$$

and the non-vanishing denominator ensures that λ is continuous on $\mathcal{D}^+ \cup \mathcal{D}^-$. Last, we know from Proposition 8 that λ can be continuously extended to 0 by taking $\lambda(0) = \frac{1}{2}$.

3. Now we prove that λ has no local maximum on \mathcal{D}^+ , and no local minimum on \mathcal{D}^- .

If λ has a local maximum in $a \in \mathcal{D}^+$, then for ε small enough, $I(a + \varepsilon)$ and $I(a - \varepsilon)$ belong to the segment $[I(a)C(s)]$ (see Figure 3.11). Then, due to the position of $C(s + a + \varepsilon)$ and $C(s + a - \varepsilon)$ relatively to $C(s + a)$, it is clear that the intersection of the σ -chords of origin $s + a$ and $s + a + \varepsilon$ lies on $[C(s + a)I(a)]$, whereas the intersection of the σ -chords of origin $s + a$ and $s + a - \varepsilon$ cannot lie on $[C(s + a)I(a)]$. But this is a contradiction with Step 1 applied to the σ -chord of origin $s + a$, since we would have $\lambda'(-\varepsilon) \geq \lambda'(\varepsilon)$ for the corresponding λ' . As a conclusion, λ has no local maximum on \mathcal{D}^+ , and a symmetric proof establishes that λ has no local minimum on \mathcal{D}^- either.

4. From Step 2 and 3 we deduce that λ is monotone on \mathcal{D}^+ (resp. on \mathcal{D}^-), and the only possibility according to Step 1 (and to the fact that $\lambda(\varepsilon) \rightarrow \frac{1}{2}$ as $\varepsilon \rightarrow 0$) is that λ is nondecreasing on \mathcal{D}^+ (resp. on \mathcal{D}^-) and remains strictly larger than $\frac{1}{2}$ on \mathcal{D}^+ (resp. strictly lower than $\frac{1}{2}$ on \mathcal{D}^-). Consequently, I does belong to $E_\sigma(\mathcal{C})$.

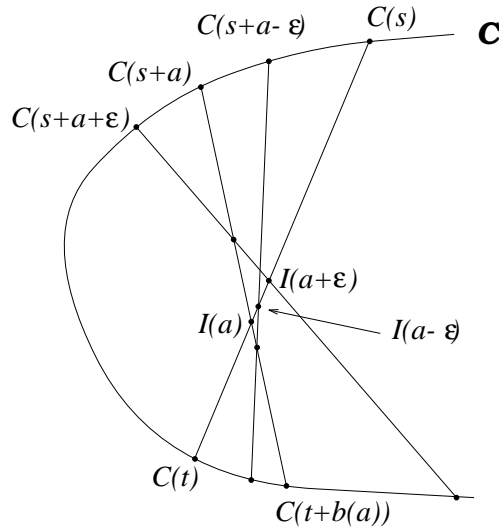


Figure 3.11: The middle property (3)

5. Now we can build a bijective and continuous correspondence between \mathcal{C} and $E_\sigma(\mathcal{C})$ as follows : given $C(s) \in \mathcal{C}$, there exists a unique $\delta(s, \sigma)$ such that $(s - \delta, s + \delta)$ is a σ -chord of C . According to Theorem 1,

$$C_\sigma(s) = \frac{1}{2}(C(s - \delta) + C(s + \delta))$$

belongs to $E_\sigma(\mathcal{C})$, and the correspondence $C(s) \mapsto C_\sigma(s)$ is one to one and clearly bicontinuous. \square

Notice that the natural correspondence between \mathcal{C} and its affine erosion gives sense to $E_\sigma(C)$, meaning the parameterization induced by C on the σ -affine erosion of the curve $C(I)$.

Corollary 2 *If \mathcal{C} is a non-trivial convex semi-closed curve and σ a regular scale of \mathcal{C} , then $E_\sigma(\mathcal{C})$ is of class C^1 .*

Proof :

If this is not the case, then we can find a $M \in E_\sigma(\mathcal{C})$ such that $T_M^+ \neq T_M^-$. But necessarily these semi-tangents arise from two distinct σ -chord segment containing M , which is impossible according to Theorem 1. \square

We shall estimate the regularity of $E_\sigma(\mathcal{C})$ more precisely later . Now, let us compute again the affine erosion of the “corner” of Proposition 1 using Theorem 1. First, it is clear that the boundary of the “corner”

$$\{O + x\mathbf{v}_1 + y\mathbf{v}_2; x > 0, y > 0\}$$

is a semi-closed curve \mathcal{C} with $\sigma_r(\mathcal{C}) = +\infty$ (any scale is regular) : thus, we know from Theorem 1 that its σ -affine erosion is exactly given by the middle of its σ -chords.

The chord set $(O, \mathbf{v}_1, \mathbf{v}_2)$ of \mathcal{C} delimited by the points $O + 2x \mathbf{v}_1$ and $O + 2y \mathbf{v}_2$ has an area equal to $2xy \cdot [\mathbf{v}_1, \mathbf{v}_2]$ (cf. figure 3.12). Consequently, the σ -affine erosion of \mathcal{C} is the set of the middle points $O + x \mathbf{v}_1 + y \mathbf{v}_2$ constrained by the area equality $2xy \cdot [\mathbf{v}_1, \mathbf{v}_2] = \sigma$, which corresponds to the hyperbola defined in Equation 3.1.

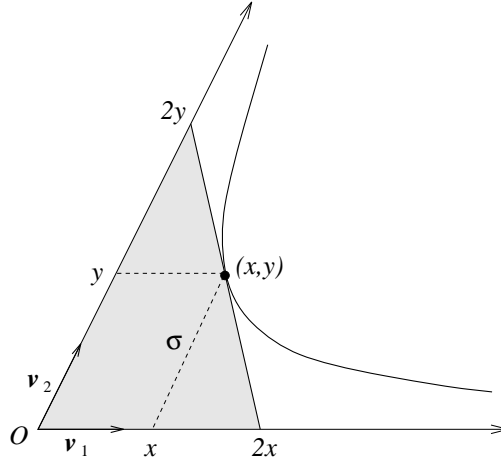


Figure 3.12: Affine erosion of a “corner” (2)

3.3.3 Regular scales

In this section, we characterize the regular scales of a non-trivial convex semi-closed curve.

Proposition 9 *Let \mathcal{C} be a non-trivial convex semi-closed curve. The set of the regular scales of \mathcal{C} is $[0, \sigma_r(\mathcal{C})[$.*

Proof :

Suppose that $\sigma_r(\mathcal{C}) < +\infty$ (otherwise there is nothing to prove), and consider $C : I \rightarrow \mathbb{R}^2$ a regular parameterization of \mathcal{C} . In what follows, we consider \mathbf{v}_0 an arbitrary nonzero vector of the plane, and the angle function $\alpha_+ : I \rightarrow S^1$ (respectively $\alpha_- : I \rightarrow S^1$) defined by $\alpha_+(s) = \angle(\mathbf{v}_0, C'_+(s))$ ($\alpha_-(s) = \angle(\mathbf{v}_0, C'_-(s))$) respectively).

1. First we show that if σ is a regular scale of \mathcal{C} and $0 \leq \sigma' \leq \sigma$, then σ' is also a regular scale of \mathcal{C} . Suppose that it is not the case, i.e. that we can find a non-regular σ' -chord (s, t) of \mathcal{C} . We can choose $\varepsilon > 0$ in such a manner that $(s, t + \varepsilon)$ is a σ -chord of \mathcal{C} . Since $\alpha_+(t) \leq \alpha_+(t + \varepsilon) \leq \alpha_-(s)$ and $\alpha_+(t) - \alpha_-(s) \in [\pi, 2\pi[$, we have $\alpha_+(t + \varepsilon) - \alpha_-(s) \in [\pi, 2\pi[$ which means that $(s, t + \varepsilon)$ is a non-regular σ -chord of \mathcal{C} . This contradiction proves that σ' is a regular scale of \mathcal{C} . Hence, the set of regular scales of \mathcal{C} is $[0, \sigma_r(\mathcal{C})[$ or $[0, \sigma_r(\mathcal{C})]$.

2. Now we prove that $\sigma_r(\mathcal{C})$ is not a regular scale of \mathcal{C} .

2.a. If \mathcal{C} is closed, then $I = S^1$, and there exist two sequences (s_n) and (t_n) such that (s_n, t_n) is a non-regular σ_n -chord of \mathcal{C} with $\sigma_n \rightarrow \sigma_r(\mathcal{C})$ as $n \rightarrow +\infty$. Since S^1 is compact, we can find

an increasing map $\varphi : \mathbb{N} \rightarrow \mathbb{N}$ such that

$$\lim_{n \rightarrow \infty} (s_{\varphi(n)}, t_{\varphi(n)}) = (a, b) \in I \times I.$$

Now, because $\text{area}(C_{s,t})$ is continuous with respect to s and t , we have

$$\text{area}(C_{a,b}) = \sigma_r(\mathcal{C}).$$

If we define $a_n = \min(a, s_{\varphi(n)})$ and $b_n = \max(b, t_{\varphi(n)})$, we have, in S^1 and for n large enough,

$$\alpha_+(b_n) - \alpha_-(a_n) \in [\pi, 2\pi[. \quad (3.4)$$

Now remark that α_- is left-continuous and α_+ is right-continuous and deduce from (3.4) that modulo 2π ,

$$\alpha_+(b) - \alpha_-(a) \in [\pi, 2\pi],$$

and since $\alpha_+(b) - \alpha_-(a) = 2\pi$ is impossible, (a, b) is a non-regular chord of C .

2.b. If \mathcal{C} is not closed, then we can suppose that $I = \mathbb{R}$ and as \mathcal{C} is a semi-closed curve,

$$\lim_{+\infty} \alpha^+ - \lim_{-\infty} \alpha^- \in [0, \pi],$$

so that if (a, b) is a non-regular σ -chord, necessarily $\alpha_+(b) - \alpha_-(a) = \pi$ and $C(]-\infty, a])$ and $C([b, +\infty[)$ must be two parallel half lines. Now define $a' = \sup\{x; \alpha_-(x) = \alpha_-(a)\}$ and $b' = \inf\{x; \alpha_+(x) = \alpha_+(b)\}$: (a', b') is a non-regular chord of C and clearly $\text{area}(C_{a'b'}) = \sigma_r(\mathcal{C})$.
□

Corollary 3 *Let \mathcal{C} be a non-trivial convex semi-closed curve, then $\sigma_r(\mathcal{C}) > 0$ if and only if no part of \mathcal{C} is a segment $[AB]$ such that $\angle(\mathbf{T}_A^-, \mathbf{T}_B^+) \in [\pi, 2\pi[$.*

Proof :

1. If $[AB]$ is a piece of \mathcal{C} such that $\angle(\mathbf{T}_A^-, \mathbf{T}_B^+) \in [\pi, 2\pi[$, then (A, B) is a non-regular 0-chord of \mathcal{C} , and consequently $\sigma_r(\mathcal{C}) = 0$.

2. Conversely, let us suppose now that $\sigma_r(\mathcal{C}) = 0$. From Proposition 9 we know that we can find a non-regular 0-chord of \mathcal{C} , i.e. a part of \mathcal{C} which is a segment $[AB]$ such that $\angle(\mathbf{T}_A^-, \mathbf{T}_B^+) \in [\pi, 2\pi[$. □

This result allows us to check that the characteristic constant σ_r is non zero for a large class of convex semi-closed curves, including C^1 ones and all polygons such that the sum of two successive angle steps remains strictly below π .

Corollary 4 *If \mathcal{C} is a convex semi-closed curve of class C^1 , then $\sigma_r(\mathcal{C}) > 0$.*

Proof :

Suppose that \mathcal{C} is a convex semi-closed curve of class C^1 for which $\sigma_r(\mathcal{C}) = 0$, from Corollary 3 a part of \mathcal{C} should be a segment $[AB]$ such that $\mathbf{T}_A^- \neq \mathbf{T}_B^+$, which is impossible since $\mathbf{T}_A^+ = \mathbf{T}_B^-$ and the regularity of \mathcal{C} forces $\mathbf{T}_B^+ = \mathbf{T}_B^-$ and $\mathbf{T}_A^+ = \mathbf{T}_A^-$. \square

Corollary 5 *If $\mathcal{C} = A_0A_1\dots A_n$ is a convex polygon, then $\sigma_r(\mathcal{C}) > 0$ iff for all i modulo n ,*

$$[A_iA_{i+1}, A_{i+2}A_{i+3}] > 0.$$

Proof :

This is a simple consequence of Corollary 3, and if $[A_iA_{i+1}, A_{i+2}A_{i+3}] > 0$ for all i we even know that

$$\sigma_r(A_1A_2\dots A_n) \geq \min_i \text{area}(A_iA_{i+1}A_{i+2}).$$

 \square

What happens for a non-regular chord ? Considering the proof of Theorem 1, we can see that if $\angle(\mathbf{T}_A^-, \mathbf{T}_B^+) \in]\pi, 2\pi[$ we have both $\lambda > \frac{1}{2}$ and $\lambda < \frac{1}{2}$, i.e. no point of the σ -chord segment $[AB]$ belongs to $E_\sigma(\mathcal{C})$. In other words, the curve described by the middle points of the σ -chord segments has “ghost parts” which must be removed to obtain the desired affine erosion. For instance, these “ghost parts” appear at any scale of erosion for a triangle, for which $\sigma_r = 0$ (see Figure 3.13).

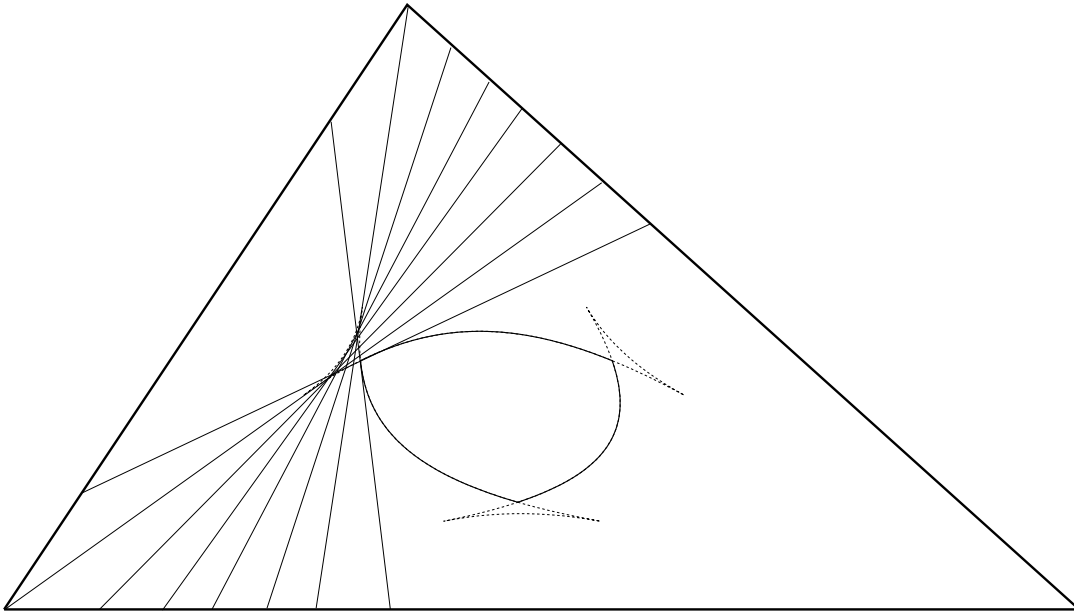


Figure 3.13: “ghost parts” always appear in the affine erosion of a triangle

The need to remove these ghost parts is in some way related to the Huygen’s principle construction used for the propagation of fronts. Behind this construction hides an entropy

condition : if the propagating front is viewed as a burning flame, then *once a particle is burnt it stays burnt and cannot burn any more* (see [65]), so that such “ghost parts” of fronts have no physical meaning.

If $\angle(\mathbf{T}_A^-, \mathbf{T}_B^+) = \pi$ (i.e. $\mathbf{T}_A^- = -\mathbf{T}_B^+$), Definition 10 makes the chord (A, B) non regular despite the fact that the middle point of the associated chord segment does belong to $E_\sigma(\mathcal{C})$. The reason why we did not allow this configuration in our definition of a regular chord is that we want not only the reverse inclusion between the middle points and the affine erosion, but also a bijective correspondence. The case of a square highlights this phenomenon : at any scale, four points of the affine erosion are the middle points of an infinite number of σ -chord segments, which produces singularities (discontinuity of the tangent) at these points (see Figure 3.14).

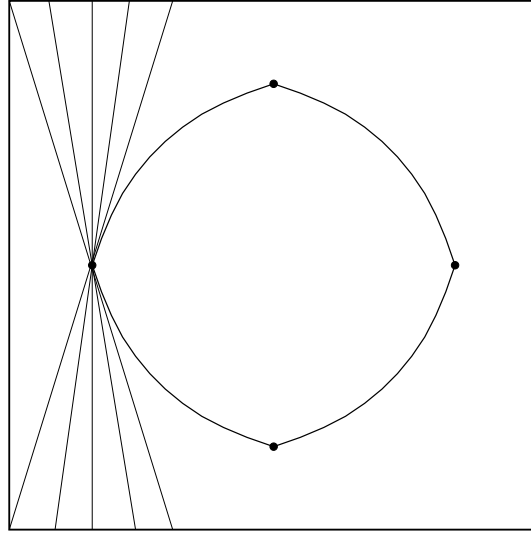


Figure 3.14: Four singularities appear in the affine erosion of a square

3.3.4 Consistency

Theorem 2 *Let $\mathcal{C} = C(I)$ be a semi-closed convex curve of class C^n with $n \geq 1$. Then for any $\sigma < \sigma_r(\mathcal{C})$, $E_\sigma(\mathcal{C})$ is a semi-closed convex curve of class C^n . If $n \geq 2$, the infinitesimal evolution as $\sigma \rightarrow 0$ of a point $C(s) \in \mathcal{C}$ is given by*

$$C_\sigma(s) = C(s) + \omega \cdot \sigma^{\frac{2}{3}} \cdot \gamma(s)^{\frac{1}{3}} \mathbf{N}(s) + o(\sigma^{\frac{2}{3}}) \quad \text{with} \quad \omega = \frac{1}{2} \left(\frac{3}{2} \right)^{\frac{2}{3}},$$

where $\gamma(s)$ and $\mathbf{N}(s)$ are respectively the curvature of \mathcal{C} and the normal vector to \mathcal{C} at point $C(s)$. Moreover, if $n \geq 3$, the remaining part is $O(\sigma^{\frac{4}{3}})$ at any point where the curvature $\gamma(s)$ is nonzero.

Proof :

1. Consider $s \mapsto C(s)$ an Euclidean length parameterization of \mathcal{C} (i.e. $|C'(s)| = 1$ everywhere). Since \mathcal{C} is convex, we know from Theorem 1 that $E_\sigma(\mathcal{C})$ is exactly made of the middle of the σ -chords of \mathcal{C} as soon as $0 < \sigma < \sigma_r(\mathcal{C})$ (which makes sense because we know from Corollary 4 that $\sigma_r(\mathcal{C}) > 0$). Let $(s - \delta, s + \delta)$ be a σ -chord of C and $C_\sigma(s)$ the middle of the associated segment (see Figure 3.15).

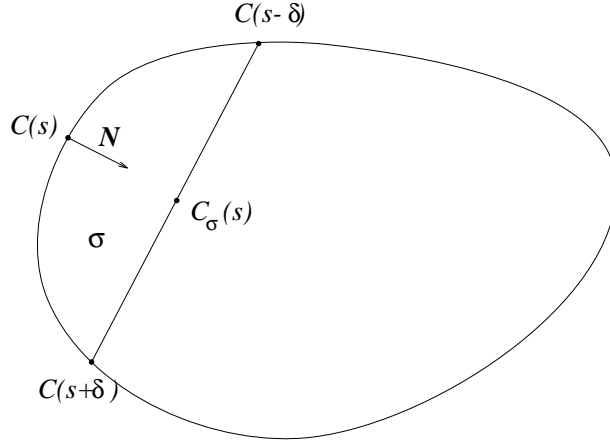


Figure 3.15: Affine erosion of a convex semi-closed curve

Since C is of class C^1 , we can use the Green formula to compute the area

$$\sigma = \frac{1}{2}F(s, \delta(s, \sigma)), \quad \text{where}$$

$$F(s, t) = \int_{s-t}^{s+t} [C(h), C'(h)] dh + [C(s+t), C(s-t) - C'(s+t)].$$

A simple computation gives

$$\frac{\partial F}{\partial t}(s, t) = [C(s+t) - C(s-t), C'(s+t) - C'(s-t)]$$

$$\text{and } \frac{\partial F}{\partial s}(s, t) = [C(s+t) - C(s-t), C'(s+t) + C'(s-t)].$$

C being convex, we have, for any distinct points $C(a)$ and $C(b)$ of C , the inequality

$$[C'(a), C(b) - C(a)] \geq 0,$$

and the equality holds if and only if the piece of curve $C([a, b])$ is a segment. Hence, the numbers $[C(s+t) - C(s-t), C'(s+t)]$ and $[C(s+t) - C(s-t), -C'(s-t)]$ are positive and their sum cannot be zero unless $\sigma = 0$, which is not the case, or unless $C(s+t) = C(s-t)$, which is impossible as soon as $0 < t \leq \delta$. As a consequence,

$$\frac{\partial F}{\partial t}(s, \delta) > 0$$

(which simply means that the area σ of the chord-set $C_{s-\delta, s+\delta}$ increases with δ), and the global inversion theorem allows us to claim that the map $s \mapsto \delta(s, \sigma)$ is of class C^n as well as the map $(s, t) \mapsto F(s, t)$.

We just proved that the function

$$s \mapsto C_\sigma(s) = \frac{1}{2} (C(s - \delta(s, \sigma)) + C(s + \delta(s, \sigma)))$$

is of class C^n . Moreover, since the vectors $C'(s - \delta(s, \sigma))$ and $C'(s + \delta(s, \sigma))$ cannot be colinear for $\sigma < \sigma_r(\mathcal{C})$, the derivative

$$2 \frac{\partial}{\partial s} C_\sigma(s) = \left(1 - \frac{\partial \delta}{\partial s}\right) C'(s - \delta) + \left(1 + \frac{\partial \delta}{\partial s}\right) C'(s + \delta) \quad (3.5)$$

never vanishes. As a consequence, the curve C_σ is of class C^n in the geometric sense (that is C_σ is a regular parameterization).

Incidentally, remark that it can easily check from Equation 3.5 that $\frac{\partial}{\partial s} C_\sigma$ and $C(s + \delta) - C(s - \delta)$ are colinear, i.e. that the σ -chord segments of \mathcal{C} are the tangents to $E_\sigma(\mathcal{C})$ as expected.

2.a. If C is of class C^2 , the curvature at point $C(s)$ is defined by $\gamma(s) = [C'(s), C''(s)]$. A simple expansion near $t = 0$ gives

$$\frac{\partial F}{\partial t}(s, t) = [2tC'(s) + o(t), 2tC''(s) + o(t)] = 4t^2 \gamma(s) + o(t^2), \quad (3.6)$$

which can be integrated to obtain

$$2\sigma = \frac{4}{3} \delta^3 \gamma(s) + o(\delta^3).$$

Thus, whenever $\gamma(s) \neq 0$ we have

$$\delta(s, \sigma) = \left(\frac{3\sigma}{2\gamma(s)} \right)^{\frac{1}{3}} + o(\sigma^{\frac{1}{3}}),$$

and finally

$$\begin{aligned} C_\sigma(s) &= \frac{1}{2} [C(s - \delta) + C(s + \delta)] \\ &= C(s) + \frac{\delta^2}{2} C''(s) + o(\delta^2) \\ &= C(s) + \frac{1}{2} \left(\frac{3}{2} \right)^{\frac{2}{3}} \sigma^{\frac{2}{3}} \cdot \gamma^{\frac{1}{3}}(s) \mathbf{N}(s) + o(\sigma^{\frac{2}{3}}), \end{aligned}$$

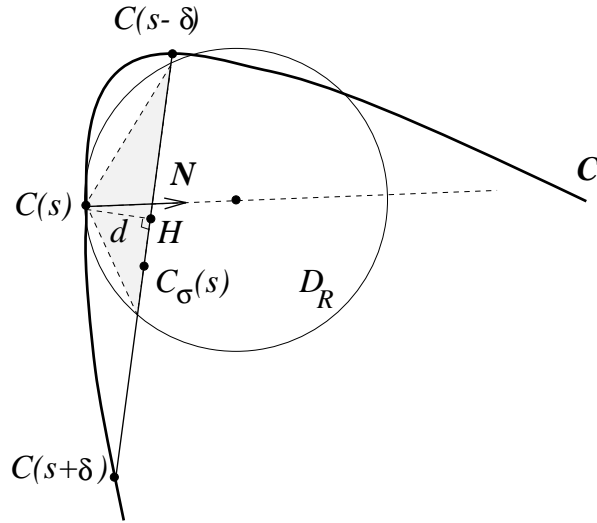
where $\mathbf{N}(s)$ is the normal vector to C in $C(s)$.

2.b. If $\gamma = 0$ we use a geometric argument. Given $\varepsilon > 0$, let $R = \varepsilon^{-3}$. Since $\gamma(s) = 0$, the disk D_R with center $C(s) + R\mathbf{N}(s)$ and radius R is locally contained in $\mathcal{I}(\mathcal{C})$ near $C(s)$ (see Figure 3.16). In particular, there exists $\sigma_0 > 0$ such that

$$\forall \sigma < \sigma_0, \quad C(s) + R\mathbf{N}(s) \notin C_{s-\delta, s+\delta} \quad \text{and} \quad D_R \cap C_{s-\delta, s+\delta} \subset \mathcal{I}(\mathcal{C})$$

(once again, δ depends on s and σ). Now, calling H the orthogonal projection of $C(s)$ on the chord segment $[C(s - \delta), C(s + \delta)]$ and writing $d = \text{dist}(C(s), H)$, we claim that

$$\sigma \geq d \sqrt{R^2 - (R - d)^2}.$$

Figure 3.16: Case $\gamma = 0$

The reason for this last inequality is that σ is larger than the shaded zone of Figure 3.16, which is itself larger than $d\sqrt{R^2 - (R-d)^2}$ (the equality happens when the chord is orthogonal to \mathbf{N}). Hence,

$$\sigma \geq d\sqrt{2Rd - d^2}$$

and

$$d^{\frac{3}{2}} \leq \frac{\sigma}{\sqrt{2R-d}} \leq \frac{\sigma}{\sqrt{R}}$$

since $d \leq R$ due to the fact that $C(s) + RN(s) \notin C_{s-\delta, s+\delta}$. Consequently,

$$d \leq \frac{\sigma^{\frac{2}{3}}}{R^{\frac{1}{3}}} \leq \varepsilon \sigma^{\frac{2}{3}},$$

which means that

$$d = o(\sigma^{\frac{2}{3}}). \quad (3.7)$$

Now, we constrain σ to be small enough in order to ensure that $\angle(C'(s-\delta), C'(s))$ and $\angle(C'(s), C'(s+\delta))$ belong to $[0, \pi/2]$. Recalling that the pieces of curve $C([s-\delta, s])$ and $C([s, s+\delta])$ have length δ , we deduce that both $\text{dist}(C(s-\delta), H)$ and $\text{dist}(H, C(s+\delta))$ belong to $[\delta-d, \delta]$, so that

$$\text{dist}(H, C_\sigma(s)) \leq \frac{d}{2}.$$

Then, Equation 3.7 implies that

$$\text{dist}(C(s), C_\sigma(s)) = o(\sigma^{\frac{2}{3}})$$

as announced.

3. If $n \geq 3$, the expansion of Equation 3.6 can be improved into

$$\frac{\partial F}{\partial t}(s, t) = 4t^2\gamma(s) + O(t^3),$$

and following the same computation as in Step 2.a, one can establish that

$$C_\sigma(s) = C(s) + \omega \cdot \sigma^{\frac{2}{3}} \cdot \gamma^{\frac{1}{3}}(s) \mathbf{N}(s) + O(\sigma^{\frac{4}{3}}).$$

□

Remark : If the curvature vanishes, we can be more precise. Suppose that C is locally C^5 near s where $\gamma(s) = 0$ and $\gamma''(s) \neq 0$. At point s , we have, writing $\mathbf{T} = C'(s)$,

$$\begin{aligned} C'' &= \gamma \mathbf{N} = \mathbf{0} \\ C''' &= -\gamma^2 \mathbf{T} + \gamma' \mathbf{N} = \gamma' \mathbf{N} \\ C^{(4)} &= -3\gamma\gamma' \mathbf{T} + (\gamma'' - \gamma^3) \mathbf{N} = \gamma'' \mathbf{N} \end{aligned}$$

Consequently,

$$\frac{\partial F}{\partial t}(s, t) = \left[2tC'(s) + O(t^3), \frac{t^3}{3}C^{(4)}(s) + O(t^5) \right] = 2\frac{t^4}{3}\gamma''(s) + O(t^6),$$

and an integration yields

$$2\sigma = \frac{2}{15}\delta^5\gamma''(s) + O(\delta^7),$$

or equivalently

$$\delta(s, \sigma) = \left(\frac{15\sigma}{\gamma''(s)} \right)^{\frac{1}{5}} + O(\sigma^{\frac{2}{5}}).$$

Therefore, the point $C(s)$ is mapped onto

$$\begin{aligned} C_\sigma(s) &= \frac{1}{2} [C(s - \delta) + C(s + \delta)] \\ &= C(s) + \frac{\delta^4}{24}C^{(4)}(s) + O(\delta^6) \\ &= C(s) + \frac{15^{\frac{1}{5}}}{24}\sigma^{\frac{4}{5}} \cdot (\gamma''(s))^{\frac{1}{5}} \mathbf{N}(s) + O(\sigma^{\frac{6}{5}}). \end{aligned}$$

Incidentally, we check that

$$C_\sigma(s) = C(s) + o(\sigma^{\frac{2}{3}}),$$

but we can see that the expansion

$$C_\sigma(s) = C(s) + O(\sigma^{\frac{4}{3}})$$

is not generally true when $\gamma(s) = 0$ (and is false as soon as $\gamma''(s) \neq 0$). □

Remark : Theorem 2 proves that the affine erosion preserves the regularity of a convex curve. Unfortunately, it does not regularize a convex curve of class C^n into a convex curve of class C^m with $m > n$. One can check this on the C^1 curve \mathcal{C} made of the half line $\{y = 0, x \leq 0\}$ and the half parabola $\{y = x^2, x > 0\}$: for any $\sigma > 0$, $E_\sigma(\mathcal{C})$ is not C^2 .

3.4 Affine erosion of non convex curves

3.4.1 Structure

Lemma 4 *If S is a simple C -set and $M \in \partial E_\sigma(S) - \partial S$, then $\partial E_\sigma(S)$ is locally a convex curve near M .*

Proof :

Let M belong to $\partial E_\sigma(S) - \partial S$. We know from Lemma 1 that M belongs to a (possibly infinite) chord segment of a component of ∂S . As S is open and $M \in S$, for $\varepsilon > 0$ small enough, the open disk $D(M, \varepsilon)$ is included in S (see Figure 3.17). But since the complementary set to any chord set of S in $D(M, \varepsilon)$ is convex, necessarily $E_\sigma(S) \cap D(M, \varepsilon)$ is convex (it is the intersection of convex subsets of $D(M, \varepsilon)$). Consequently, $\partial E_\sigma(S)$ is near M a convex curve, because it is locally the boundary of a convex set. \square

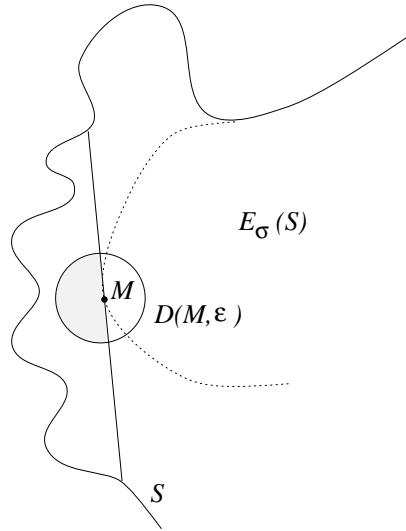


Figure 3.17: local convexity in $M \in \partial E_\sigma(S) - S$

Lemma 5 *If S is a simple C -set and $M \in \partial E_\sigma(S) \cap \partial S$ with $\sigma > 0$, then ∂S is not locally concave near M .*

Proof :

Suppose that $M \in \partial E_\sigma(S) \cap \partial S$ and ∂S is not locally concave near M . Using a parameterization C of ∂S near $M = C(s)$, we have for $\varepsilon > 0$ small enough,

$$[C(s - \varepsilon)C(s), C(s)C(s + \varepsilon)] > 0.$$

Thus, M belongs to the topological opening of a σ -chord set $C_{s-\varepsilon, s+\varepsilon}$ for $\varepsilon > 0$ small enough, which is in contradiction with $M \in \partial E_\sigma(S)$. \square

According to Lemma 4 and Lemma 5, the boundary of the affine erosion of a simple C-set is everywhere locally concave or locally convex. Thus, it is a collection of curves. Hence, we can give sense to the affine erosion of a piecewise convex semi-closed curve as a collection of semi-closed curves (and we shall prove later that these curves are also piecewise convex).

Definition 12 *The σ -affine erosion of a piecewise convex semi-closed curve \mathcal{C} is the collection of semi-closed curves*

$$E_\sigma(\mathcal{C}) = \partial E_\sigma(\mathcal{I}(\mathcal{C})).$$

Proposition 10 *The affine erosion of a piecewise convex semi-closed curve \mathcal{C} is, up to a finite number of points, the disjoint union of a finite union of concave curves (\mathcal{C}_i) and convex curves (\mathcal{D}_j), with*

- $\forall i, \mathcal{C}_i \subset \mathcal{C}$, and no concave sub-curve of \mathcal{C} contains more than one \mathcal{C}_i .
- $\forall j, \mathcal{D}_j \cap \mathcal{C} = \emptyset$.

Proof :

Let us define the curves \mathcal{C}_i as the connected components of $E_\sigma(\mathcal{C}) \cap \mathcal{C}$ (minus their extremal points if any). According to Lemma 5, these curves are concave, and if \mathcal{C}_i and $\mathcal{C}_{i'}$ belong to the same concave component of \mathcal{C} , necessarily $i = i'$ (a nonnegative chord segment of \mathcal{C} cannot have both its endpoints on the same concave component of \mathcal{C}). Hence, there is a finite number of curves \mathcal{C}_i . Now, call \mathcal{D}_j the connected components of

$$E_\sigma(\mathcal{C}) \setminus \bigcup_i \overline{\mathcal{C}_i}.$$

We have to prove that there is a finite number of such curves.

First, there can be only a finite number of non semi-closed \mathcal{D}_j , because these \mathcal{D}_j are connected to some \mathcal{C}_i according to Lemma 5. Second, let us choose an arbitrary direction \mathbf{v} of the plane, and consider the multivalued map φ which associate, to any line D directed by \mathbf{v} , all area values of all chord sets of \mathcal{C} defined from a piece of D . Because \mathcal{C} has a finite number of components, φ can be described by a finite set of continuously increasing single-valued maps (φ_k) (only a finite number of accidents happen to φ when D sweeps the plane). Then, to each map φ_k is associated at most one closed \mathcal{D}_j , so that the number of closed \mathcal{D}_j 's is finite. Last, as for the semi-closed but nonclosed \mathcal{D}_j 's, there is at most two of them. \square

Corollary 6 *The affine erosion of a piecewise convex semi-closed curve is a collection of piecewise convex semi-closed curves. Equivalently, the affine erosion of a C-set is a C-set.*

Proof :

The first part is a direct consequence of Proposition 10. As for a C-set S , it is sufficient to notice that the boundary of $E_\sigma(S)$ is included in the affine erosion of the components of ∂S . \square

3.4.2 Inflexion points

We would like to prove that the number of inflexion points (in a generalized sense) cannot increase when we compute the affine erosion of a piecewise convex closed curve. This is another stability property of the affine erosion, complementary to the inclusion principle.

Let $\mathcal{C} = C(I)$ be a piecewise convex curve. We define a canonical decomposition of \mathcal{C} into convex curves. We say that a point M of \mathcal{C} is

- convex if \mathcal{C} is locally convex near M ,
- concave if \mathcal{C} is locally concave near M ,

We consider the sub-curves \mathcal{C}_i^+ of \mathcal{C} defined as the open connected components of the set of all convex points of \mathcal{C} , and the concave sub-curves \mathcal{C}_j^- symmetrically defined. If a convex curve \mathcal{C}_i^+ and a concave curve \mathcal{C}_j^- overlap, either they are equal to the same segment, or, if not, they have each a segment in common at one of their endpoints. In that case, we remove from \mathcal{C}_i^+ and \mathcal{C}_j^- half of this segment. This way, we obtain a canonical (and minimal) decomposition of \mathcal{C} into convex and concave parts. A junction between some \mathcal{C}_i^+ and some \mathcal{C}_j^- is called a **simple junction**, while a junction between two \mathcal{C}_i^+ 's or two \mathcal{C}_j^- 's is called a **double junction** (see Figure 3.18).

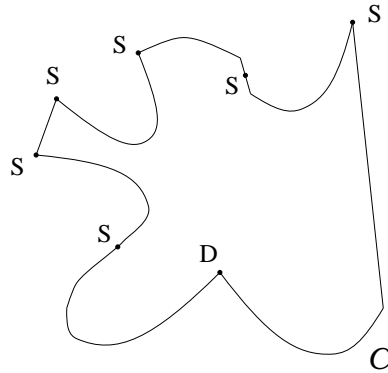


Figure 3.18: Simple (S) and double (D) junctions of a closed curve \mathcal{C} .

We define $\#\mathcal{J}(\mathcal{C})$, the **number of junctions** of \mathcal{C} as the number of simple junctions of \mathcal{C} plus twice the number of double junctions of \mathcal{C} . If \mathcal{C} is a C^2 closed curve whose curvature vanishes at a finite number of points, the junctions of \mathcal{C} are all simple and correspond to the inflexion points of \mathcal{C} . A polygon has no double junction either.

Proposition 11 *If \mathcal{C} is a piecewise convex closed curve and $\sigma > 0$, then $E_\sigma(\mathcal{C})$ has no double junction and*

$$\#\mathcal{J}(E_\sigma(\mathcal{C})) \leq \#\mathcal{J}(\mathcal{C}).$$

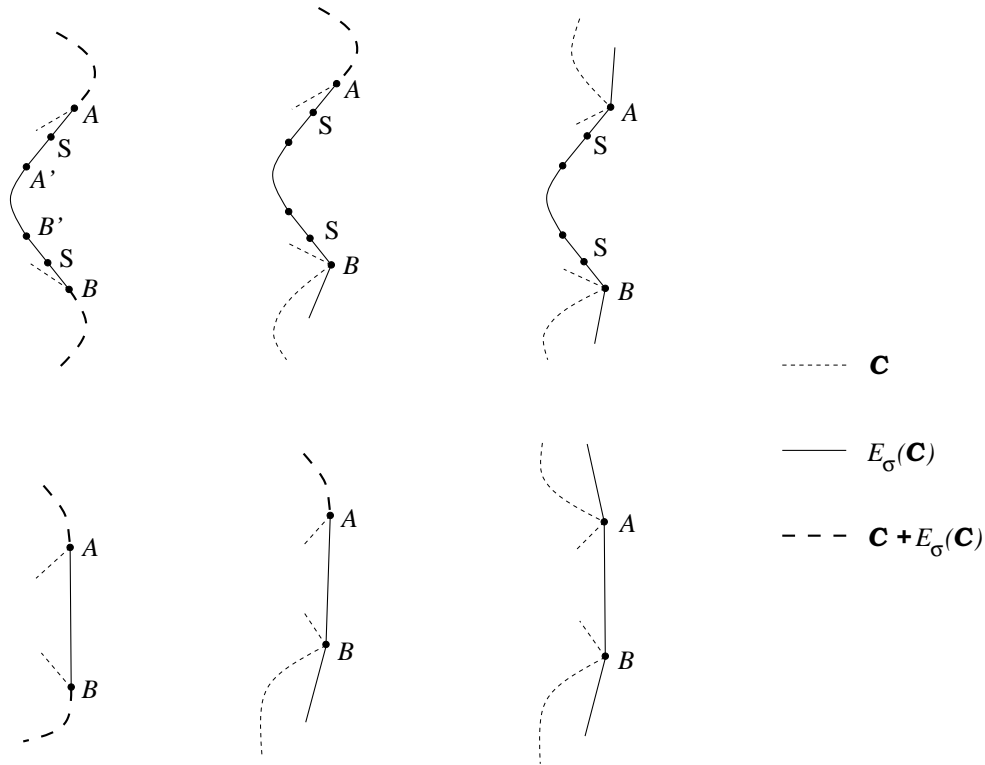


Figure 3.19: Simple junctions of $E_\sigma(\mathcal{C})$.

Proof :

1. Suppose that a component $D(J)$ of $E_\sigma(\mathcal{C})$ has a double junction $M = D(s)$. Since $D(I)$ is not locally convex near M , necessarily M belongs to $\mathcal{C} = C(I)$ and \mathcal{C} is locally concave near M . Hence, near M , $\mathcal{C} \cap D(J) = \{M\}$. This means that $D(]s - \varepsilon, s])$ and $D(]t, t + \varepsilon])$ are segments for $\varepsilon > 0$ small enough. Thus, M cannot be a double junction of $D(J)$, which is a contradiction. We deduce that $E_\sigma(\mathcal{C})$ has no double junction as soon as $\sigma > 0$.

2. We prove that

$$\#\mathcal{J}(E_\sigma(\mathcal{C})) \leq \#\mathcal{J}(\mathcal{C}).$$

2.a. Let us consider \mathcal{D}_j a maximum convex piece of $E_\sigma(\mathcal{C})$, i.e. such that $E_\sigma(\mathcal{C})$ is not locally convex at the extremal points A and B of \mathcal{D}_j . From Lemma 4 we know that A and B must belong to \mathcal{C} .

If $\mathcal{D}_j \subset \mathcal{C}$, it is a segment and neither \mathcal{C} nor $E_\sigma(\mathcal{C})$ can have any junction on $\overline{\mathcal{D}_j}$. If $\mathcal{D}_j \not\subset \mathcal{C}$ but \mathcal{D}_j is a segment, then $E_\sigma(\mathcal{C})$ has no junction between A and B (see Figure 3.19). Last, if \mathcal{D}_j is not a segment, then $E_\sigma(\mathcal{C})$ has exactly two simple junctions between A and B (see Figure 3.19). But since the piece of \mathcal{C} between A and B cannot be concave (it has a nonzero positive chord), the number of junctions of \mathcal{C} between A and B included is at least 2 (with the convention that a double junction in A (or in B) is counted once for each of the two \mathcal{D}_j it belongs to). Hence, in all cases, between A and B (included), $E_\sigma(\mathcal{C})$ has not more junctions than \mathcal{C} .

2.b. We claim that $E_\sigma(\mathcal{C})$ cannot have any junction outside a piece of curve $\overline{\mathcal{D}_j}$ of the previous kind. The reason is that on these remaining parts, $E_\sigma(\mathcal{C})$ is strictly concave (i.e. nowhere locally convex), so that any junction between these remaining parts should be a double junction, which is impossible according to Step 1. Hence, we have

$$\#\mathcal{J}(E_\sigma(\mathcal{C})) \leq \#\mathcal{J}(\mathcal{C})$$

as announced. □

3.4.3 Consistency

Theorem 3 *If \mathcal{C} is a piecewise convex semi-closed curve of class piecewise C^n , then $E_\sigma(\mathcal{C})$ is a collection of piecewise convex semi-closed curves of class piecewise C^n . If $n \geq 2$, each point M of \mathcal{C} can be associated to a point M_σ of $E_\sigma(\mathcal{C})$ such that*

$$M_\sigma = M + \omega \cdot \sigma^{\frac{2}{3}} \cdot (\gamma^+)^{\frac{1}{3}} \mathbf{N} + o(\sigma^{\frac{2}{3}}),$$

where γ and \mathbf{N} are respectively the curvature of \mathcal{C} and the normal vector¹ to \mathcal{C} at point M . As usual, we set $\omega = \frac{1}{2} \left(\frac{3}{2}\right)^{\frac{2}{3}}$ and $\gamma^+ = \max(0, \gamma)$.

Proof :

1. From Proposition 10, we know that $E_\sigma(\mathcal{C})$ is made of a finite number of curves of three kinds : pieces of \mathcal{C} , which are C^n , segments, which are C^∞ , and new convex pieces, which can be proved to be C^n using the arguments of Theorem 2. Hence, $E_\sigma(\mathcal{C})$ is piecewise C^n .

2. Consider M a point of \mathcal{C} , and call γ the curvature of \mathcal{C} in M .

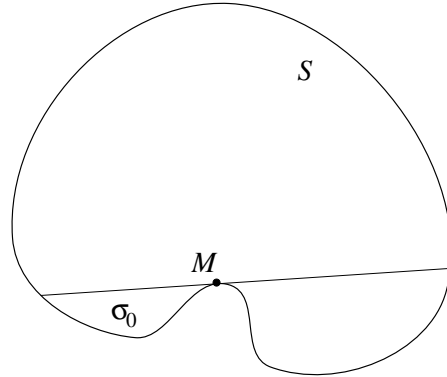


Figure 3.20: Case $\gamma < 0$

2.a. If $\gamma < 0$, call \mathbf{T} the tangent to \mathcal{C} in M , and let σ_0 be the nonzero area of the C-set delimited by a segment of the kind $]M - a\mathbf{T}, M + b\mathbf{T}[$, where both a and b are positive. Any

¹If $\gamma = 0$, \mathbf{N} is not uniquely defined but any choice is convenient since $(\gamma^+)^{\frac{1}{3}} \mathbf{N} = \mathbf{0}$.

chord-set of \mathcal{C} containing M contains the previous chord set (see Figure 3.20), and consequently its area must be larger than σ_0 . In other words, for any $\sigma < \sigma_0$, M belongs to $E_\sigma(\mathcal{C})$ and taking $M_\sigma = M$ closes the case.

2.b. If $\gamma > 0$, call \mathcal{C}_i the largest convex component of \mathcal{C} containing M . For σ small enough, any σ -chord set of \mathcal{C} containing M is defined by two points of \mathcal{C}_i , so that the “evolution” of M is given by Theorem 2 and the proof is complete.

2.c. If $\gamma = 0$, the geometric argument used in the proof of Theorem 2 still applies. □

3.4.4 Other possible definitions of the affine erosion

The affine erosion of a convex set S is obtained in a simple way, by removing from S any part of S with area σ of the kind $H \cap S$, where H is a half plane. This may be the simplest way to obtain a global affine invariant set-shortening process tangent to the affine scale space. Now, if one wants to generalize this definition to non-convex sets, one must be careful, and the natural generalization (removing from S any connected component of $H \cap S$ with area σ) is not that good : this definition does not ensure a very important property, the global inclusion principle (see Figure 3.21), which states that $E_\sigma(S_1) \subset E_\sigma(S_2)$ when $S_1 \subset S_2$. This principle has strong consequences for the iterated operator, and guarantees numerical stability.

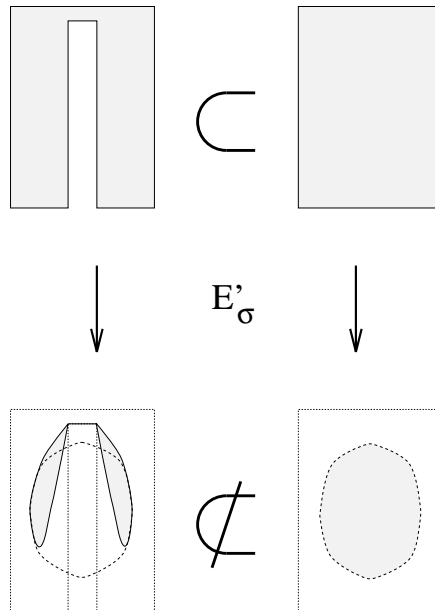


Figure 3.21: Inclusion principle is lost for the alternative definition of the affine erosion

With our definition of the affine erosion, the global inclusion principle is satisfied, but the connectedness is not preserved (whereas it is preserved for the former definition). Notice, however, that these two definitions yield the same infinitesimal evolution (for scales small enough).

Chapter 4

Comparison between affine erosion and scale space

In this chapter, we compute exactly the affine erosion and the affine scale space of conics. We show that for these curves the affine erosion remains a good approximation of its tangent operator not only for infinitesimal areas : this suggests that we can build a fast scheme for the affine scale space by iterating the affine erosion with rather large scale steps.

4.1 Affine scale space of curves

From now on, we note $t \mapsto ASS_t(\mathcal{C})$ the affine scale space of a curve \mathcal{C} , when it exists. In other words, if we can find a function $(s, t) \mapsto C(s, t)$ such that $s \mapsto C(s, 0)$ is a parameterization of \mathcal{C} , we say that $s \mapsto C(s, t)$ is a parameterization of $ASS_t(\mathcal{C})$ if we have for all s and $t \geq 0$,

$$\frac{\partial C}{\partial t}(s, t) = \gamma(s, t)^{\frac{1}{3}} \mathbf{N}(s, t), \quad (4.1)$$

where $\gamma(s, t)$ and $\mathbf{N}(s, t)$ represent the curvature and the unit normal vector of the curve $C(\cdot, t)$ at point $C(s, t)$. As before, we take the convention that if r is a negative number, $r^{1/3} = -|r|^{1/3}$. At an inflexion point, \mathbf{N} is not defined but since we have $\gamma = 0$, the right hand term of Equation 4.1 is naturally equal to zero. Notice that Equation 4.1 assumes that C is derivable with respect to t and twice derivable with respect to s .

If the curves $(ASS_t(\mathcal{C}))_{t>0}$ can be represented by functions of the kind $x \mapsto (x, y(x, t))$ in an orthonormal basis, then Equation 4.1 is equivalent to

$$\frac{\partial y}{\partial t} = \left(\frac{\partial^2 y}{\partial x^2} \right)^{\frac{1}{3}}. \quad (4.2)$$

Indeed, let us denote by y' and y'' the first and second order derivatives of y with respect to x . For such a Cartesian parameterization we have

$$\gamma(x, t) = \frac{y''}{(1 + y'^2)^{\frac{3}{2}}},$$

and in the associated orthonormal basis, the unit tangent and normal vectors to the curve are respectively

$$\mathbf{T}(x, t) = \frac{1}{\sqrt{1+y'^2}} (1, y')$$

and

$$\mathbf{N}(x, t) = \frac{1}{\sqrt{1+y'^2}} (-y', 1).$$

Thus, we have in the same basis,

$$(0, 1) = \frac{1}{\sqrt{1+y'^2}} (\mathbf{N} + y' \mathbf{T}),$$

so that Equation 4.2 is equivalent to

$$\frac{\partial C}{\partial t} = (y'')^{\frac{1}{3}} \cdot (0, 1) = \gamma^{\frac{1}{3}} \mathbf{N} + \frac{y''^{1/3} y'}{\sqrt{1+y'^2}} \mathbf{T}. \quad (4.3)$$

It has been proven (see [68],[29]) that the tangential component is of no influence on the whole curve evolution since it corresponds to a renormalization of the space parameter s (i.e. a movement of each point $C(s, t)$ along the curve $C(\cdot, t)$). Therefore, Equation 4.3 is equivalent to Equation 4.1.

Theorem 2 states that for regular convex curves the operator $E_{h^{3/2}}$ is tangent to the the operator $ASS_{\omega, h}$ when $h \rightarrow 0$, provided we set

$$\omega = \frac{1}{2} \left(\frac{3}{2} \right)^{\frac{2}{3}}.$$

In this chapter, we compute explicitly the affine scale space and the affine erosion for several convex curves, and we check that these operators are very close for small scales. In fact, for conics (ellipses, hyperbolae, parabolae, and “corners” as degenerated hyperbolae), both the affine erosion and the affine scale space can be exactly computed.

4.2 Affine erosion and scale space of an ellipse

4.2.1 Affine erosion

Proposition 12 *The σ -affine erosion of an ellipse with area A_0 is an ellipse with same axes and excentricity and with area*

$$A(\sigma) = A_0 \cos^2 \frac{\theta(\sigma)}{2},$$

where $\theta(\sigma)$ is defined by

$$\theta(\sigma) - \sin \theta(\sigma) = \frac{2\pi\sigma}{A_0}.$$

In particular, for an infinitesimal erosion, we have the following canonical expansion

$$A^{\frac{2}{3}}(t^{\frac{3}{2}}) = A_0^{\frac{2}{3}} - \sqrt[3]{\frac{2\pi^2}{3}} \cdot t + O(t^2). \quad (4.4)$$

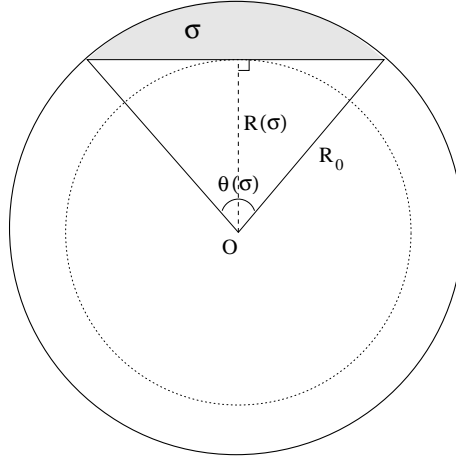


Figure 4.1: Affine erosion of a circle

Proof :

1. Consider the parameterization of the ellipse

$$M(t) = \sqrt{\frac{A_0}{\pi}} (\cos t \mathbf{v}_1 + \sin t \mathbf{v}_2)$$

satisfying $[\mathbf{v}_1, \mathbf{v}_2] = 1$. We can find a linear map ϕ with determinant 1 which transforms the affine basis $(\mathbf{v}_1, \mathbf{v}_2)$ into an orthogonal basis, in which $\phi(M(t))$ describes a circle enclosing the same area A_0 . Then, because the affine erosion commutes with the rotations, the affine erosion of a circle with radius R_0 cannot be anything but a circle with same center and with radius $R(\sigma) < R_0$. On Figure 4.1 we can see that

$$\begin{aligned} R(\sigma) &= R_0 \cos \frac{\theta(\sigma)}{2} \\ \text{and } \sigma &= R_0^2 \left(\frac{\theta}{2} - \frac{\sin \theta}{2} \right). \end{aligned}$$

Hence, as ϕ commutes with the affine erosion and with the homothetic transformations, we deduce that on the ellipse as well as on the circle, the affine erosion acts as a homothetic transformation with ratio $\cos \frac{\theta(\sigma)}{2}$, which proves the first result of Proposition 12.

2. Let us evaluate now $A(\sigma) = A_0 \cos^2 \frac{\theta(\sigma)}{2}$ when σ tends towards 0. From

$$\theta - \sin \theta = \frac{2\pi\sigma}{A_0}$$

we see that $\theta(\sigma) \rightarrow 0$ as $\sigma \rightarrow 0$, and

$$\frac{\theta^3(\sigma)}{6} (1 + O(\theta^2(\sigma))) = \frac{2\pi\sigma}{A_0},$$

which gives $\theta(\sigma) = O(\sigma^{\frac{1}{3}})$ and

$$\theta(\sigma) = \left(\frac{12\pi\sigma}{A_0} \right)^{\frac{1}{3}} + O(\sigma).$$

In this way, we obtain

$$A(\sigma) = A_0 \left(1 - \sin^2 \frac{\theta(\sigma)}{2} \right) = A_0 - \frac{A_0}{4} \left(\frac{12\pi\sigma}{A_0} \right)^{\frac{2}{3}} + O(\sigma^{\frac{4}{3}}) = A_0 - A_0^{\frac{1}{3}} \left(\frac{3\pi\sigma}{2} \right)^{\frac{2}{3}} + O(\sigma^{\frac{4}{3}}).$$

The “canonical” expansion of $A(\sigma)$ is

$$A^{\frac{2}{3}}(t^{\frac{3}{2}}) = A_0^{\frac{2}{3}} - \omega \cdot t + O(t^2),$$

with

$$\omega = \frac{2}{3} \left(\frac{3\pi}{2} \right)^{\frac{2}{3}} = 3\sqrt{\frac{2\pi^2}{3}}.$$

We remark incidentally that as σ goes near its critical value $\sigma_e = \frac{A_0}{2}$ corresponding to the ellipse extinction, we have

$$\theta(\sigma_e + h) = \pi - \frac{2\pi}{A_0}h + o(h)$$

and consequently

$$\cos \frac{\theta(\sigma_e + h)}{2} = -\frac{\pi}{4} \cdot \frac{2h}{A_0} + o(h).$$

It follows that the ratio $\sqrt{\frac{A(\sigma)}{A_0}} = \cos \frac{\theta(\sigma)}{2}$ admits a linear expansion near its extinction value.

Figure 4.2 shows the value of the normalized area $\frac{A}{A_0}$ and the ratio $\sqrt{\frac{A}{A_0}}$ depending on the normalized erosion parameter $\frac{\sigma}{\sigma_e}$.

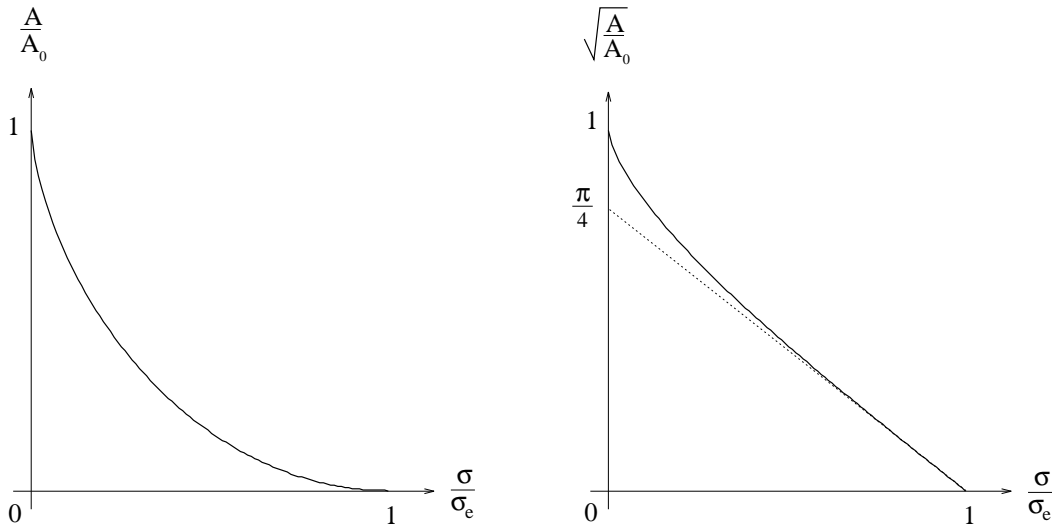


Figure 4.2: Area for the affine erosion of an ellipse

4.2.2 Affine scale space

Proposition 13 *The affine scale space at scale t of an ellipse with area A_0 is an ellipse with same axes and excentricity, whose area $A(t)$ satisfies*

$$A^{\frac{2}{3}}(t) = A_0^{\frac{2}{3}} - \frac{4}{3}\pi^{\frac{2}{3}} t. \quad (4.5)$$

Proof :

As for the affine erosion, the affine invariance of the affine scale space reduces the problem to the computation of the affine scale space of a circle. Because of the rotation invariance, the ASS of a circle is a family of circles $(\mathcal{C}_t)_{t>0}$ with same center O and radius $R(t)$. A trigonometric parameterization of the circles \mathcal{C}_t satisfies Equation 4.1 as soon as we have for any $t \geq 0$,

$$R'(t) = - \left(\frac{1}{R} \right)^{\frac{1}{3}} .$$

The solution of this ordinary differential equation is given by

$$R^{\frac{4}{3}}(t) = R^{\frac{4}{3}}(0) - \frac{4}{3}t,$$

and Equation 4.5 simply arises from the equality $A(t) = \pi R^2(t)$. \square

If we compare Equations 4.5 and 4.4, we can check that the operator $ASS_{\omega,h}$ is tangent to $E_{h^{3/2}}$, simply because

$$\frac{4}{3}\pi^{\frac{2}{3}} \cdot \omega = \sqrt[3]{\frac{2\pi^2}{3}}.$$

This property is illustrated on Figure 4.3. The normalized area $(A(\cdot)/A_0)^{\frac{2}{3}}$ is represented both for the affine erosion E_σ and for the normalized affine scale space ASS_t (with $t = \omega \cdot \sigma^{\frac{2}{3}}$ for the reason we explained before).

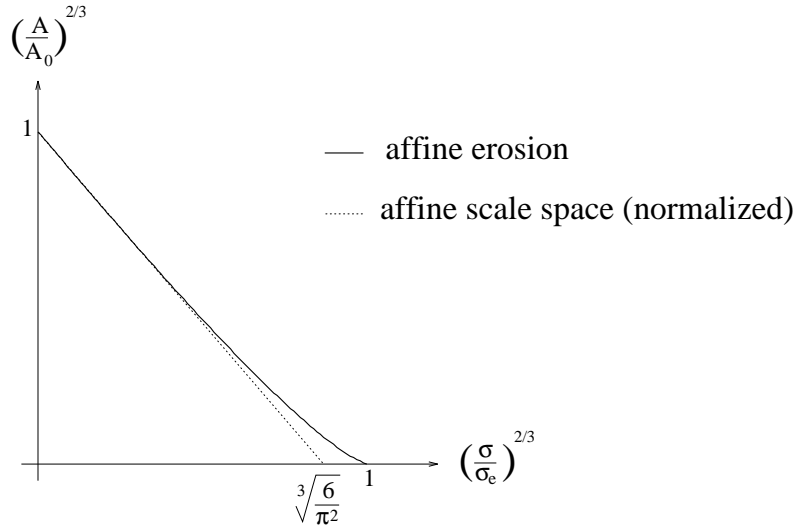


Figure 4.3: Comparison between the affine erosion and scale space of an ellipse

As we can see, the action of the affine erosion on ellipses is very close to the one of its tangent operator, the ASS, even for large scales. This suggests that we can build a fast scheme for the ASS by iterating the affine erosion with rather large scale steps.

4.3 Affine erosion and scale space of a hyperbola

4.3.1 Affine erosion

Proposition 14 *The σ -affine erosion of a hyperbola with apparent area A_0 is a hyperbola with same axes and with apparent area*

$$A(\sigma) = A_0 \operatorname{ch}^2 \frac{\theta(\sigma)}{2}, \quad (4.6)$$

where $\theta(\sigma)$ is defined by

$$\theta(\sigma) - \operatorname{sh} \theta(\sigma) = \frac{2\sigma}{A_0}.$$

In particular, for an infinitesimal erosion, we have the canonical expansion

$$A^{\frac{2}{3}}(t^{\frac{3}{2}}) = A^{\frac{2}{3}}(0) + \sqrt[3]{\frac{2}{3}} \cdot t + O(t^2).$$

Proof :

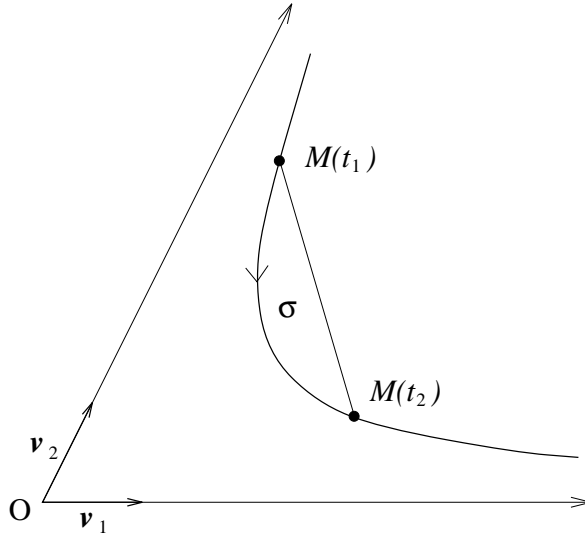


Figure 4.4: Affine erosion of a hyperbola

Let $(O, \mathbf{v}_1, \mathbf{v}_2)$ be an affine basis with same axes as the hyperbola \mathcal{C} . In this basis, a parametric equation of \mathcal{C} is given by

$$M(t) = (X(t), Y(t)) = a(e^t, e^{-t}), \quad \text{with } a^2 = \frac{A_0}{2[\mathbf{v}_1, \mathbf{v}_2]}.$$

Let us now consider two points $M(t_1)$ and $M(t_2)$ of \mathcal{C} with $t_1 = t - \frac{\theta}{2}$ and $t_2 = t + \frac{\theta}{2}$ (see Figure 4.4). In order that the chord set (t_1, t_2) of \mathcal{C} has area σ , we should have

$$\frac{\sigma}{[\mathbf{v}_1, \mathbf{v}_2]} = \frac{1}{2} \int_{t_1}^{t_2} [M'(t), M(t)] dt + \frac{1}{2} [M(t_1) - M(t_2), M(t_2)]$$

$$\begin{aligned}
&= \frac{1}{2} \int_{t_1}^{t_2} Y \frac{dX}{dt} - X \frac{dY}{dt} dt + \frac{1}{2} (X(t_1)Y(t_2) - Y(t_1)X(t_2)) \\
&= \frac{a^2}{2} \int_{t_1}^{t_2} e^{-t} e^t + e^t e^{-t} dt + \frac{a^2}{2} (e^{-\theta} - e^\theta) \\
&= a^2(\theta - \operatorname{sh} \theta).
\end{aligned}$$

Since $\sigma_r(\mathcal{C}) = +\infty$, Theorem 1 ensures that the affine erosion of \mathcal{C} is the set of the middle points of such σ -chord segments, i.e.

$$P(t) = \frac{a}{2} \cdot \left(e^{t-\frac{\theta}{2}} + e^{t+\frac{\theta}{2}}, e^{-t+\frac{\theta}{2}} + e^{-t-\frac{\theta}{2}} \right) = a \operatorname{ch} \frac{\theta}{2} \cdot (e^t, e^{-t}).$$

As θ does not depend on t , this proves that the affine erosion acts on \mathcal{C} as a homothetic transformation with center O and ratio $\operatorname{ch} \frac{\theta}{2}$, and

$$\theta - \operatorname{sh} \theta = \frac{\sigma}{a^2 [\mathbf{v}_1, \mathbf{v}_2]} = \frac{2\sigma}{A_0}.$$

As regards the canonical expansion of $A(t)$ near $t = 0$, the computation is the same as for the ellipse, except that the constant π disappears, so that the coefficient $\sqrt[3]{\frac{2\pi^2}{3}}$ becomes $\sqrt[3]{\frac{2}{3}}$. \square

Remark : One can be surprised that θ does not depend on t . It can be simply explained by the fact that the parametric representation of the hyperbola we used is, up to a multiplicative factor, the affine abscissa representation, and since the affine curvature of a hyperbola is constant, the area of a σ -chord set $(t, t+x)$ only depends on x .

Let us now evaluate $A(\sigma)$ when σ tends to infinity. We have

$$\frac{e^{\theta(\sigma)}}{2} + O(e^{-\theta(\sigma)}) = \frac{2\sigma}{A_0},$$

which gives

$$e^{\theta(\sigma)} = \frac{4\sigma}{A_0} + O\left(\frac{1}{\sigma}\right).$$

Replacing this expression in Equation 4.6 yields

$$\begin{aligned}
A(\sigma) &= \frac{A_0}{4} \left(e^{\theta(\sigma)} + 2 + O(e^{-\theta(\sigma)}) \right) \\
&= \sigma + \frac{A_0}{2} + O\left(\frac{1}{\sigma}\right).
\end{aligned}$$

Hence, $A(\sigma)$ admits an asymptotic linear expansion at infinity. Figure 4.5 represents the normalized apparent area $\frac{A}{A_0}$ depending on the normalized erosion parameter $\frac{\sigma}{A_0}$, for the affine erosion of a hyperbola.

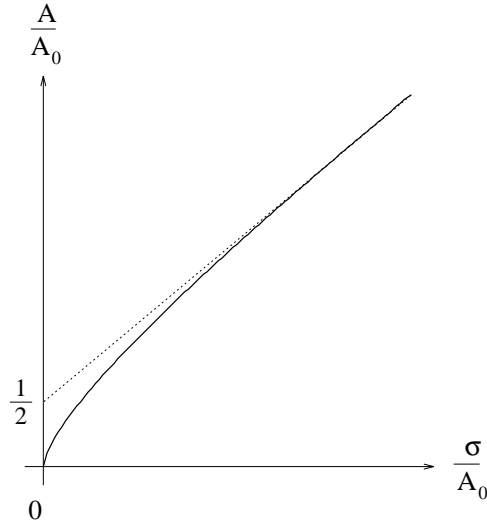


Figure 4.5: Area evolution for the affine erosion of a hyperbola

4.3.2 Affine scale space

The affine scale space of a hyperbola has been computed by Alvarez and Morales in [5]. Here we use a different parameterization.

Proposition 15 *The affine scale space at scale t of a hyperbola with apparent area A_0 is a hyperbola with same axes and whose apparent area satisfies*

$$A^{\frac{2}{3}}(t) = A_0^{\frac{2}{3}} + \frac{4}{3}t. \quad (4.7)$$

Proof :

Let H_0 be a hyperbola with apparent area A_0 and $\mathcal{R} = (O, \mathbf{v}_1, \mathbf{v}_2)$ an orthonormal basis of the plane, we can find an affine map with determinant 1 which transforms the axes of H_0 into (O, \mathbf{v}_1) and (O, \mathbf{v}_2) , so that $\tilde{H}_0 = \phi(H_0)$ can be represented in \mathcal{R} by the function

$$y(x) = \frac{A_0}{2x}.$$

Now, let us consider a family of hyperbolae $\tilde{H}_t = M(\cdot, t)$ of apparent area $A(t) > 0$ defined by

$$y(x, t) = \frac{A(t)}{2x}.$$

On one hand,

$$\frac{\partial y}{\partial t} = \frac{A'(t)}{2x},$$

and on the other hand,

$$\left(\frac{\partial^2 y}{\partial x^2} \right)^{\frac{1}{3}} = \frac{A^{\frac{1}{3}}(t)}{x}.$$

Consequently, the family \tilde{H}_t is the scale space of \tilde{H}_0 as soon as Equation 4.2 is satisfied, i.e. as soon as $A(t)$ is solution of the differential equation

$$A'(t) = 2A^{\frac{1}{3}}(t).$$

Solving this equation yields

$$A^{\frac{2}{3}}(t) = A_0^{\frac{2}{3}} + \frac{4}{3}t. \quad (4.8)$$

Hence, the scale space of H_0 , given by $\phi^{-1}(\tilde{H}_t)$, is the one announced in Proposition 15, and since the apparent area is invariant under ϕ^{-1} , Equation 4.8 remains true. \square

Figure 4.6 represents the compared apparent areas obtained on a hyperbola with the affine erosion E_σ and with the normalized affine scale space ASS_t ($t = \omega\sigma^{\frac{2}{3}}$). As for ellipses, notice how close the affine scale space and the affine erosion behave.

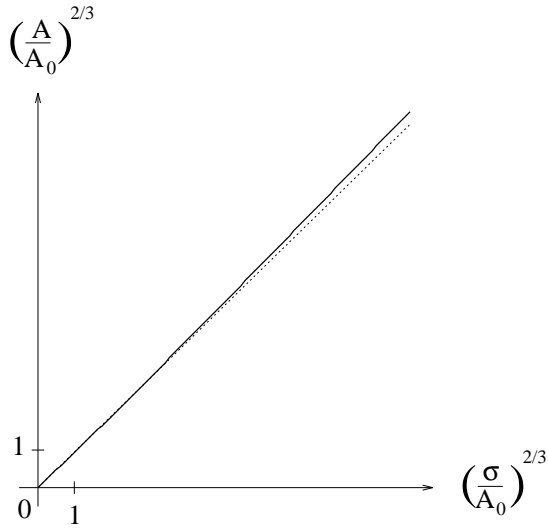


Figure 4.6: Canonical area evolution for the affine erosion of a hyperbola

4.4 Affine erosion and scale space of a parabola

Proposition 16 *The σ -affine erosion of the parabola of equation $y = px^2$ in an orthonormal basis is the translated parabola of equation*

$$y = px^2 + p^{\frac{1}{3}}\sigma^{\frac{2}{3}}\left(\frac{3}{4}\right)^{\frac{2}{3}} \quad (4.9)$$

in the same basis. In particular, $E_{h^{3/2}}$ acts as a semi-group operator upon the family of parabolae $P_\lambda : y = px^2 + \lambda$ since

$$E_{(h_1)^{3/2}} \circ E_{(h_2)^{3/2}}(P_\lambda) = E_{(h_1+h_2)^{3/2}}(P_\lambda).$$

A consequence is the exact equality

$$ASS_{\omega \cdot h}(P_\lambda) = E_{h^{3/2}}(P_\lambda),$$

where as usual

$$\omega = \frac{1}{2} \left(\frac{3}{2} \right)^{\frac{2}{3}}.$$

Proof :

Since a parabola is a semi-closed convex curve with $\sigma_r = +\infty$, we know from Theorem 1 that its σ -affine erosion is given by the set of the middle points of its σ -chord segments. Consider a σ -chord $(x - \delta, x + \delta)$ of the parabola $y = px^2$, the resulting middle point is $(x, y_\sigma(x))$ where

$$y_\sigma(x) = p \frac{(x - \delta)^2 + (x + \delta)^2}{2} = p(x^2 + \delta^2).$$

Besides, a simple computation yields

$$\begin{aligned} \sigma &= \delta p [(x - \delta)^2 + (x + \delta)^2] - \int_{x-\delta}^{x+\delta} ps^2 ds \\ &= 2\delta p(x^2 + \delta^2) - \frac{p}{3} [(x + \delta)^3 - (x - \delta)^3] \\ &= \frac{4}{3} \delta^3, \end{aligned}$$

and finally,

$$y_\sigma(x) = px^2 + p \left(\frac{3\sigma}{4} \right)^{\frac{2}{3}} = px^2 + p^{\frac{1}{3}} \sigma^{\frac{2}{3}} \left(\frac{3}{4} \right)^{\frac{2}{3}}.$$

Consequently, $E_{h^{3/2}}(P_\lambda) = P_{\lambda+\alpha h}$ where $\alpha = p^{\frac{1}{3}} \left(\frac{3}{4} \right)^{\frac{2}{3}}$, which establishes the announced semi-group property. But since $ASS_{\omega \cdot h}$ is the tangent operator to $E_{h^{3/2}}$, we have (as we shall prove later)

$$ASS_{\omega \cdot h}(P_\lambda) = \lim_{n \rightarrow \infty} \left[E_{(h/n)^{3/2}} \right]^n (P_\lambda) = E_{h^{3/2}}(P_\lambda).$$

We can also check this result directly by using Equation 4.2. Taking the second order derivative with respect to x in Equation 4.9 yields

$$\frac{\partial^2 y}{\partial x^2} = 2p,$$

so that $x \mapsto y(x, t)$ represents the affine scale space of P_0 as soon as

$$\frac{\partial y}{\partial t} = (2p)^{\frac{1}{3}}.$$

Consequently, $ASS_{\omega \cdot h}(P_0)$ is the curve given by

$$y(x, t) = px^2 + (2p)^{\frac{1}{3}} \cdot \omega h = px^2 + p^{\frac{1}{3}} h \left(\frac{3}{4} \right)^{\frac{2}{3}}.$$

□

4.5 Affine erosion of a triangle

The complete description of the affine erosion of a polygon will be given further. Here we just deal with the simplest case, namely the triangle. This case is interesting because all triangles are equivalents in Affine Geometry. One may refer to Chapter 6 (numerical scheme) for the precise description on the affine erosion of a general polygon.

Proposition 17 *The affine erosion of a triangle is a “hyperbolic triangle”, i.e. the concatenation of three hyperbola pieces, each one given in barycentric coordinates by the equation*

$$(e^t, e^{-t}, \frac{2}{\sqrt{\sigma}} - e^t - e^{-t}), \quad |t| \leq \ln \left(\frac{1}{\sqrt{\sigma}} - \sqrt{\frac{1}{\sigma} - 2} \right)$$

In particular, the extinction scale of a unit area triangle is

$$\sigma_e = \frac{4}{9} = 0,444\dots$$

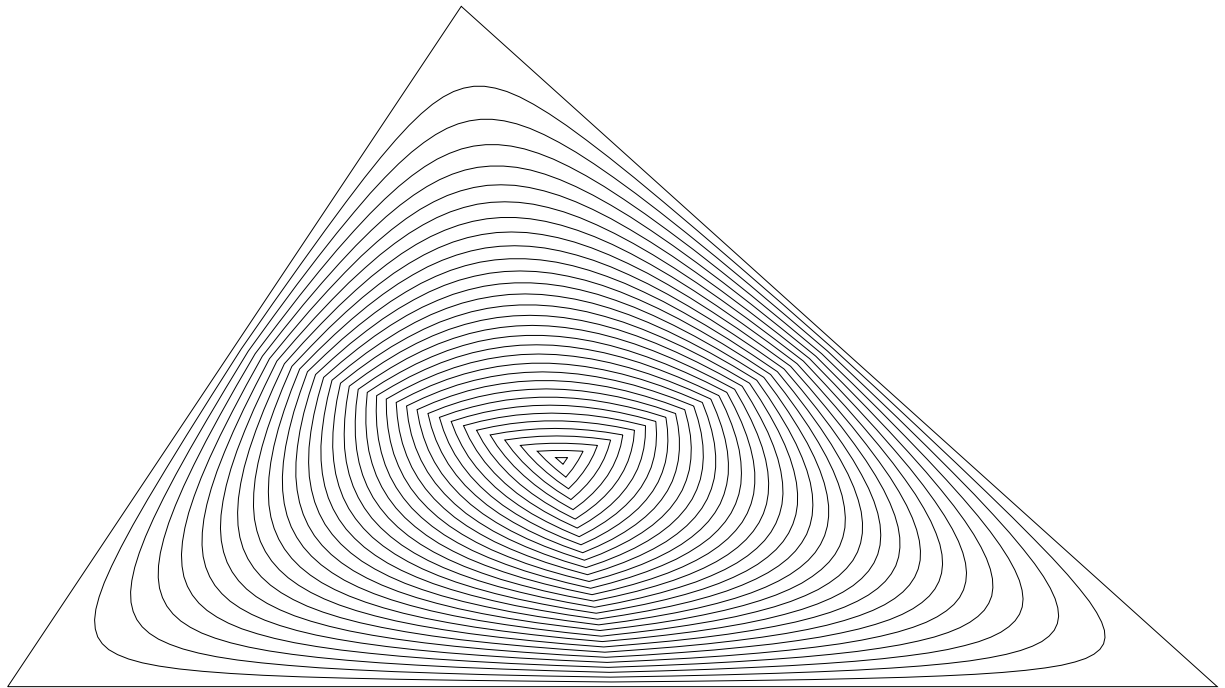


Figure 4.7: Affine erosions of a triangle for different scales

Notice that this is NOT the scale space spanned by the iteration of the affine erosion ! Each curve represents the action of the affine erosion on the initial triangle, for different values of the erosion area.

Proof :

1. First, notice that we can find an affine map which transforms a given triangle into a unit area equilateral triangle. Thus, it is sufficient to establish the proof for such a triangle thanks to the affine invariance of the affine erosion (see Proposition 5). By symmetry, it is clear that the

extinction point of an equilateral triangle is its center. As a consequence, the extinction point of any triangle must be the barycenter of its vertices (notice that this property is false for other polygons in general). One can check easily that the chord set of minimum area which contains the barycenter of a unit area equilateral triangle has area $\frac{4}{9}$ (see Figure 4.8). Consequently, the extinction scale of any triangle is $\frac{4}{9}$ of its area.

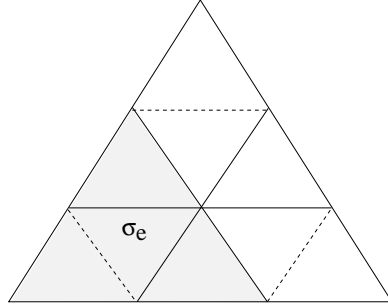


Figure 4.8: Extinction area of a triangle

2. Consider the σ -chords segments of the triangle whose endpoints lie on two fixed edges of the triangle. The middle points of these σ -chord segments span a piece of hyperbola, simply because the affine erosion of a “corner” is, as we saw previously in Proposition 1, a piece of hyperbola. Consequently, Proposition 8 ensures that the affine erosion of a triangle is the concatenation of three pieces of hyperbola (there are exactly three different pairs of edges for a triangle).

3. The previous hyperbolae can be described in barycentric coordinates by an equation of the kind

$$(e^t, e^{-t}, K(\sigma) - e^t - e^{-t}), \quad t_1 \leq t \leq t_2. \tag{4.10}$$

(we recall that (a, b, c) are barycentric coordinates of M in the affine basis (A, B, C) if and only if $(a + b + c) OM = a OA + b OB + c OC$ for any point O of the plane). Let us compute $K(\sigma)$. Remember that if $\mathbf{v}_1, \mathbf{v}_2, \mathbf{v}_3$ are three vectors of \mathbb{R}^2 , one has

$$[\mathbf{v}_1, \mathbf{v}_2] \mathbf{v}_3 + [\mathbf{v}_2, \mathbf{v}_3] \mathbf{v}_1 + [\mathbf{v}_3, \mathbf{v}_1] \mathbf{v}_2 = \mathbf{0}.$$

Applying this to MA, MB and MC where ABC is a triangle with unit area, we get

$$M = \frac{1}{2} [MA, MB] C + \frac{1}{2} [MB, MC] A + \frac{1}{2} [MC, MA] B.$$

In other words, a system of barycentric coordinates of M in the basis (A, B, C) is given by the areas of the triangles MBC, MCA and MAB . Now, if we make $t = 0$ in Equation 4.10, we obtain the point M of Figure 4.9, which, according to the previous remark, can be represented in the basis (A, B, C) by $(\frac{1-S}{2}, \frac{1-S}{2}, S)$. Moreover, one can see easily that $S = \frac{C'M}{CM}$ and $\sigma = \left(\frac{CM}{C'C'}\right)^2$. Now, identifying the previous coordinates (up to a multiplicative factor) with $(1, 1, K(\sigma) - 2)$, we get

$$\frac{1-S}{2}(K(\sigma) - 2) = S,$$

so that

$$K(\sigma) = \frac{2}{1-S} = \frac{2}{\sqrt{\sigma}}.$$

Now, a simple computation resulting from the permutation of the affine bases gives the bound value

$$|t| \leq \ln \left(\frac{1}{\sqrt{\sigma}} - \sqrt{\frac{1}{\sigma} - 2} \right).$$

Then, by solving the equation

$$\frac{1}{\sqrt{\sigma}} - \sqrt{\frac{1}{\sigma} - 2} = 1,$$

we find again the extinction scale $\sigma = \frac{4}{9}$. □

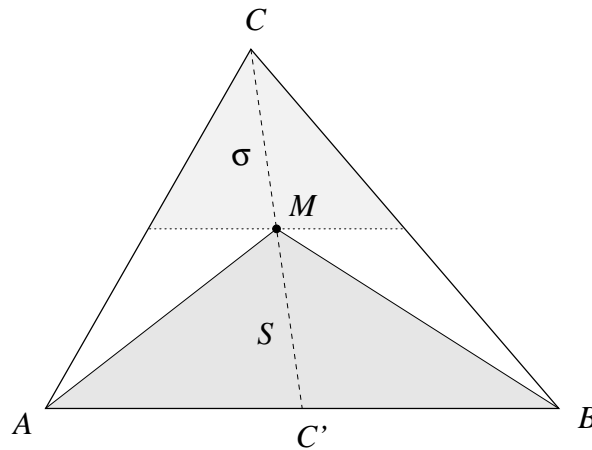


Figure 4.9: Computing $K(\sigma)$

Remark : As announced in the previous chapter, the triangle is an example of a simple convex C-set whose extinction area is less than half of its area.

As far as we know, the affine scale space of a triangle has not been computed exactly, and it is uncertain that there exists a simple analytic expression for it. However, we can observe that for the reasons previously explained, the affine invariance constrains the extinction point of a triangle to be its barycenter. Numerical simulations give for the normalized extinction area of the affine scale space of a triangle the value $\sigma'_e \simeq 0,42$ (it means that a unit area triangle and an ellipse of area $2\sigma'_e$ disappear simultaneously).

Chapter 5

Affine erosion of grey-level images

In this chapter, we first extend the affine erosion to any set of the plane and to lower semi-continuous grey level images. Then, we study its asymptotic behaviour and prove the convergence of the iterated affine erosion+dilation towards the affine morphological scale space. We also compare the affine erosion to classical affine inf-sup operators, and we establish the link with Matheron's Theorem (characterization of morphological operators).

5.1 Morphological principles

Suppose that we want to analyze an image u , given as a map $u : \mathbb{R}^2 \rightarrow \mathbb{R}$. The first question we should answer is : what relevant informations does contain u , physically speaking ? A important remark is that our interpretation of an image does not depend on its absolute contrast, but rather on the fact that some objects are brighter than others (we can check this each time we put on sunglasses). Hence, we should consider that a given image u (i.e. a map $u : \mathbb{R}^2 \rightarrow \mathbb{R}$) carries the same information as any image of the kind $g(u)$, where g is an arbitrary contrast change, that is to say an increasing and continuous scalar function. This point of view has been successfully adopted by Mathematical Morphology (in the case of flat grey-scale kernels) to design efficient operators for image analysis. Formally, we are led to consider equivalence classes of the relation

$$u \sim v \Leftrightarrow \exists g, v = g(u).$$

According to this equivalence, an image u reduces to the decreasing collection of its level sets¹

$$\chi_\lambda(u) = \{\mathbf{x} \in \mathbb{R}^2; u(\mathbf{x}) > \lambda\}.$$

Conversely, any image u can be recovered from the family of its level sets by the relation

$$u(\mathbf{x}) = \sup\{\lambda; \mathbf{x} \in U_\lambda\},$$

¹For our study, it is more convenient to consider the open level sets rather than the closed ones defined by

$$\chi_\lambda(u) = \{\mathbf{x} \in \mathbb{R}^2; u(\mathbf{x}) \geq \lambda\}.$$

and two images having the same collection of level sets are equivalent (see [41]).

From this point of view, it is natural to say that an operator T acting on images is a **morphological operator** if it satisfy the morphological invariance described in Chapter 2 :

[**Morphological Invariance**] : For any increasing continuous function g ,

$$T(g \circ u) = g \circ T(u).$$

Although this idea is directly inspired from Mathematical Morphology, we must mention that the previous definition of a morphological operator is different from what Serra calls a morphological filter². As well, the affine erosion we defined in Chapter 3 is not an erosion on a lattice in Serra's sense (see [70]). The reason is that the relation

$$E_\sigma(A \cap B) = E_\sigma(A) \cap E_\sigma(B)$$

is false in general (whereas it is true for the Euclidean erosion).

5.2 From sets to images

Let us consider an operator T acting on sets : we would like to define a corresponding operator \tilde{T} on an image u by applying T to the level sets of u . In other words, we ask the following question : is there an operator \tilde{T} which satisfies $\chi_\lambda(\tilde{T}(u)) = T(\chi_\lambda(u))$ for any λ and a certain class of images u ? Obviously, T must satisfy some hypotheses because the level sets of an image u satisfy the inclusion

$$\lambda \geq \mu \quad \Rightarrow \quad \chi_\lambda(u) \subset \chi_\mu(u)$$

and

$$\chi_{\lambda+\varepsilon}(u) \nearrow \chi_\lambda(u) \quad \text{as} \quad \varepsilon \searrow 0.$$

This last relation means that $\varepsilon \mapsto \chi_{\lambda+\varepsilon}(u)$ is nonincreasing and that

$$\forall \lambda, \quad \chi_\lambda(u) = \bigcup_{\varepsilon > 0} \chi_{\lambda+\varepsilon}(u);$$

it is equivalent to say that

$$\forall \mathbf{x}, \quad u(\mathbf{x}) = \sup\{\lambda; \mathbf{x} \in \chi_\lambda(u)\}. \quad (5.1)$$

From now on, \mathcal{O} denotes the set of the open sets of \mathbb{R}^2 , and $LSC(\mathbb{R}^2)$ the set of the lower semi-continuous functions defined on \mathbb{R}^2 . We recall that $u : \mathbb{R}^2 \rightarrow \mathbb{R}$ is lower semi-continuous (l.s.c.) if and only if each level set of u is open.

Definition 13 *An operator T acting on sets is nondecreasing if*

$$\forall X, Y, \quad X \subset Y \quad \Rightarrow \quad T(X) \subset T(Y).$$

²in [70], an operator ψ is a morphological filter if it is both nondecreasing ($u \leq v \Rightarrow \psi(u) \leq \psi(v)$) and idempotent ($\psi \circ \psi = \psi$).

Definition 14 A nondecreasing operator $T : \mathcal{O} \mapsto \mathcal{O}$ is \nearrow -continuous if

$$\forall (X_n) \in \mathcal{O}^{\mathbb{N}}, \quad X_n \nearrow_n X \Rightarrow T(X_n) \nearrow_n T(X).$$

For a nondecreasing operator $T : \mathcal{O} \mapsto \mathcal{O}$, it is equivalent to say that T is \nearrow -continuous or that it is lower-semi-continuous for the so-called “hit and miss” topology³ (see [69]).

Proposition 18 If $T : \mathcal{O} \mapsto \mathcal{O}$ is a nondecreasing \nearrow -continuous operator, then the relation

$$\chi_\lambda(\tilde{T}(u)) = T(\chi_\lambda(u)) \tag{5.2}$$

defines a unique operator $\tilde{T} : LSC(\mathbb{R}^2) \rightarrow LSC(\mathbb{R}^2)$. Moreover, \tilde{T} is a nondecreasing, morphological and 1-Lipschitz operator.

Proof :

1. If \tilde{T} exists, then it is unique. The reason is that Equation 5.1 rewritten for $\tilde{T}(u)$ yields

$$\forall \mathbf{x}, \quad \tilde{T}(u)(\mathbf{x}) = \sup\{\lambda; \mathbf{x} \in \chi_\lambda(\tilde{T}(u))\},$$

and if \tilde{T} satisfies Equation 5.2, it is completely defined from T by

$$\tilde{T}(u)(\mathbf{x}) = \sup\{\lambda; \mathbf{x} \in T(\chi_\lambda(u))\}. \tag{5.3}$$

2. Let us now consider the operator defined by Equation 5.3, and prove that it satisfies Equation 5.2. On one hand,

$$\begin{aligned} \mathbf{x} \in \chi_\lambda(\tilde{T}(u)) &\Rightarrow \tilde{T}(u)(\mathbf{x}) > \lambda \\ &\Rightarrow \exists \lambda_0 > \lambda, \mathbf{x} \in T(\chi_{\lambda_0}(u)) \\ &\Rightarrow \mathbf{x} \in T(\chi_\lambda(u)), \end{aligned}$$

the last inference arising from the monotonicity of T , because

$$\lambda < \lambda_0 \Rightarrow \chi_{\lambda_0}(u) \subset \chi_\lambda(u) \Rightarrow T(\chi_{\lambda_0}(u)) \subset T(\chi_\lambda(u)).$$

On the other hand, remember that

$$\chi_{\lambda+\varepsilon}(u) \nearrow \chi_\lambda(u) \quad \text{as} \quad \varepsilon \searrow 0,$$

and since T is lower semi-continuous we have

$$T(\chi_{\lambda+\varepsilon}(u)) \nearrow T(\chi_\lambda(u)) \quad \text{as} \quad \varepsilon \searrow 0$$

³This topology on open sets of the plane is spanned by the sets

$$\mathcal{O}_{G_1, G_2, \dots, G_p}^K = \{O \in \mathcal{O}, K \subset O \text{ and } \forall i, G_i \not\subset O\},$$

where K is a compact set and each G_i is an open set.

and in particular

$$\bigcup_{\varepsilon > 0} T(\chi_{\lambda+\varepsilon}(u)) = T(\chi_{\lambda}(u)) = T\left(\bigcup_{\varepsilon > 0} \chi_{\lambda+\varepsilon}(u)\right).$$

Hence,

$$\begin{aligned} \mathbf{x} \in T(\chi_{\lambda}(u)) &\Rightarrow \mathbf{x} \in \bigcup_{\varepsilon > 0} T(\chi_{\lambda+\varepsilon}(u)) \\ &\Rightarrow \exists \varepsilon > 0, \mathbf{x} \in T(\chi_{\lambda+\varepsilon}(u)) \\ &\Rightarrow \exists \varepsilon > 0, \tilde{T}(u)(\mathbf{x}) \geq \lambda + \varepsilon \\ &\Rightarrow \tilde{T}(u)(\mathbf{x}) > \lambda \\ &\Rightarrow \mathbf{x} \in \chi_{\lambda}(\tilde{T}(u)). \end{aligned}$$

As a consequence, \tilde{T} defined in Equation 5.3 satisfies Equation 5.2.

3. Let us check the announced properties of \tilde{T} .

3.a. T is nondecreasing, and \tilde{T} inherits this property because of Equation 5.3. Indeed, if u_1 and u_2 are two l.s.c. images such that $u_1 \leq u_2$, then we have for any λ , $\chi_{\lambda}(u_1) \subset \chi_{\lambda}(u_2)$, and consequently $\tilde{T}(u_1) \leq \tilde{T}(u_2)$ because of Equation 5.3.

3.b. \tilde{T} is morphological because if g is a contrast change, i.e. an increasing continuous scalar function, we have

$$\chi_{\lambda}(u) = \chi_{g(\lambda)}(g(u)),$$

and Equation 5.3 ensures that

$$\tilde{T}(g(u)) = g(\tilde{T}(u)).$$

3.c. Let us prove that \tilde{T} is 1-Lipschitz. Let u and v be two l.s.c. images such that for any \mathbf{x} , $|u(\mathbf{x}) - v(\mathbf{x})| \leq k$. The monotonicity of \tilde{T} yields

$$\forall \mathbf{x}, \quad \tilde{T}(u - k)(\mathbf{x}) \leq \tilde{T}(v)(\mathbf{x}) \leq \tilde{T}(u + k)(\mathbf{x}),$$

and since $\tilde{T}(u + k) = \tilde{T}(u) + k$, we have for any \mathbf{x} ,

$$|\tilde{T}(u)(\mathbf{x}) - \tilde{T}(v)(\mathbf{x})| \leq k.$$

Hence, we proved that \tilde{T} is 1-Lipschitz, i.e.

$$\|\tilde{T}(u) - \tilde{T}(v)\|_{\infty} \leq \|u - v\|_{\infty}.$$

A consequence is that \tilde{T} restricted to L^{∞} is uniformly continuous. \square

5.3 Affine erosion of grey level images

We would like to extend the affine erosion to grey-level images through the morphological level set decomposition. For that purpose, we first need to define the affine erosion of any subset

of the plane (or, at least, of any open set). But the geometrical definition of the affine erosion (Definition 5) does not make sense for any subset of the plane, since in general its boundary is not a curve in a reasonable sense.

We could use the following result due to E. Giusti [38] : if u is of bounded variation, then its λ -level sets are Caccioppoli sets for almost any λ . This result could be of great interest for our purpose since up to a negligible set of points, the essential boundary of a Caccioppoli set is made of a countable number of closed curves, for we have

$$\|u\|_{BV} = \int \text{length}(\partial\chi_\lambda(u)) d\lambda.$$

We prefer, however, to define the affine erosion of an image in a more simple way, using the inclusion property.

Definition 15 *The σ -affine erosion of a set $U \subset \mathbb{R}^2$ is the set*

$$E_\sigma(U) = \bigcup_{S \text{ C-set}, S \subset U} E_\sigma(S).$$

This definition makes sense because if U is a C-set, we know that for any C-set S subset of U we have $E_\sigma(S) \subset E_\sigma(U)$. Moreover, the extended operator E_σ is clearly nondecreasing because if $U \subset V$, any C-set subset of U is also subset of V , that is

$$\{S \text{ C-set}; S \subset U\} \subset \{S \text{ C-set}; S \subset V\}$$

and consequently

$$\bigcup_{S \text{ C-set}, S \subset U} E_\sigma(S) \subset \bigcup_{S \text{ C-set}, S \subset V} E_\sigma(S).$$

Lemma 6 *For any set $U \subset \mathbb{R}^2$, $E_\sigma(U)$ is open.*

Proof :

By Corollary 1 we know that for any C-set S , $E_\sigma(S)$ is open, and consequently

$$E_\sigma(U) = \bigcup_{S \text{ C-set}, S \subset U} E_\sigma(S)$$

is open as a reunion of open sets. □

Lemma 7 *For any set $U \subset \mathbb{R}^2$, we have*

$$E_\sigma(U) = \bigcup_{S \text{ bounded C-set}, \overline{S} \subset U} E_\sigma(S).$$

Proof :

Since

$$E_\sigma(U) = \bigcup_{S \text{ C-set}, S \subset U} S,$$

we only need to prove Lemma 7 when U is a C-set.

1. We claim that there exists a nondecreasing sequence S_n of bounded C-sets such that $U = \bigcup_n S_n$ and $\overline{S_n} \subset U$ for all n . Let us define

$$A_{i,j}^n = \left[\frac{i}{2^n}, \frac{i+1}{2^n} \right] \times \left[\frac{j}{2^n}, \frac{j+1}{2^n} \right], \quad (i,j) \in \mathbf{Z}^2,$$

and consider K_n an increasing sequence of compact sets such that $\mathbb{R}^2 = \bigcup_n K_n$. The increasing sequence S_n , defined as the topological opening of the union of the $A_{i,j}^n$ for which $\overline{A_{i,j}^n} \subset U \cap K_n$, satisfies the previous constraints.

2. Let $M \in E_\sigma(U)$, and suppose that $M \notin \bigcup_n E_\sigma(S_n)$ (we are going to prove that this is not possible). If we define D_α as the line going through M and oriented by $\alpha \in S^1$, then for any n we can find $\alpha_n \in S^1$ and a σ_n -chord segment of S_n included in D_{α_n} (and with the same orientation), such that $\sigma_n \leq \sigma$. Now, up to a subsequence extraction, we can suppose that the sequence (α_n, σ_n) converges towards $(\tilde{\alpha}, \tilde{\sigma}) \in S^1 \times [0, \sigma]$.

Since $E_\sigma(U)$ is open and $M \in E_\sigma(U)$ we can find a closed disk $\overline{D}(M, \varepsilon)$ with center M and radius $\varepsilon > 0$ such that $\overline{D}(M, \varepsilon) \subset E_\sigma(U)$. Consider N the intersection between $\partial D(M, \varepsilon)$ and $D_{\tilde{\alpha}+\pi/2}$ (see Figure 5.1). The line going through N and oriented by $\tilde{\alpha}$ defines on U a bounded chord set K containing N , and for n large enough we have $D_{\alpha_n} \cap K = \emptyset$, so that $\sigma_n \geq \text{area}(K)$, and letting n tend to infinity yields $\text{area}(K) \leq \tilde{\sigma} \leq \sigma$, which is in contradiction with $N \in E_\sigma(U)$.

□

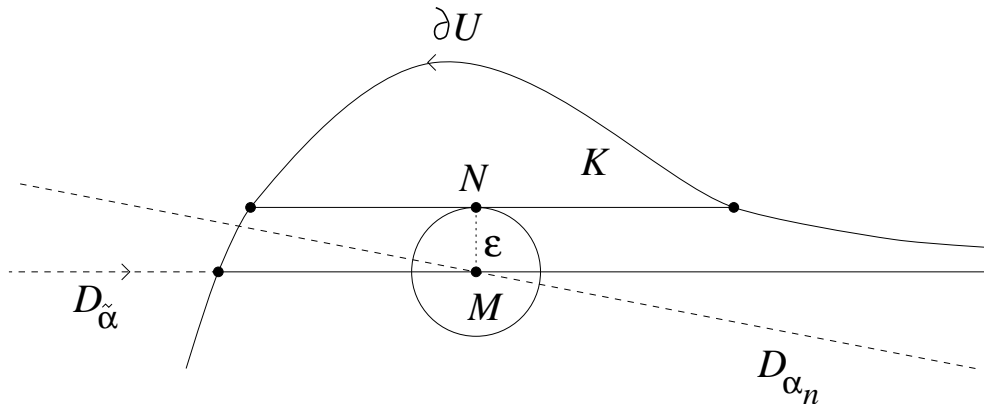


Figure 5.1: For n large enough, $D_{\alpha_n} \cap K = \emptyset$.

Proposition 19 *The restriction $E_\sigma : \mathcal{O} \rightarrow \mathcal{O}$ is \nearrow -continuous.*

Proof :

Since E_σ is nondecreasing, we have to prove that for any nondecreasing sequence (X_n) of open sets,

$$\bigcup_{n \in \mathbb{N}} E_\sigma(X_n) \supset E_\sigma\left(\bigcup_{n \in \mathbb{N}} X_n\right).$$

Let $X = \bigcup_n X_n$, consider a bounded C-set S such that $\overline{S} \subset \bigcup X_n$, and suppose that for any n we can find $x_n \in S \setminus X$. Since \overline{S} is compact, we can extract from (x_n) a subsequence which converges towards $x \in \overline{S}$. But for any n , $\overline{S} \setminus X_n$ is closed, and as $x_k \in \overline{S} \setminus X_n$ for any $k \geq n$, we have $x \in \overline{S} \setminus X_n$ for all n . This means $x \in \overline{S} \setminus X$, which is impossible, this set being empty since $\overline{S} \subset X$.

Consequently, there exists $n_0 \in \mathbb{N}$ such that $S \subset X_{n_0}$, which proves that

$$E_\sigma(S) \subset E_\sigma(X_{n_0}) \subset \bigcup_{n \in \mathbb{N}} E_\sigma(X_n).$$

The last inclusion being true for any bounded C-set S such that $\overline{S} \subset X$, we deduce from Lemma 7 that

$$E_\sigma(X) = \bigcup_{S \text{ bounded C-set, } \overline{S} \subset X} E_\sigma(S) \subset \bigcup_{n \in \mathbb{N}} E_\sigma(X_n).$$

□

Now, since $E_\sigma : \mathcal{O} \rightarrow \mathcal{O}$ is nondecreasing and \nearrow -continuous, we can define the affine erosion of a lower semi-continuous image according to Proposition 18.

Definition 16 *The σ -affine erosion of a l.s.c. image $u : \mathbb{R}^2 \rightarrow \mathbb{R}$ is the image*

$$E_\sigma(u) : \mathbf{x} \mapsto \sup\{\lambda \in \mathbb{R}; \mathbf{x} \in E_\sigma(\chi_\lambda(u))\},$$

where $\chi_\lambda(u) = \{\mathbf{x}; u(\mathbf{x}) > \lambda\}$ is the λ -level set of u .

Once again, we use the same notation for the affine erosion of an image, without risk of confusion.

Lemma 8 *$E_\sigma : LSC(\mathbb{R}^2) \rightarrow LSC(\mathbb{R}^2)$ is a nondecreasing, morphological, 1-Lipschitz and affine invariant operator.*

Proof :

The first three properties are a consequence of Proposition 18. As regards the affine invariance, we have to prove that for any affine map ϕ ,

$$E_{\sigma \cdot |\det \phi|}(u) \circ \phi = E_\sigma(u \circ \phi).$$

This is a consequence of Proposition 5, since $\chi_\lambda(u \circ \phi) = \phi(\chi_\lambda(u))$. □

Lemma 9 For any image u , $E_\sigma(u)$ is nonincreasing with respect to σ , i.e.

$$\sigma_1 \leq \sigma_2 \quad \Rightarrow \quad E_{\sigma_1}(u) \geq E_{\sigma_2}(u).$$

Proof :

This is a consequence of Lemma 2. □

Lemma 10 If u is k -Lipschitz, so is $E_\sigma(u)$.

Proof :

The map u being k -Lipschitz, we have

$$u(\mathbf{x}) - k\|y\| \leq u(\mathbf{x} + y) \leq u(\mathbf{x}) + k\|y\|.$$

Considering this last inequality as the comparison between three functions of \mathbf{x} (i.e. with y fixed), the monotonicity and the translation invariance of E_σ yield

$$E_\sigma(u)(\mathbf{x}) - k\|y\| \leq E_\sigma(u)(\mathbf{x} + y) \leq E_\sigma(u)(\mathbf{x}) + k\|y\|,$$

which proves that $E_\sigma(u)$ is k -Lipschitz. □

We just saw that the affine erosion satisfies three main axioms of the affine morphological scale space, namely

[Global Comparison Principle] : $u \leq v \quad \Rightarrow \quad E_\sigma(u) \leq E_\sigma(v)$.

[Morphology] : For every increasing continuous function g , $E_\sigma(g \circ u) = g \circ E_\sigma(u)$.

[Affine invariance] : For every affine map ϕ , $E_{\sigma \cdot |\det \phi|}(u) \circ \phi = E_\sigma(u \circ \phi)$.

We shall prove later that the **[Local Comparison Principle]** is also satisfied by the affine erosion. Thus, the major differences between the affine erosion and the AMSS are :

- The axiom **[Contrast reversal]** : $T_t(-u) = -T_t(u)$, which is satisfied by the AMSS but not by the affine erosion. This leads us to define the dual operator to the affine erosion, called affine dilation and satisfying

$$D_\sigma(u) = -E_\sigma(-u)$$

for any continuous image u . The relation

$$E_\sigma \circ D_\sigma(-u) = -D_\sigma \circ E_\sigma$$

ensures that the **[Contrast reversal]** axiom is asymptotically satisfied when the operator $D_\sigma \circ E_\sigma$ (or, equivalently, $E_\sigma \circ D_\sigma$) is iterated.

- The semi-group property

$$T_{t+t'} = T_t \circ T_{t'},$$

which is not satisfied by the affine erosion, even for any scale normalization of the kind $T_t = E_{f(t)}$. This is the reason why we need to iterate the affine erosion (or, to be precise, an associated alternate operator) in order to build a good approximation of the AMSS.

5.4 Comparison with the inf-sup operators

In this section, we compare the action of E_σ with the one of the inf-sup operator associated to the basis \mathcal{B}_c made of all closed convex sets with area 1 and symmetrical with respect to $\mathbf{0}$. We define

$$SI_\sigma(u)(\mathbf{x}) = \sup_{B \in \mathcal{B}_c} \inf_{\mathbf{y} \in B} u(\mathbf{x} + \sqrt{\sigma} \cdot \mathbf{y}), \quad \text{and}$$

$$IS_\sigma(u)(\mathbf{x}) = \inf_{B \in \mathcal{B}_c} \sup_{\mathbf{y} \in B} u(\mathbf{x} + \sqrt{\sigma} \cdot \mathbf{y}).$$

We know from [41] that if we iterate n times on a continuous periodic image u_0 the alternated operator $SI_\sigma \circ IS_\sigma$, then as $n \rightarrow +\infty$, $\sigma \rightarrow 0$ with $n\sigma^{\frac{2}{3}} \rightarrow t$, we obtain the flow of images $u(\cdot, t)$ which is a viscosity solution of the equation

$$\frac{\partial u}{\partial t} = c |Du| \text{curv}(u)^{\frac{1}{3}}$$

with initial condition $u(\cdot, 0) = u_0$, c being a positive constant. Notice that these morphological operators on images can be simply extended to sets via Equation 5.2. For any subset U of the plane, we define

$$SI_\sigma(U) = \{\mathbf{x} \in \mathbb{R}^2, SI_\sigma(1_U(\mathbf{x})) = 1\},$$

which is equivalent to

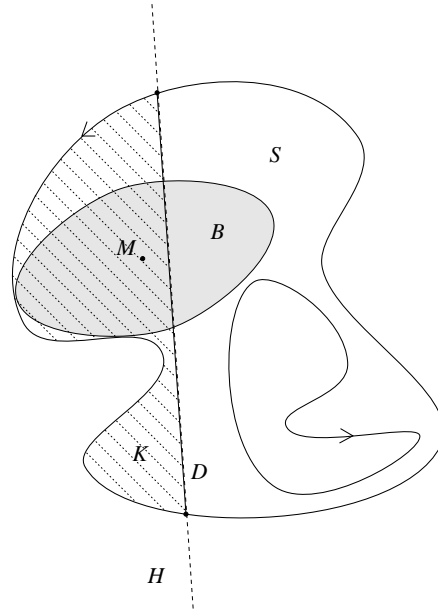
$$SI_\sigma(U) = \{\mathbf{x} \in U, \exists B \in \mathcal{B}, \mathbf{x} + \sqrt{\sigma} \cdot B \subset U\}.$$

Proposition 20 *For any open set U and any scale σ ,*

$$SI_{2\sigma}(U) \subset E_\sigma(U) \subset U.$$

Equivalently, for any lower semi-continuous image u ,

$$SI_{2\sigma}(u) \leq E_\sigma(u) \leq u.$$

Figure 5.2: $SI_{2\sigma}(S) \subset E_{\sigma}(S)$.

This result simply means that E_{σ} “erodes” a shape less than $SI_{2\sigma}$ does.

Proof :

1. We first establish the proof for a C-set S . If M belongs to $SI_{2\sigma}(S)$, then there exists a convex closed set B of area 2σ , symmetrical with respect to M , and contained in S . Now, if D is a positive chord segment of S such that the associated chord set K contains M , let H be the half plane containing K and delimited by the line supporting D (cf. Figure 5.2). Then, $B \cap H$ is connected (as the intersection of two convex sets) and contains M , so that it is contained in K . Consequently, the symmetry of B yields

$$\text{area}(K) > \frac{1}{2}\text{area}(B) = \sigma$$

(the inequality is strict because B is closed and S is open), which means that M belongs to $E_{\sigma}(S)$. Hence, for any C-set S we have $SI_{2\sigma}(S) \subset E_{\sigma}(S)$.

2. If U is an open subset of the plane we have

$$\bigcup_{S \text{ C-set}, S \subset U} SI_{2\sigma}(S) \subset \bigcup_{S \text{ C-set}, S \subset U} E_{\sigma}(S) = E_{\sigma}(U) \subset U. \quad (5.4)$$

Now, if $\mathbf{x} \in SI_{2\sigma}(U)$, we can find $B \in \mathcal{B}_c$ such that $\mathbf{x} + \sqrt{2\sigma}B \subset U$. Let $S_{\varepsilon} = \mathbf{x} + (\sqrt{2\sigma} + \varepsilon) \overset{\circ}{B}$, where $\overset{\circ}{B}$ is the topological opening of B . Since B is compact and ${}^{\circ}U$ is closed, the distance between these disjoint sets is nonzero and consequently $S_{\varepsilon} \subset U$ for a certain $\varepsilon > 0$ small enough. Thus, S_{ε} is a C-set included in U and such that $\mathbf{x} \in SI_{2\sigma}(S_{\varepsilon})$, and we get

$$\mathbf{x} \in \bigcup_{S \text{ C-set}, S \subset U} SI_{2\sigma}(S).$$

We just proved the inclusion

$$SI_{2\sigma}(U) \subset \bigcup_{S \text{ } C\text{-set}, S \subset U} SI_{2\sigma}(S). \quad (5.5)$$

Finally, Equations (5.4) and (5.5) imply as required

$$SI_{2\sigma}(U) \subset E_\sigma(U) \subset U \quad (5.6)$$

for any open set U .

3. If u_1 and u_2 are two images such that

$$\forall \lambda, \chi_\lambda(u_1) \subset \chi_\lambda(u_2),$$

then $\forall \mathbf{x}, u_1(\mathbf{x}) \leq u_2(\mathbf{x})$. Now, if u is a lower semi-continuous image, we can apply Equation 5.6 to $\chi_\lambda(u)$ to obtain

$$\forall \lambda, SI_{2\sigma}(\chi_\lambda(u)) \subset E_\sigma(\chi_\lambda(u)) \subset \chi_\lambda(u),$$

and since Equation 5.2 defines $E_\sigma(u)$ and $SI_{2\sigma}(u)$, we have

$$\forall \lambda, \chi_\lambda(SI_{2\sigma}(u)) \subset \chi_\lambda(E_\sigma(u)) \subset \chi_\lambda(u),$$

which proves that

$$\forall \mathbf{x}, SI_{2\sigma}(u)(\mathbf{x}) \leq E_\sigma(u)(\mathbf{x}) \leq u(\mathbf{x}).$$

□

Remark : The preceding result is not true for a closed set in general : for a closed disk D , $SI_{2\sigma}(D)$ is the closure of the open disk $E_\sigma(D)$. One may also wonder if the reverse inclusion $E_\sigma(U) \subset SI_{2\sigma}(U)$ happens. For a triangle T with unit area, we have $SI_{2\sigma}(T) = \emptyset \Leftrightarrow \sigma \geq \frac{1}{3}$ (see Figure 5.3), whereas the corresponding extinction scale for E_σ is $\frac{4}{9}$. More precisely, one can prove that $E_\sigma(T) \neq SI_{2\sigma}(T)$ for any scale $0 < \sigma < \frac{4}{9}$. However, for regular convex sets and small scales, this reverse inclusion happens.

Proposition 21 *If S is a closed convex set whose boundary is C^1 , then there is a limit scale $\sigma_1(S) > 0$ such that $SI_{2\sigma}(S) = E_\sigma(S)$ for all $\sigma < \sigma_1(S)$.*

Proof :

1. Let S be a closed convex set whose boundary \mathcal{C} is defined by a regular parameterization $C : I \rightarrow \mathcal{C}$ of class C^1 . We first prove that for $\sigma > 0$ small enough and for any σ -chord set $C_{s,t}$, the set symmetrical to $C_{s,t}$ with respect to the middle point of $[C(s)C(t)]$ is included in \overline{S} .

1.a. Define $\sigma_1 = \text{area}(S)/2$. For any $s \in I$ and $0 \leq \sigma \leq \sigma_1$, consider the unique σ -chord segment $[C(s)C(t)]$ (where t depends on s and σ) and $I(s)$ the intersection between \mathcal{C}

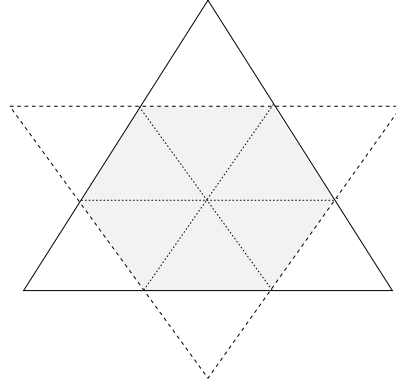


Figure 5.3: The largest symmetric convex set contained in a unit area triangle has area $2/3$.

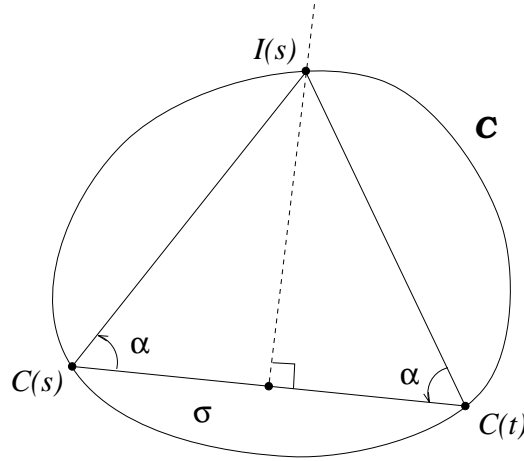


Figure 5.4: Definition of $\alpha(s, \sigma)$

and the midperpendicular of $(C(s), C(t))$ (see Figure 5.4). If $\sigma = 0$, $C(s) = C(t)$ and this midperpendicular is the line which goes through $C(s)$ and which is orthogonal to the tangent to C in $C(s)$. We call $\alpha(s, \sigma)$ the measure in $]0, \frac{\pi}{2}[$ of the angle between $C(s)C(t)$ and $C(s)I(s)$. Since $(s, \sigma) \mapsto \alpha(s, \sigma)$ is continuous on the compact set $I \times [0, \sigma_1]$, necessarily

$$\alpha_0 = \inf_{(s, \sigma) \in I \times [0, \sigma_1]} \alpha(s, \sigma)$$

is nonzero and for any $\sigma \leq \sigma_1$ and $s \in I$, we have $\alpha(s, \sigma) \geq \alpha_0$.

1.b. For any $s \in I$, consider $\sigma(s)$ the area of the largest C-set $C_{s,t}$ such that

$$\angle(C'(s), C'(t)) = \frac{1}{2}\alpha_0$$

(such a C-set exists because the map $t \mapsto \angle(C'(s), C'(t))$ increases continuously from 0 towards 2π). Notice that if we had $\sigma(s) = 0$ for some s , then $C([s, t])$ would be a segment, which is impossible since $\angle(C'(s), C'(t)) \neq 0$. Hence, $\sigma(s) = 0$ is nonzero for all $s \in I$, and since $s \mapsto \sigma(s)$ is continuous on the compact set I , we have

$$\sigma_2 = \inf_{s \in I} \sigma(s) > 0.$$

1.c. Now we claim that for any $\sigma \leq \min(\sigma_1, \sigma_2)$ and for any σ -chord set $C_{s,t}$, the set $\tilde{C}_{s,t}$ symmetric to $C_{s,t}$ with respect to the middle point of $[C(s)C(t)]$ is included in \bar{S} . Define Ω the intersection between the tangents to \mathcal{C} in $C(s)$ and $C(t)$, and $\tilde{\Omega}$ the point symmetric to Ω with respect to the middle point of $[C(s)C(t)]$. Since $\sigma \leq \sigma_2$, we have

$$\beta = \angle(C'(s), C'(t)) \in]0, \alpha_0],$$

and as $\sigma \leq \sigma_1$ we know that the triangle $C(s)C(t)J$ is included in \bar{S} , J being defined by

$$\angle(C(s)C(t), C(s)J) = \angle(C(t)J, C(t)C(s)) = \alpha_0$$

(see Figure 5.5). Now, as $\tilde{C}_{s,t}$ is included in the triangle $C(s)C(t)\tilde{\Omega}$, it is sufficient to prove that $\tilde{\Omega}$ belongs to the triangle $C(s)C(t)J$. But this is a simple consequence of $\beta \leq \alpha_0$, because

$$0 \leq \angle(C(s)C(t), C(s)\tilde{\Omega}) \leq \beta$$

as well as

$$0 \leq \angle(C(t)\tilde{\Omega}, C(t)C(s)) \leq \beta.$$

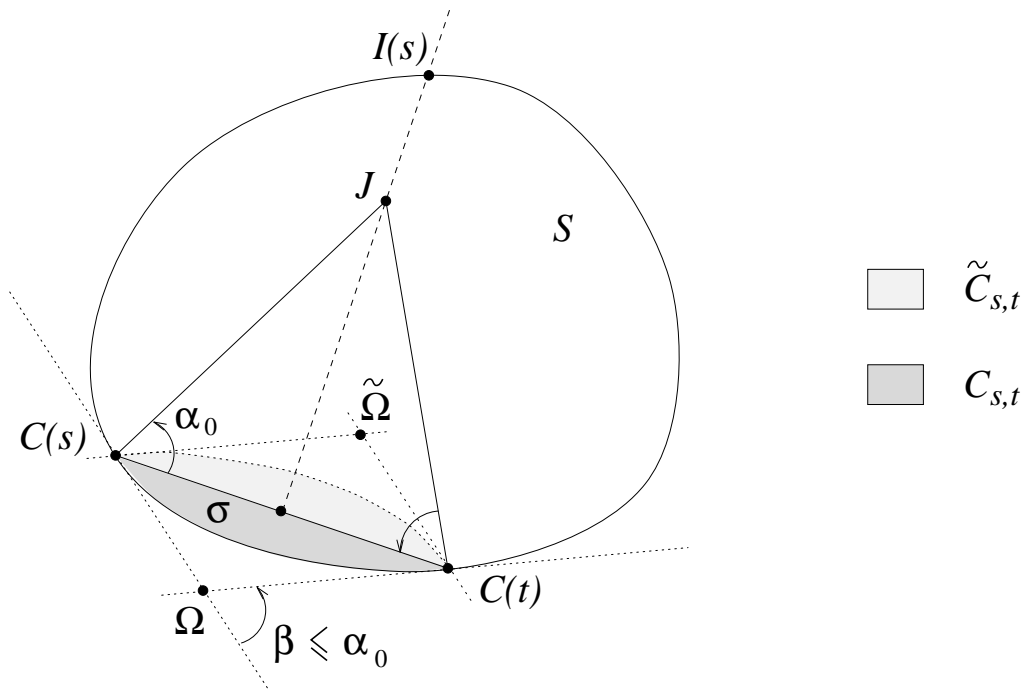


Figure 5.5: $\tilde{C}_{s,t}$ is included in S

2. In order to prove Proposition 21, according to Proposition 20 it is sufficient to check that for $\sigma' \leq \min(\sigma_1, \sigma_2)$, $E_{\sigma'}(S) \subset SI_{2\sigma'}(S)$. Consider a point $M \in E_{\sigma'}(S)$: necessarily, any σ -chord segment of S whose middle point is M is such that $\sigma > \sigma'$ (and since S is convex, there exists at least one such chord segment). But in this case, we proved on Step 1.c that we can find a convex closed set B with area 2σ (made from the symmetrization of a chord-set, see

Figure 5.5), symmetrical with respect to M and contained in \overline{S} . Applying on B a homothetic transformation with center M and ratio $\sqrt{\sigma'/\sigma} < 1$, we obtain a convex closed set B' with area $2\sigma'$, symmetrical with respect to M and contained in S . Consequently, $M \in SI_{2\sigma'}(S)$, and the proof is complete. \square

5.5 Asymptotic behaviour of the affine erosion

In the previous chapter, we investigated the asymptotic behaviour of the geometrical affine erosion, and we proved that it was consistent with the affine scale space of curves. Hence, we can expect the affine erosion of images to be consistent with the affine morphological scale space (AMSS).

In [41], F.Guichard and J.-M.Morel proved that SI_σ is (semi-)consistent with the AMSS. We prove the same result for the affine erosion, i.e. that

$$E_\sigma(u) = u + \omega \cdot \sigma^{\frac{2}{3}} \cdot |Du| [\text{curv}^-(u)]^{\frac{1}{3}} + O(\sigma^{\frac{3}{4}}).$$

Here, r^- means $\min(r, 0)$ and we keep the convention that if $r < 0$, $r^{\frac{1}{3}} = -|r|^{\frac{1}{3}}$. Using the dual operator to affine erosion, the affine dilation (defined by $D_\sigma(u) = -E_\sigma(-u)$ as we saw previously), we shall obtain the exact consistency with AMSS (i.e. $\text{curv}(u)$ instead of $\text{curv}^-(u)$) by considering the alternate operator $D_\sigma \circ E_\sigma$ (or $E_\sigma \circ D_\sigma$).

The classical way (see [41]) to estimate the asymptotic behaviour of such operators is to reduce the problem to quadratic forms by using a local comparison principle.

5.5.1 A local comparison principle

First, we need to define the concept of C-images (which are to images what C-sets are to sets) and establish an approximation lemma.

Definition 17 *An image u is a **C-image** if all of its non trivial level sets are C-sets.*

By trivial set, we mean either the empty set or the whole plane.

Lemma 11 *Consider a Lipschitz image u . Then, for any compact subset K of the plane and any $\varepsilon > 0$, there exists a C-image u_ε such that $|u - u_\varepsilon| \leq \varepsilon$ on K .*

Proof :

u being k -Lipschitz on the compact set K , we first define the family of squares

$$A_{i,j} = [a_i, a_{i+1}] \times [a_j, a_{j+1}], \quad (i, j) \in \mathbb{Z}^2, \quad \text{where} \quad a_n = \frac{n\varepsilon}{k \cdot \sqrt{2}}.$$

Now, we can let

$$u_\varepsilon(\mathbf{x}) = \inf\{u(\mathbf{y})1_K(\mathbf{y}); \exists(i, j), (\mathbf{x}, \mathbf{y}) \in A_{i,j}^2\},$$

where 1_K is the characteristic function of K (i.e. which equals 1 on K and 0 outside). This definition ensures that all non trivial level sets of u_ε are C-sets (their boundaries are made of polygons), and moreover we have

$$\forall \mathbf{x}, \quad 0 \leq u(\mathbf{x})1_K(\mathbf{x}) - u_\varepsilon(\mathbf{x}) \leq k \cdot \text{diam}(A_{i,j}) = \varepsilon.$$

Hence, u_ε satisfies $|u - u_\varepsilon| \leq \varepsilon$ on K . □

Proposition 22 (Local Comparison Principle) *Let u and v be two k -Lipschitz images such that $u \geq v$ on the disk with center \mathbf{x}_0 and radius r . Then we have, for any $\sigma \geq 0$,*

$$E_\sigma(u)(\mathbf{x}_0) \geq E_\sigma(v)(\mathbf{x}_0) - \frac{k\sigma}{r}.$$

Proof :

Given $\varepsilon > 0$, by Lemma 11 we can find a C-image w such that $|w - u| \leq \varepsilon$ on the open disk $D(\mathbf{x}_0, r)$. Besides, we define w^+ (respectively w^-) as the C-image equal to w on $D(\mathbf{x}_0, r)$ and equal to $+\infty$ outside (resp. equal to w on $\overline{D}(\mathbf{x}_0, r)$ and to $-\infty$ outside). Notice that infinite values are convenient here, but we could use finite (and large enough) values as well. We are going to prove that

$$E_\sigma(w^-)(\mathbf{x}_0) \geq E_\sigma(w^+)(\mathbf{x}_0) - \frac{k\sigma}{r} + O(\varepsilon) \quad (5.7)$$

as $\varepsilon \rightarrow 0$. For that purpose, we consider α, β such that

$$E_\sigma(w^-)(\mathbf{x}_0) < \alpha < \beta < E_\sigma(w^+)(\mathbf{x}_0)$$

(if $E_\sigma(w^-)(\mathbf{x}_0) = E_\sigma(w^+)(\mathbf{x}_0)$, this is not possible, but we are done since Equation 5.7 is clearly satisfied).

The definition of E_σ states the existence of a chord (A, B) of the level set $\chi_\beta(w^+)$ such that $\mathbf{x}_0 \in [AB]$ and the associated chord set K has an area not larger than σ (see Figure 5.6). The construction of w^+ ensures that K is bounded. Besides, no piece of $[AB]$ can define a chord set of $\chi_\alpha(w^-)$ contained in K because since this chord set would have an area not larger than σ , it would be a contradiction to the fact that $\alpha > E_\sigma(w^-)(\mathbf{x}_0)$. As a consequence, the set $\mathcal{C} = \partial\chi_\alpha(w^-) \cap K \cap D(\mathbf{x}_0, r)$ “attains” the boundary of the circle $\partial D(\mathbf{x}_0, r)$. If we define as well $\mathcal{C}' = \partial\chi_\beta(w^+) \cap K \cap D(\mathbf{x}_0, r)$ and

$$d = \inf\{|\mathbf{x} - \mathbf{x}'|; (\mathbf{x}, \mathbf{x}') \in \mathcal{C} \times \mathcal{C}'\},$$

on the one side we have

$$\beta - \alpha \leq 2\varepsilon + kd, \quad (5.8)$$

because u is k -Lipschitz and $|w - u| \leq \varepsilon$ on $D(\mathbf{x}_0, r)$. On the other side, one can easily inscribe in K a triangle with basis r and height d , which proves that $\text{area}(K) \geq rd$, and consequently

$$\sigma \geq rd. \quad (5.9)$$

Finally, Equations 5.8 and 5.9 give

$$\beta - \alpha \leq \frac{k\sigma}{r} + 2\varepsilon,$$

and considering the limits $\alpha \rightarrow E_\sigma(w^-)(\mathbf{x}_0)$ and $\beta \rightarrow E_\sigma(w^+)(\mathbf{x}_0)$, we obtain the desired Equation 5.7.

Last, as we have both $u \geq w^- - \varepsilon$ and $v \leq w^+ + \varepsilon$ on \mathbb{R}^2 , we can apply twice the monotonicity of E_σ to deduce from Equation 5.7 that

$$E_\sigma(u)(\mathbf{x}_0) \geq E_\sigma(v)(\mathbf{x}_0) - \frac{k\sigma}{r} + O(\varepsilon),$$

and letting $\varepsilon \rightarrow 0$ achieves the proof. \square

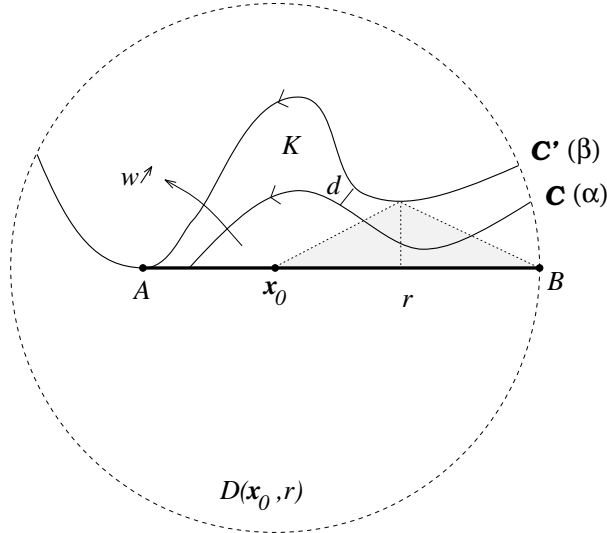


Figure 5.6: A local comparison principle

Corollary 7 (Uniform Local Comparison Principle) *Let u and v be two k -Lipschitz images such that $u \geq v$ on $D(\mathbf{x}_0, r)$. Then,*

$$\forall \mathbf{x} \in D(\mathbf{x}_0, \frac{r}{2}), \quad E_\sigma(u)(\mathbf{x}) \geq E_\sigma(v)(\mathbf{x}) - \frac{2k\sigma}{r}.$$

Proof :

For any $\mathbf{x} \in D(\mathbf{x}_0, \frac{r}{2})$ we can apply Proposition 22 since $u \geq v$ on $D(\mathbf{x}, \frac{r}{2})$ and we obtain the desired inequality. \square

5.5.2 Consistency

Lemma 12 (Locality) *Let u and v be two k -Lipschitz images such that*

$$u(\mathbf{x}) - v(\mathbf{x}) = O(|\mathbf{x} - \mathbf{x}_0|^3) \quad \text{as } \mathbf{x} \rightarrow \mathbf{x}_0.$$

Then,

$$E_\sigma(u)(\mathbf{x}_0) - E_\sigma(v)(\mathbf{x}_0) = O(\sigma^{\frac{3}{4}}) \quad \text{as } \sigma \rightarrow 0.$$

Proof :

We borrow the proof from [41]. Since $u(\mathbf{x}) - v(\mathbf{x}) = O(|\mathbf{x} - \mathbf{x}_0|^3)$, we can find two positive numbers R and C such that

$$\forall r < R, \forall \mathbf{x} \in D(\mathbf{x}_0, r), \quad v(\mathbf{x}) - Cr^3 \leq u(\mathbf{x}) \leq v(\mathbf{x}) + Cr^3.$$

These three functions are k -Lipschitz, so we can apply the local comparison principle (Proposition 22) to obtain, for any σ ,

$$E_\sigma(v)(\mathbf{x}_0) - Cr^3 - \frac{2k\sigma}{r} \leq E_\sigma(u)(\mathbf{x}_0) \leq E_\sigma(v)(\mathbf{x}_0) + Cr^3 + \frac{2k\sigma}{r}.$$

Choosing $\sigma = r^4$, we get as announced

$$E_\sigma(u)(\mathbf{x}_0) - E_\sigma(v)(\mathbf{x}_0) = O(\sigma^{\frac{3}{4}}) \quad \text{as } \sigma \rightarrow 0.$$

□

Remark : Lemma 12 remains true if we write “uniformly with respect to \mathbf{x}_0 ” for the hypothesis and the conclusion.

Lemma 13 *If u is a polynomial whose degree is at most 2, then for any $\mathbf{x}_0 \in \mathbb{R}^2$,*

$$E_\sigma(u)(\mathbf{x}_0) = u(\mathbf{x}_0) + \omega \cdot \sigma^{\frac{2}{3}} \cdot |Du|(\mathbf{x}_0) [\gamma^-(u)(\mathbf{x}_0)]^{\frac{1}{3}} + O(\sigma^{\frac{3}{4}}). \quad (5.10)$$

Proof :

If the degree of u is strictly less than 2, then $E_\sigma(u) = u$, and Equation 5.10 is clearly satisfied. Otherwise, according to the morphological invariance of E_σ , we can assume that $u(\mathbf{x}_0) = 0$. Moreover, we can chose a (positively oriented) system of coordinates such that $\mathbf{x}_0 = (x_0, y_0)^T$ and either

$$u((x, y)^T) = ax^2 + by^2$$

or

$$u((x, y)^T) = ax^2 + by,$$

where $(a, b) \in \mathbb{R} \times \{-1, 1\}$. If $u((x, y)^T)$ does not depend on x , the level lines of u are straight lines and Equation 5.10 is clearly satisfied. Hence, we suppose $a \neq 0$ in the following.

1. Case $u((x, y)^T) = ax^2 + by$.

We deal with the case $b = 1$, the case $b = -1$ being similar. The level lines of u are parabolae, so that we can use Proposition 16 to compute

$$\begin{aligned} E_\sigma(u)(\mathbf{x}_0) = \lambda &\Rightarrow \mathbf{x}_0 \in E_\sigma(\{y = -ax^2 + \lambda\}) \\ &\Rightarrow \mathbf{x}_0 \in \{y = -ax^2 + \omega((-2a)^+)^{\frac{1}{3}}\sigma^{\frac{2}{3}} + b\lambda\}, \end{aligned}$$

so that

$$E_\sigma(u)(\mathbf{x}_0) = u(\mathbf{x}_0) + \omega((2a)^-)^{\frac{1}{3}}\sigma^{\frac{2}{3}}.$$

On the other hand,

$$\mathcal{A}(u)(\mathbf{x}_0) = \left[\left((u_x)^2 u_{yy} - 2u_x u_y u_{xy} + (u_y)^2 u_{xx} \right)^- \right]^{\frac{1}{3}}(\mathbf{x}_0) = (2a^-)^{\frac{1}{3}},$$

so that u satisfies Equation 5.10 (with no remainder).

2. Case $u((x, y)^T) = ax^2 + by^2$, $ab > 0$.

The case $b = 1$ is obvious since $E_\sigma(u) = u$ and $\mathcal{A}(u) = 0$. Thus we suppose that $b = -1$ and $a < 0$. The level line $\{u(\mathbf{x}) = \lambda\}$ is empty if $\lambda > 0$, and it is an ellipse with area $\pi|\lambda||a|^{-1/2}$ otherwise. Hence, we can apply Proposition 12 and a simple computation based on the asymptotic expansion (4.4) yields

$$E_\sigma(u)(\mathbf{x}_0) = u(\mathbf{x}_0) + \omega(8a u(\mathbf{x}_0))^{\frac{1}{3}}\sigma^{\frac{2}{3}} + O(\sigma^{\frac{4}{3}}),$$

and

$$\mathcal{A}(u)(\mathbf{x}_0) = (8a(ax_0^2 - y_0^2))^{\frac{1}{3}}$$

as expected.

3. Case $u((x, y)^T) = ax^2 + by^2$, $ab < 0$.

The level lines of u are hyperbolae, and the reasoning is similar to Step 2 using Proposition 14. □

Proposition 23 (Consistency) *Let u be a k -Lipschitz image of class C^3 near \mathbf{x}_0 , then as $\sigma \rightarrow 0$,*

$$\begin{aligned} E_\sigma(u)(\mathbf{x}_0) &= u(\mathbf{x}_0) + \omega \cdot \sigma^{\frac{2}{3}} \cdot |Du|(\mathbf{x}_0) [\gamma^-(u)(\mathbf{x}_0)]^{\frac{1}{3}} + O(\sigma^{\frac{3}{4}}), \\ D_\sigma(u)(\mathbf{x}_0) &= u(\mathbf{x}_0) + \omega \cdot \sigma^{\frac{2}{3}} \cdot |Du|(\mathbf{x}_0) [\gamma^+(u)(\mathbf{x}_0)]^{\frac{1}{3}} + O(\sigma^{\frac{3}{4}}), \end{aligned}$$

Proof :

u being a C^3 near \mathbf{x}_0 , we can consider \tilde{u} , its Taylor expansion at order 2 near \mathbf{x}_0 . Thus,

$$u(\mathbf{x}) = \tilde{u}(\mathbf{x}) + O(|\mathbf{x} - \mathbf{x}_0|^3)$$

as $\mathbf{x} \rightarrow \mathbf{x}_0$. From Lemma 12, we deduce that as $\sigma \rightarrow 0$,

$$E_\sigma(u)(\mathbf{x}_0) - E_\sigma(\tilde{u})(\mathbf{x}_0) = O(\sigma^{\frac{3}{4}}),$$

and using Lemma 13 we get as expected

$$E_\sigma(u)(\mathbf{x}_0) = u(\mathbf{x}_0) + \omega \cdot \sigma^{\frac{2}{3}} \cdot |Du|(\mathbf{x}_0) [\gamma^-(u)(\mathbf{x}_0)]^{\frac{1}{3}} + O(\sigma^{\frac{3}{4}}).$$

The consistency for D_σ follows immediatly since $D_\sigma(u) = -E_\sigma(-u)$. □

Remark : In fact, the consistency is uniform in a neighborhood of \mathbf{x}_0 .

Next, we extend this consistency property to the alternate operators $D_\sigma \circ E_\sigma$ and $E_\sigma \circ D_\sigma$. We first prove that they satisfy a Local Comparison Principle.

Lemma 14 *Let u and v be two k -Lipschitz images such that $u \geq v$ on $D(\mathbf{x}_0, r)$. Then,*

$$\forall \mathbf{x} \in D(\mathbf{x}_0, \frac{r}{4}), \quad D_\sigma \circ E_\sigma(u)(\mathbf{x}) \geq D_\sigma \circ E_\sigma(v)(\mathbf{x}) - \frac{6k\sigma}{r},$$

and the same inequality holds for $E_\sigma \circ D_\sigma$.

Proof :

The proof is a direct consequence of Lemma 7. We know that for $\mathbf{x} \in D(\mathbf{x}_0, \frac{r}{2})$, we have

$$E_\sigma(u)(\mathbf{x}) \geq E_\sigma(v)(\mathbf{x}) - \frac{2k\sigma}{r},$$

which we rewrite

$$-E_\sigma(v)(\mathbf{x}) \geq -E_\sigma(u)(\mathbf{x}) - \frac{2k\sigma}{r}.$$

Now, from Lemma 10, $-E_\sigma(u)$ is also k -Lipschitz, as well as $-E_\sigma(v) - \frac{2k\sigma}{r}$. Hence, we can apply the Uniform Local Comparison Principle once again to obtain

$$\forall \mathbf{x} \in D(\mathbf{x}_0, \frac{r}{4}), \quad E_\sigma[-E_\sigma(v)(\mathbf{x})] \geq E_\sigma\left[-E_\sigma(u)(\mathbf{x}) - \frac{2k\sigma}{r}\right] - \frac{4k\sigma}{r},$$

which yields

$$D_\sigma \circ E_\sigma(u)(\mathbf{x}) \geq D_\sigma \circ E_\sigma(v)(\mathbf{x}) - \frac{6k\sigma}{r}$$

as announced. □

Theorem 4 (Consistency) *Let u be a k -Lipschitz image of class C^3 near \mathbf{x}_0 , then as $\sigma \rightarrow 0$,*

$$T_\sigma(u)(\mathbf{x}_0) = u(\mathbf{x}_0) + \omega \cdot \sigma^{\frac{2}{3}} \cdot |Du|(\mathbf{x}_0) [\gamma(u)(\mathbf{x}_0)]^{\frac{1}{3}} + O(\sigma^{\frac{3}{4}}),$$

for both $T_\sigma = D_\sigma \circ E_\sigma$ and $T_\sigma = E_\sigma \circ D_\sigma$.

Proof :

We check that the proof of Proposition 23 can be applied here. First, the consistency of the alternate operators for second order polynomials is straightforward since for such polynomials $E_\sigma \circ D_\sigma(u)$ and $D_\sigma \circ E_\sigma(u)$ are both equal to either $E_\sigma(u)$ or $D_\sigma(u)$. Last, the locality property of Lemma 12 for $D_\sigma \circ E_\sigma$ and $E_\sigma \circ D_\sigma$ is a direct consequence of Lemma 14. \square

Remark : As for E_σ , one easily proves that the consistency property of Theorem 23 is uniform near \mathbf{x}_0 .

5.6 Using Matheron's Theorem

There is another way to establish the consistency of the operator E_σ : it is based on Matheron's characterization of monotone morphological operators and on a consistency Theorem due to F.Guichard and J.-M.Morel (see [41]).

Theorem 5 (Matheron) *Let T be a translation invariant monotone⁴ morphological⁵ operator on a set of functions \mathcal{F} containing the characteristic functions of all the level sets of the elements of \mathcal{F} . Then, one can find a family \mathcal{B} of subsets of \mathbb{R}^2 such that*

$$\forall u \in \mathcal{F}, \quad T(u)(\mathbf{x}) = \sup_{B \in \mathcal{B}} \inf_{\mathbf{y} \in B} u(\mathbf{x} + \mathbf{y}).$$

Indeed, the operator E_σ being translation invariant, nondecreasing and morphological, the Matheron's characterization applies and we can write, for any l.s.c. image u ,

$$E_\sigma(u)(\mathbf{x}) = \sup_{B \in \mathcal{B}_e} \inf_{\mathbf{y} \in B} u(\mathbf{x} + \sqrt{\sigma} \cdot \mathbf{y}).$$

We should take

$$\mathcal{B}_e = \{X \subset \mathbb{R}^2; 0 \in E_1(X)\},$$

but from Lemma 7 we know that it is sufficient to take

$$\mathcal{B}_e = \{X \text{ bounded C - set; } 0 \in E_1(X)\}.$$

Thus, E_σ belongs to the class of affine invariant inf-sup operators which have been studied in [41]. In particular, we can expect to use the following consistency theorem :

⁴i.e. nondecreasing

⁵i.e. satisfying [Morphological Invariance].

Theorem 6 (F.Guichard, J.-M.Morel) *Let \mathcal{B} be a localizable set of plane closed nonempty bounded sets which is invariant by the special linear group $SL(\mathbb{R}^2)$. Then, there exists two constants c^+ and c^- depending on \mathcal{B} such that, for any image $u \in C^3$ in a neighbourhood of \mathbf{x}_0 ,*

$$\inf_{B \in \mathcal{B}_e} \sup_{\mathbf{y} \in B} u(\mathbf{x} + \sqrt{s} \cdot \mathbf{y}) = u(\mathbf{x}_0) + s^{2/3} |Du(\mathbf{x}_0)| g(\text{curv}(u)(\mathbf{x}_0)) + o(s^{2/3}),$$

$$\begin{aligned} \text{where } g(r) &= c^+ r^{\frac{1}{3}} \text{ if } r \geq 0 \\ &= c^- (-r)^{\frac{1}{3}} \text{ if } r < 0. \end{aligned}$$

To apply Theorem 6 to the affine erosion, the only requirement we have to check is that the basis \mathcal{B}_e is localizable in the following sense (see [41]).

Proposition 24 (Localizability) *The basis \mathcal{B}_e associated with the affine erosion operator is localizable, i.e. there exists a constant $c > 0$ such that*

$$\forall r \geq \sqrt{c}, \forall B \in \mathcal{B}_e, \exists B' \in \mathcal{B}_e, B' \subset D(0, r) \text{ and } \delta(B', B) \leq \frac{c}{r}.$$

Here, the notation $D(0, r)$ represents the open disk of radius r centered at the origin, and $\delta(B', B)$ means the Hausdorff semi-distance between B' and B , given by

$$\delta(B', B) = \sup_{\mathbf{x}' \in B'} d(\mathbf{x}', B) = \sup_{\mathbf{x}' \in B'} \inf_{\mathbf{x} \in B} |\mathbf{x} - \mathbf{x}'|.$$

Proof :

The proof is similar to the proof of the Local Comparison Principle (Proposition 22), which is not surprising.

1. Given $r \geq 1$ and a set B element of \mathcal{B}_e , we have $0 \in E_1(B)$ and by Definition of $E_1(B)$ we can find a C-set A included in B such that $0 \in E_1(A)$ (i.e. $A \in \mathcal{B}_e$). We consider the $\frac{1}{r}$ -Euclidean dilation of A restrained to the disk $D(0, r)$, i.e.

$$B' = \{\mathbf{x} \in D(0, r); d(\mathbf{x}, A) \leq \frac{1}{r}\}.$$

B' is a C-set containing $A \cap D(0, r)$, contained in $D(0, r)$, and

$$\delta(B', B) \leq \delta(B', A) + \delta(A, B) \leq \frac{1}{r} + 0.$$

Now we are going to prove that $B' \in \mathcal{B}_e$, that is to say that $0 \in E_1(B')$.

Suppose that 0 belongs to D , a chord segment of B' associated to a chord set K of area σ (see Figure 5.7). Two cases can be distinguished.

1.a. If $A \cap K \subset D(0, r)$, then a subset of K defines a chord set of A containing 0 and of area no more than σ . But since $A \in \mathcal{B}_e$, we necessarily have $\sigma > 1$.

1.b. If $A \cap K$ is not a subset of $D(0, r)$, which means that $K \cap \partial D(0, r)$ is not empty, then we can easily inscribe in K a triangle of base larger than r and height $\frac{1}{r}$ (see Figure 5.7), so that we get $\sigma = \text{area}(K) > 1$.

In both cases, 0 belongs to no 1-chord set of B' , so that $B' \in \mathcal{B}_e$. Consequently, we proved that

$$\forall r \geq \sqrt{c}, \forall B \in \mathcal{B}_e, \exists B' \in \mathcal{B}_e \text{ (C-set)}, \quad B' \subset D(0, r) \quad \text{and} \quad \delta(B', B) \leq \frac{1}{r},$$

which ensures that \mathcal{B}_e is localizable with a constant $c = 1$. □

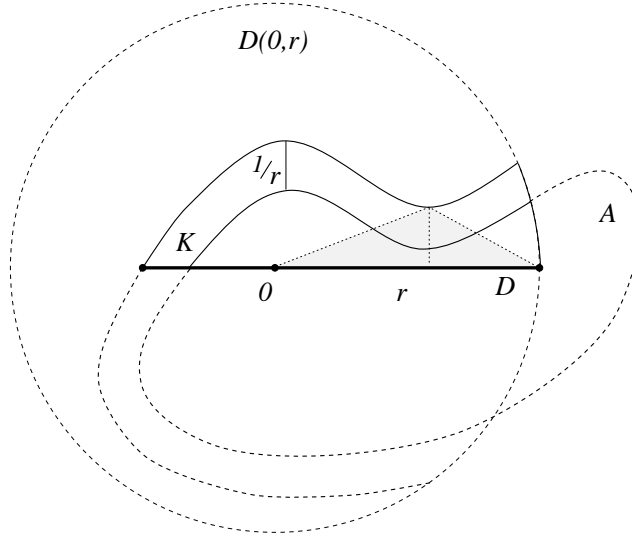


Figure 5.7: Area of K is greater than 1

Hence, Theorem 6 applies to \mathcal{B}_e and we have, for any image C^3 near \mathbf{x}_0 ,

$$E_\sigma(u)(\mathbf{x}_0) = \sup_{B \in \mathcal{B}_e} \inf_{\mathbf{y} \in B} u(\mathbf{x}_0 + \sqrt{\sigma} \cdot \mathbf{y}) = u(\mathbf{x}_0) + |Du(\mathbf{x}_0)|g(\text{curv}(u)(\mathbf{x}_0)) \sigma^{\frac{2}{3}} + o(\sigma^{\frac{2}{3}}), \quad (5.11)$$

$$\begin{aligned} \text{where } g(r) &= c^+ r^{\frac{1}{3}} \text{ if } r \geq 0 \\ &= c^- (-r)^{\frac{1}{3}} \text{ if } r < 0. \end{aligned}$$

At this stage, one easily checks that $c^+ = 0$ and $c^- = \omega = \frac{1}{2} \left(\frac{3}{2}\right)^{2/3}$.

In [41], the consistency of the alternate operators is proved only when \mathcal{B} is made of all unit area convex sets symmetrical with respect to $\mathbf{0}$, and the proof is based on a more precise estimation of the inf-sup and sup-inf operators in this case.

However, it seems that the method we used in the previous section still works for any localizable basis of structuring elements invariant by $SL(\mathbb{R}^2)$ (and in particular for \mathcal{B}_e). Since

the consistency mainly requires a local comparison principle, we only need to check that the alternate operators $IS_s \circ SI_s$ and $SI_s \circ IS_s$ satisfy the following local comparison principle. The proof is more or less the same as for Lemma 14.

Lemma 15 *If \mathcal{B} is localizable and invariant by $SL(\mathbb{R}^2)$, and if u and v are two k -Lipschitz functions in $D(\mathbf{x}_0, r)$ satisfying $u \leq v$ in $D(\mathbf{x}_0, r)$, then for any $s \leq c^{-1}r^2$,*

$$IS_s \circ SI_s(u)(\mathbf{x}_0) \leq IS_s \circ SI_s(v)(\mathbf{x}_0) + kc \frac{s}{r}, \quad (5.12)$$

where c depends only on \mathcal{B} . The same property holds for $IS_s \circ SI_s$.

Proof :

First, we know from [41] that (5.12) is satisfied for both SI_s and IS_s , taking $c = c_{\mathcal{B}}$. But since $c^{-1}r^2$ does not depend on \mathbf{x}_0 , (5.12) is satisfied for SI_s and IS_s in the whole disk $D(\mathbf{x}_0, \frac{r}{2})$ as soon as $s \leq 2c^{-1}r^2/4$, provided that we take $c = 2c_{\mathcal{B}}$. Hence, we can apply once again the Local Comparison Principle to deduce that for any $s \leq c^{-1}r^2$, (5.12) is satisfied for $IS_s \circ SI_s$ and $SI_s \circ IS_s$, with $c = 4c_{\mathcal{B}}$. \square

Hence, we can generalize the consistency property of [41] for the alternate operators $IS_s \circ SI_s$ and $SI_s \circ IS_s$ for any localizable and affine-invariant basis of structuring elements.

5.7 Convergence

As we know that the affine erosion of images is consistent with the AMSS, it is natural to wonder whether the iterated infinitesimal affine erosion spans exactly the affine morphological scale space. The answer is yes, and the proof is classical (see [9], [22], [41] and [20]). The only refinement we bring is that we allow non uniform subdivisions.

Definition 18 *A subdivision of an interval $[a, b]$ is a finite sequence $s = (s_0, s_1, \dots, s_n)$ such that $a = s_0 \leq s_1 \leq \dots \leq s_n = b$. The step of s is*

$$|s| = \sup_{1 \leq i \leq n} (s_i - s_{i-1}).$$

In the following definition, $\mathcal{S}(\mathbb{R}^2)$ is the set of 2×2 symmetric real matrices.

Definition 19 *A function $F : \mathcal{S}(\mathbb{R}^2) \times \mathbb{R}^2 \rightarrow \mathbb{R}^2$ is **elliptic** if*

$$\forall (p, X, Y) \in \mathbb{R}^2 \times \mathcal{S}(\mathbb{R}^2) \times \mathcal{S}(\mathbb{R}^2), \quad X \leq Y \Rightarrow F(X, p) \geq F(Y, p).$$

Theorem 7 *Let F be a continuous elliptic function, and T_h an operator on Lipschitz images (the Lipschitz constant being preserved). Suppose that T_h commutes with additions of constants, contrast changes and translations, and that for any $u \in C^3$ near \mathbf{x}_0 ,*

$$T_h(u)(\mathbf{x}_0) = u(\mathbf{x}_0) + h F(D^2u(\mathbf{x}_0), Du(\mathbf{x}_0)) + o(h). \quad (5.13)$$

Given a Lipschitz image u_0 , we define, for any subdivision s of $[0, t]$,

$$u_s(\mathbf{x}, 0) = u_0(\mathbf{x}) \quad \text{and}$$

$$u_s(\mathbf{x}, s_{i+1}) = T_{s_{i+1}-s_i} u_s(\mathbf{x}, s_i).$$

Then, as $|s| \rightarrow 0$, $u_s(\cdot, t)$ converges uniformly on every compact subset of the plane towards a function $\mathbf{x} \mapsto u(\mathbf{x}, t)$, the unique viscosity solution of

$$\begin{cases} \frac{\partial u}{\partial t} = F(D^2u, Du) \\ u(\mathbf{x}, 0) = u_0(\mathbf{x}). \end{cases}$$

The proof can be found in [41] for example.

Corollary 8 *Let u_0 be a Lipschitz image, and $u_s(\cdot, s_i)$ the filtered images obtained as in theorem 7. Then, as $|s| \rightarrow 0$, $u_s(\cdot, t)$ converges uniformly on every compact subset of the plane to the unique viscosity solution of the AMSS partial differential equation*

$$\frac{\partial u}{\partial t} = \omega \cdot |Du|g(\text{curv}(u)),$$

subject to initial condition $u(\mathbf{x}, 0) = u_0(\mathbf{x})$, where

$$\begin{aligned} g(c) &= (c^+)^{\frac{1}{3}} \quad \text{if } T_h = E_{h^{3/2}}, \\ &= (c^-)^{\frac{1}{3}} \quad \text{if } T_h = D_{h^{3/2}}, \\ &= c^{\frac{1}{3}} \quad \text{if } T_h = E_{h^{3/2}} \circ D_{h^{3/2}} \quad \text{or} \quad T_h = D_{h^{3/2}} \circ E_{h^{3/2}}. \end{aligned}$$

with as usual $\omega = \frac{1}{2} \left(\frac{3}{2}\right)^{\frac{2}{3}}$.

Proof :

We apply the previous theorem to the operators $E_{h^{3/2}}, D_{h^{3/2}}, \dots$ and their associated continuous elliptic function

$$F(D^2u, Du) = \omega \cdot |Du|g(\text{curv}(u)).$$

The required consistency property (Equation 5.13) is a direct consequence of Theorem 4. \square

Remark : Following [22], we could also use the mean

$$M_h = \frac{1}{2}(E_{h^{3/2}} + D_{h^{3/2}})$$

instead of the alternate operators $E_{h^{3/2}} \circ D_{h^{3/2}}$ and $D_{h^{3/2}} \circ E_{h^{3/2}}$. The consistency follows immediatly from the consistency of $E_{h^{3/2}}$ and $D_{h^{3/2}}$, and the convergence theorem still applies. This ‘‘mean’’ operator has one advantage : it is symmetric, so that the resulting scheme is fully invariant under a contrast reversal (whereas the alternate scheme is only *asymptotically* invariant under a contrast reversal). However, M_h does not satisfy the morphological invariance axiom, and it creates new grey levels on images.

Chapter 6

Numerical scheme

Numerically, a curve is nothing but a finite set of numbers which are interpreted as coordinates or parameters to produce a continuous curve. The simplest way to represent a curve numerically is to define it as a polygon, but some higher order representations, e.g. splines, have appeared to be more efficient for some applications.

Many reasons lead to choose the polygonal representation to implement the affine erosion on curves. The polygonal representation is very simple, affine invariant, and the level lines of a grey-level discrete image are naturally defined as polygons if we consider the pixels as squares. But the major advantage of this representation in our case is, as we shall see further, that we can compute *exactly* the affine erosion of a polygon. The lack of regularity of polygons (not C^1 everywhere) shall not be a problem, since most of the previous analyses apply to piecewise C^1 curves.

Obviously, neither the affine erosion nor the AMSS of a polygon is a polygon. But since no simple dense set of parameterized curves satisfies this property (as far as we know), an approximation is always required to iterate the affine erosion. The main advantage of being able to compute exactly the affine erosion of a polygon is that *we can fully dissociate the two approximate operations required to compute the AMSS : the scale quantization step* (we have to iterate the affine erosion several times) *and the space quantization step*, which is necessary to work on discrete data. By processing these two steps successively and independently, we avoid a classical trap which prevents geometrical algorithms from satisfying the [**Inclusion Principle**] and [**Affine Invariance**] properties. In particular, our method sets no *a priori* relation between the number of vertices of a polygon and the number of vertices of the polygon resulting on the approximation of its affine scale space at any scale : this number can drastically increase (case of a triangle) or decrease as well (case of a very “noisy” curve). In other words, our algorithm processes a polygon *as a curve* and not as a set of points, and for that reason it is not a point evolution scheme.

In this chapter, we describe exactly the affine erosion of a polygon, convex or not. Then we give a simple numerical algorithm to compute the affine erosion of convex polygons, as well

as an exact algorithm in the general case. We also present briefly a simplified algorithm which runs faster, and produces similar results.

6.1 Affine erosion of a polygon

6.1.1 Regular convex case

Proposition 25 *Let $\mathcal{P} = P_1P_2\dots P_n$ be a convex polygon, and $0 < \sigma < \sigma_r(\mathcal{P})$. The σ -affine erosion of \mathcal{P} is a C^1 curve made of the concatenation of the pieces of hyperbolae $H_{i,k}$ defined by Equations 6.2 to 6.7, the couples (i,k) satisfying Equation 6.1 and being sorted in lexical order.*

Proof :

If $\mathcal{P} = P_1P_2\dots P_n$ is a (positively oriented) convex polygon and $0 < \sigma < \sigma_r(\mathcal{P})$, we know from Theorem 1 that $E_\sigma(\mathcal{P})$ is made exactly of the middle points of the σ -chord segments of \mathcal{P} . Consider two non-parallel edges $[P_{i-1}P_i]$ and $[P_kP_{k+1}]$, then there exists σ -chords whose endpoints lie on $[P_{i-1}P_i]$ and $[P_kP_{k+1}]$ if and only if

$$\frac{1}{2}[IP_k, IP_i] \leq \sigma + \sigma_{i,k} \leq \frac{1}{2}[IP_{k+1}, IP_{i-1}], \quad (6.1)$$

where I is defined as

$$I := (P_{i-1}P_i) \cap (P_kP_{k+1}). \quad (6.2)$$

and

$$\sigma_{i,k} := \text{area}(IP_i\dots P_k) \quad (6.3)$$

(see Figure 6.1). In this case, we know from Proposition 1 that the middles of the σ -chord segments whose endpoints lie on $[P_{i-1}P_i]$ and $[P_kP_{k+1}]$ span a piece of hyperbola

$$H_{i,k} : M(t) = I + \lambda(e^t IP_k + e^{-t} IP_i), \quad t_1 \leq t \leq t_2 \quad (6.4)$$

whose apparent area is

$$\sigma + \sigma_{i,k} = 2\lambda^2 [IP_k, IP_i],$$

so that

$$\lambda = \sqrt{\frac{\sigma + \sigma_{i,k}}{2 [IP_k, IP_i]}}. \quad (6.5)$$

We need to compute the endpoints of $H_{i,k}$, i.e. the value of t_1 and t_2 . Two cases happen for t_1 : if $\text{area}(IP_{i-1}P_k) > \sigma + \sigma_{i,k}$, there exists a σ -chord segment $[P_{i-1}J]$ where $J \in [P_kP_{k+1}]$ (see Figure 6.1), otherwise there exists a σ -chord $[JP_k]$ where $J \in [P_{i-1}P_i]$. In the first case, we have

$$I + 2\lambda \cdot e^{-t_1} IP_i = P_{i-1},$$

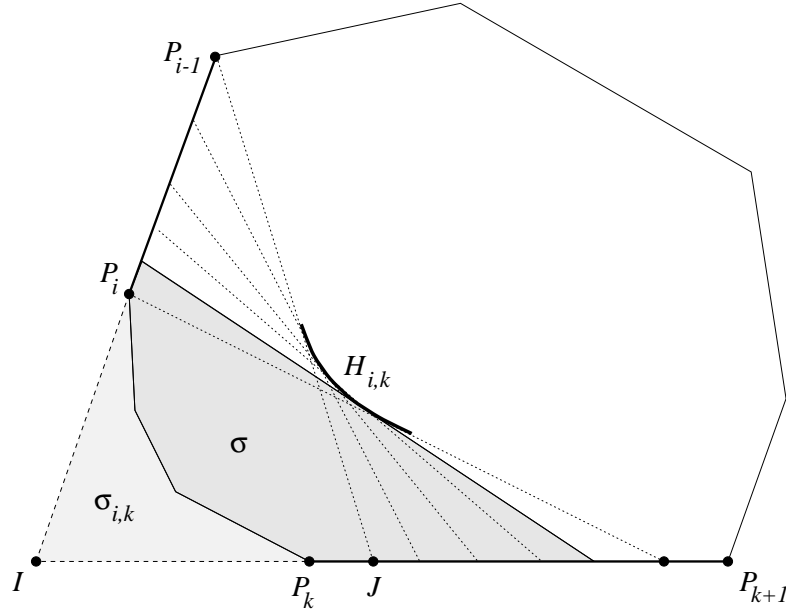


Figure 6.1: Piece of hyperbola resulting from two edges.

whereas

$$I + 2\lambda \cdot e^{t_1} IP_k = P_k$$

for the alternative case. Symmetrically, one easily checks that if $\text{area}(IP_i P_{k+1}) > \sigma + \sigma_{i,k}$ we have

$$I + 2\lambda \cdot e^{t_2} IP_k = P_{k+1},$$

and

$$I + 2\lambda \cdot e^{-t_2} IP_i = P_i \quad \text{otherwise.}$$

In other words,

$$t_1 = -\ln \frac{\text{dist}(I, P_{i-1})}{2\lambda \cdot \text{dist}(I, P_i)} \quad \text{if } \text{area}(IP_{i-1}P_k) > \sigma + \sigma_{i,k}, \quad t_1 = -\ln(2\lambda) \quad \text{otherwise,} \quad (6.6)$$

$$t_2 = \ln \frac{\text{dist}(I, P_{k+1})}{2\lambda \cdot \text{dist}(I, P_k)} \quad \text{if } \text{area}(IP_i P_{k+1}) > \sigma + \sigma_{i,k}, \quad t_2 = \ln(2\lambda) \quad \text{otherwise.} \quad (6.7)$$

The admissible hyperbolae $H_{i,k}$ are encountered on $E_\sigma(\mathcal{P})$ in lexical order, that is $H_{i,k} < H_{i',k'}$ means either “ $i < i'$ ” or “ $i = i'$ and $k - i < k' - i < k - i + n$ modulo n ”. The reason is very simple : as we know that $E_\sigma(\mathcal{P})$ is convex, we must consider the σ -chords segments of \mathcal{P} in such an order that the angles of their directions increase continuously on S^1 . Thus, the previous assertion simply results from the inequality

$$i \leq j \leq k \Rightarrow \alpha(P_i P_j) \leq \alpha(P_i P_k) \leq \alpha(P_j P_k) < \alpha(P_i P_j) + 2\pi,$$

where $\alpha(\mathbf{v})$ measures on S^1 the angle between a fixed vector and the vector \mathbf{v} . \square

6.1.2 Non regular convex case (removing ghosts parts)

When \mathcal{P} is a convex polygon and $\sigma \geq \sigma_r(\mathcal{P})$, we noticed in Chapter 3 (see Figure 3.13 for example) that “ghosts parts” can appear in the curve made of the middle points of the σ -chord segments of \mathcal{P} . We cannot avoid this situation since $\sigma_r(\mathcal{P}) = 0$ for some polygons. Moreover, we saw in Chapter 4 that we could hope to iterate the affine erosion with rather large scale steps ; to this aim, we must be able to compute the affine erosion of any polygon with arbitrary large scales, and not only when $\sigma < \sigma_r(\mathcal{P})$.

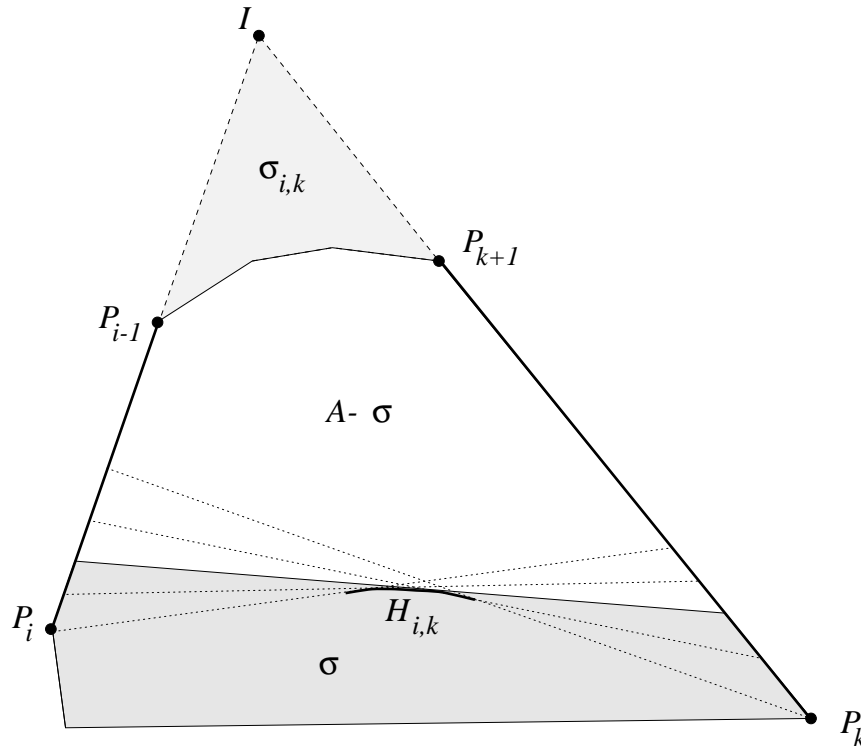


Figure 6.2: Non regular chords span “ghost” hyperbolae.

We can see on Figure 6.2 that non-regular chords span “ghost parts”, which do not take part of the affine erosion of \mathcal{P} . By the way, these “ghost parts” are also hyperbolae, and their apparent area is equal to $A - \sigma + \sigma_{i,k}$, A being the area of \mathcal{P} . Thus, we can forget these ghost hyperbolae, and $E_\sigma(\mathcal{P})$ is included in the collection of hyperbolae defined in Proposition 25, with the restriction

$$[P_{i-1}P_i, P_kP_{k+1}] > 0.$$

Now, in order to compute exactly the affine erosion of \mathcal{P} , we have to compute hyperbolae intersections in order to remove the remaining “ghost parts”. In general, computing the intersection between two hyperbolae reduces to an algebraic equation of degree 4, but in the situation we are facing, one can see that when two pieces of hyperbola have a common intersection, they must have a common axis, so that the problem reduces to a second degree equation which can be

solved exactly. Hence, *it is quite simple to compute the exact affine erosion of a convex polygon for arbitrary large scales*. In the next section, we investigate the general (and more complicated) case of non-convex polygons.

6.1.3 General case (non convex polygons)

Proposition 26 *The affine erosion of a (possibly non convex) polygon is one or several generalized “hyperbolic polygon”, resulting from the concatenation of segments and convex pieces of hyperbolae.*

The proof is straightforward from Proposition 10, because the affine erosion can only “create” segments and hyperbolae pieces. If $\mathcal{P} = P_1P_2 \dots P_n$ is a polygon, we can write

$$E_\sigma(\mathcal{P}) = \mathcal{I}(\mathcal{P}) - \bigcup_{1 \leq i, k \leq n} C_\sigma(P_i \dots P_k),$$

where $C_\sigma(P_i \dots P_k)$ is the union of the chord sets of \mathcal{P} , with area smaller than σ , and resulting from chord segments whose endpoints lie on the edges $[P_iP_{i+1}]$ and $[P_{k-1}P_k]$ (with the circular conventions $P_0 = P_n$, $P_{n+1} = P_1$ and when $k < i$, $P_i \dots P_k = P_iP_{i+1} \dots P_nP_1 \dots P_{k-1}P_k$).

Let $P_i \dots P_k$ be a polygonal curve, and consider two points $(A, B) \in [P_iP_{i+1}] \times [P_{k-1}P_k]$. We shall say that the segment $[AB]$ is **occluded** if it is not a chord segment of $\mathcal{P} = P_i \dots P_k$, i.e. if for some $j \in \{i+1, \dots, k-2\}$,

$$[AB] \cap [P_jP_{j+1}] \neq \emptyset.$$

Now, we shall say that the polygonal curve $\mathcal{P} = P_i \dots P_k$ is

- **partially occluded** if for at least one $(A, B) \in [P_i, P_{i+1}] \times [P_{k-1}, P_k]$, the segment $[AB]$ is occluded,
- **totally occluded** if all segments $[AB]$, $(A, B) \in [P_i, P_{i+1}] \times [P_{k-1}, P_k]$ are occluded.

If $P_i \dots P_k$ is totally occluded, it is clear that $C_\sigma(P_i \dots P_k) = \emptyset$. It is equivalent to say that (P_iP_k) is not a chord of \mathcal{P} .

Lemma 16 *Suppose that $P_i \dots P_k$ is partially (but not totally) occluded, and $[P_iP_{i+1}, P_{k-1}P_k] > 0$. Then one can find $(A, B) \in [P_iP_{i+1}] \times [P_{k-1}P_k]$ such that $P_iAP_{i+1} \dots P_{k-1}BP_k$ is not occluded and*

$$C_\sigma(P_i \dots P_k) = C_\sigma(P_iAP_{i+1} \dots P_{k-1}BP_k).$$

Proof :

More than a proof, we give an effective construction of A and B . The first remark is that if $C_\sigma(P_i \dots P_k) = \emptyset$, we can choose $A = P_i$ and $B = P_k$. Hence, we suppose that $C_\sigma(P_i \dots P_k) \neq \emptyset$ in the following.

Since $[P_i P_{i+1}, P_{k-1} P_k] > 0$, we can find an affine map ϕ such that $\det \phi = 1$ and $\phi(P_j) = (x_j, y_j)$ in an orthonormal basis, with $x_i = x_{i+1} = y_{k-1} = y_k = 0$, $x_k > 0$, $y_i > 0$, $x_{k-1} < x_k$ and $y_{i+1} < y_i$ (see Figure 6.3).

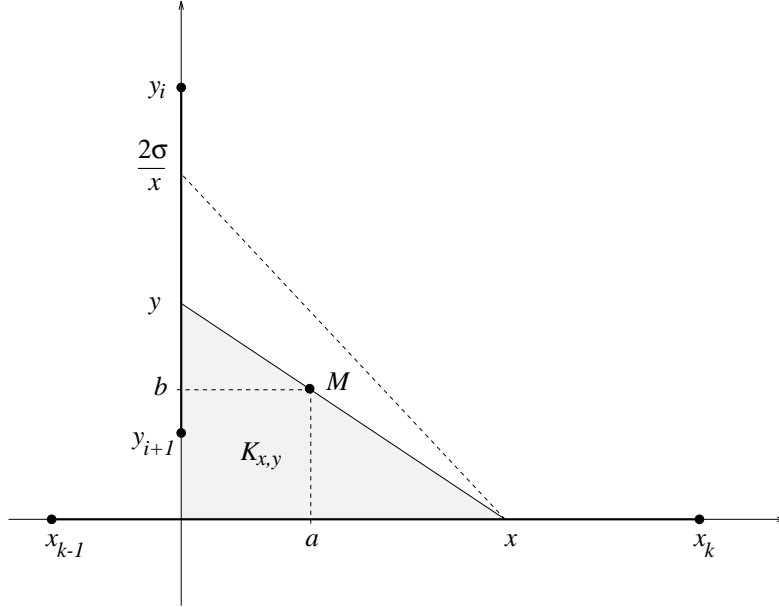


Figure 6.3: Solving partial occlusions.

Now, consider four positive real numbers a, b, x, y and look at Figure 6.3. The point $M(a, b)$ belongs to the boundary of the chord set $K_{x,y}$ of the corner $C = \mathbb{R}_+ \times \mathbb{R}_+$ if and only if

$$\frac{a}{x} + \frac{b}{y} = 1.$$

In this case, we have

$$\text{area}(K_{x,y}) = ab + \frac{b(x-a)}{2} + \frac{a(y-b)}{2} = ab + \frac{b(x-a)}{2} + \frac{ab^2}{2(x-a)},$$

and we can deduce that the σ -chord set of C defined from the segment $[(x, 0), (0, \frac{2\sigma}{x})]$ contains M if and only if x belongs to the interval

$$I_\sigma(a, b) = \left\{ x, ab + \frac{b(x-a)}{2} + \frac{ab^2}{2(x-a)} \leq \sigma \right\}.$$

An explicit computation gives

$$I_\sigma(a, b) = \left[\frac{\sigma}{b} \left(1 - \sqrt{1 - \frac{2ab}{\sigma}} \right), \frac{\sigma}{b} \left(1 + \sqrt{1 - \frac{2ab}{\sigma}} \right) \right],$$

with the conventions $I_\sigma(a, b) = \emptyset$ if the square root is not defined, and $I_\sigma(a, b) = \mathbb{R}$ if one of a, b is not positive.

Let us now define

$$J_1 = \bigcap_{i+2 \leq j \leq k-2} I_\sigma(x_j, y_j)$$

(with the convention $J_1 = \mathbb{R}$ if $i+2 > k-2$), and

$$J_2 = [\max(0, x_{k-1}), x_k] \cap \left[\frac{2\sigma}{y_i}, \frac{2\sigma}{\max(0, y_{i+1})} \right]$$

(with the convention $1/0 = +\infty$). Since we supposed $C_\sigma(P_i \dots P_k) \neq \emptyset$, $J_1 \cap J_2$ is not empty and we can write $J_1 \cap J_2 = [z_1, z_2]$. Then, one checks easily that the two points

$$A = \phi^{-1} \left(\left(0, \frac{2\sigma}{z_2} \right) \right) \quad \text{and} \quad B = \phi^{-1}((z_1, 0))$$

satisfy the conclusion of the Lemma. \square

We investigate the possible “shapes” of $C_\sigma(P_i \dots P_k)$. According to the previous Lemma, we can suppose without loss of generality that no occlusions appear. In the following, area $(P_i \dots P_k)$ means the algebraic area of the polygon $P_i P_{i+1} \dots P_k$, defined for example by

$$\text{area}(P_i \dots P_k) = \frac{1}{2} \sum_{i < j < k} [P_i P_j, P_i P_{j+1}].$$

If $\text{area}(P_{i+1} \dots P_{k-1}) > \sigma$, any chord segment whose endpoints lie on $[P_i P_{i+1}]$ and $[P_{k-1} P_k]$ defines a chord set of area greater than σ , so that $C_\sigma(P_i \dots P_k) = \emptyset$. Hence, we shall suppose that $\text{area}(P_{i+1} \dots P_{k-1}) \leq \sigma$ in the three following cases which remain.

- **case 1 (regular case)** : If $\text{area}(P_i \dots P_k) > \sigma$ and $[P_i P_{i+1}, P_{k-1} P_k] > 0$, the inside boundary of $C_\sigma(P_i \dots P_k)$ is made of a piece of hyperbola, completed with two half-chord segments at its endpoints (see Figure 6.4).

- **case 2 (reverse case)** : If $\text{area}(P_i \dots P_k) > \sigma$ and $[P_i P_{i+1}, P_{k-1} P_k] \leq 0$ the inside boundary of $C_\sigma(P_i \dots P_k)$ is a polygonal curve of the kind $A\Omega B$, where $(A, B) \in [P_i P_{i+1}] \times [P_{k-1} P_k]$. The point Ω is obtained as the intersection between the two σ -chord segments defined from A and B . Remember that as in the convex case, either $A = P_i$ or (A, P_{k-1}) is a σ -chord (and a symmetrical alternative holds for B). As we noticed previously, the ghost hyperbola spanned by the σ -chord segments is strictly contained in $C_\sigma(P_i \dots P_j)$ and does not contribute to its boundary (see Figure 6.5).

- **case 3 (sub-area case)** : If $\text{area}(P_i \dots P_j) \leq \sigma$, the inside boundary of $C_\sigma(P_i \dots P_j)$ is simply the segment $P_i P_{j+1}$.

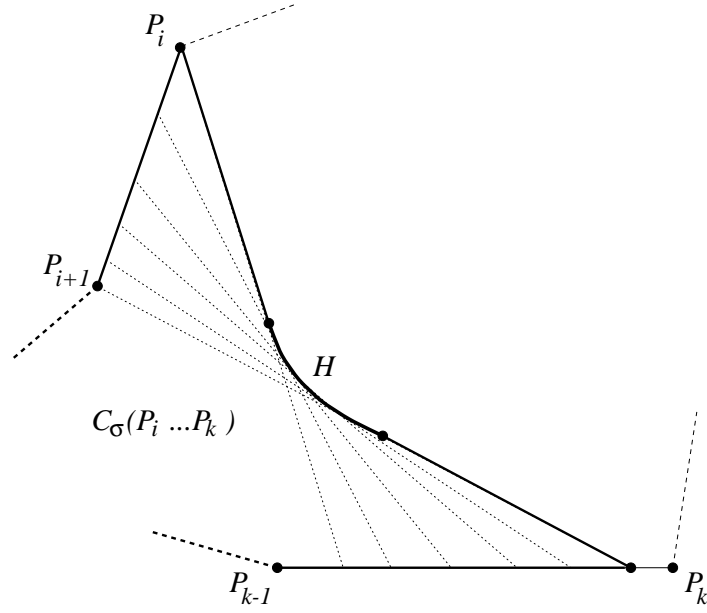


Figure 6.4: Regular case.

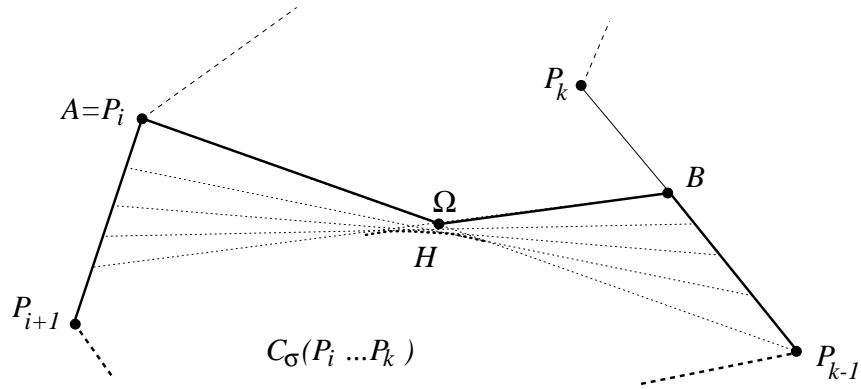


Figure 6.5: Reverse case.

6.2 Algorithm

Now are now in position to describe an *exact* algorithm to compute the affine erosion of any polygon. It consists of three steps.

Step A : We collect all the pieces of curves which can possibly be part of $E_\sigma(\mathcal{P})$. As we noticed previously, these pieces are of three kinds (see Figure 6.6).

1. The valid pieces of hyperbola $H_{i,k}$ described previously, completed with their two half chord segments at their endpoints. As we noticed before, the interval $[t_1, t_2]$ defining each piece of hyperbola (Equation 6.4) may have to be shortened in case of partial occlusions (see Lemma 16).
2. The two “limit” σ -chord segments of each ghost piece of hyperbola resulting from non-regular chords.
3. The σ' -chord segments ($0 \leq \sigma' \leq \sigma$) defined by two vertices in the sub-area case.

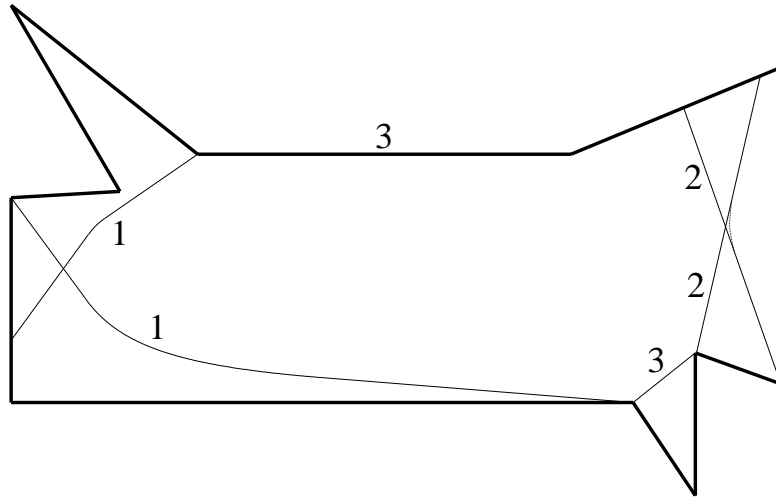


Figure 6.6: The three kinds of curves encountered in the affine erosion of a polygon

Step B : We remove the useless pieces of curves according to their position. More precisely, with each piece of curve \mathcal{C} obtained in step A we associate two numbers $a(\mathcal{C}), b(\mathcal{C})$ representing the starting point of the first chord segment spanning \mathcal{C} and the endpoint of the last chord segment spanning \mathcal{C} : since these points belong to the polygon \mathcal{P} , we can represent them as numbers $i + \alpha$, meaning the point $(1 - \alpha)P_i + \alpha P_{i+1}$. The key point of this representation is that two pieces of curves \mathcal{C}_1 and \mathcal{C}_2 obtained in Step A have a common intersection if and only if the intervals $[a_1, b_1]$ and $[a_2, b_2]$ are not disjoint. Therefore, if $a_1 < a_2 < b_2 < b_1$, the piece of curve \mathcal{C}_2 is useless and can be removed.

Step C : We compute the intersections between the remaining pieces of curves (sorted with respect with their starting number a). At this stage, we may have to compute intersections between

two segments, between a segment and an hyperbola, or between two hyperbolae. The two first cases reduce to equations of degree 1 and 2 respectively. The last case (intersection of two hyperbolae) can be more difficult. If the two hyperbolae have a common axis, then the intersection equation is of degree 2 and can be solved easily. However, in more general cases (which happen), we can have to solve an algebraic equation of degree 4 ; if so, we compute the intersection by using Newton's algorithm, which converges in a few iterations. Now, for each intersection, we remove from each of the two curves the parts which are "on the right" of the other one, according to the definition of the affine erosion. We have to maintain — at least, formally— two data structures to process this step correctly : one is the original set of curves obtained from step B, the other is a copy of these curves, updated iteratively as we just explained.

We must mention that many intersections simply result from two successive hyperbolae as in the convex case ; to process these intersections, no computation is required : one only needs to remove the two corresponding half-chord segments.

Finally, we obtain the affine erosion of the polygon as the concatenation (in the natural order) of the pieces of curves obtained from step C. This algorithm is a bit heavy (about 1600 lines of C source code), but not too slow for reasonable polygons (1 second or so for a polygon with 100 vertices). One must be careful when computing the intersections, because of the finite numerical precision of the computer (this can be done by considering point equalities modulo a relative error, for instance).

Figures 6.7, 6.8 and 6.9 are an example of the results we obtain after steps A, B and C.

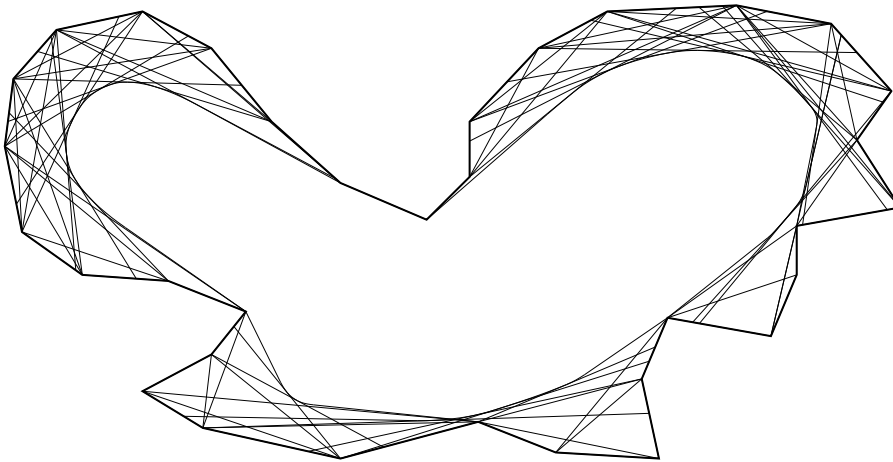


Figure 6.7: curves obtained after step A

In this algorithm, we did not mention the problem of topological changes that occurs when the initial polygon breaks into non connected parts (remember that the affine erosion does not always preserve the connectedness). This problem is not very difficult to handle, but requires a

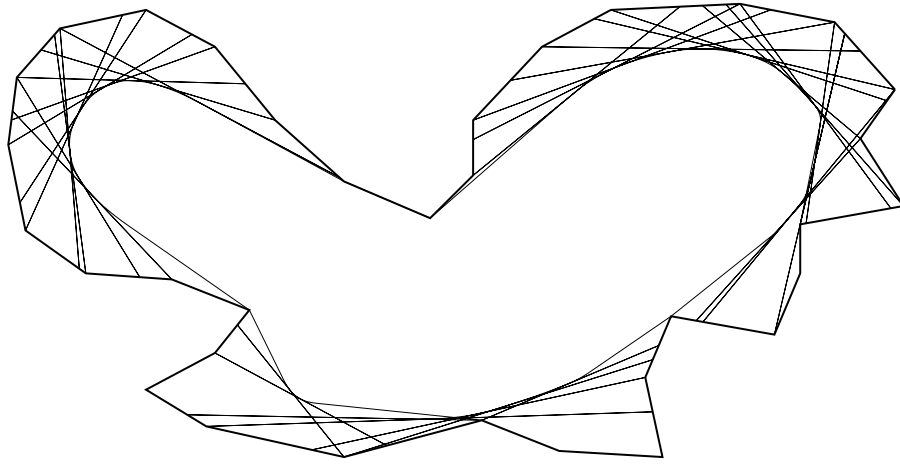


Figure 6.8: curves obtained ater step B

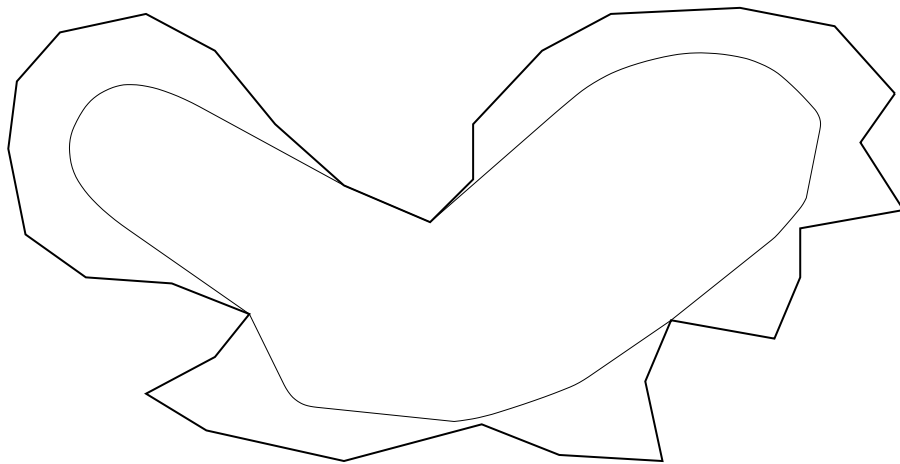


Figure 6.9: curve obtained ater step C

high computation cost : each time an hyperbola or a segment is computed, one must look for a possible intersection with an edge of the polygon, and break the resulting curve into several parts when the case happens. Fortunately, such external occlusions are seldom.

6.3 Affine subsampling and iteration

So far, we know how to compute exactly the affine erosion of a polygon. To iterate this process, we need to quantize the resulting curve (which is, as we shown, a concatenation of hyperbola pieces and segments) in order to get a new polygon. Fortunately, there is a simple way to sample a piece of hyperbola in an affine-invariant way. Consider the parameterization

$$H : M(t) = \lambda(e^t \mathbf{v}_1 + e^{-t} \mathbf{v}_2), \quad t_1 \leq t \leq t_2 :$$

then $(t, t+x)$ is an ε -chord set of H if and only if $\varepsilon = \lambda^2(\text{sh } x - x)$, where sh denotes the hyperbolic sine (see the proof of Proposition 14). Hence, the polygon $P_0 P_1 \dots P_n$ defined by

$$P_k = M\left(\left(1 - \frac{k}{n}\right)t_1 + \frac{k}{n}t_2\right)$$

is a discrete affine invariant quantization of H with “area step”

$$\varepsilon(n) = \lambda^2\left(\text{sh } \frac{1}{n} - \frac{1}{n}\right).$$

Given $\varepsilon > 0$, we can quantize the affine erosion of a polygon up to the area step ε by choosing, for each piece of hyperbola, the minimum entire value of n such that $\varepsilon(n) \leq \varepsilon$. This can be done, for instance, by tabling the inverse function $n(\varepsilon/\lambda^2)$ for the small values and using, for the large ones, the expansion

$$n \simeq \left(\frac{\lambda^2}{6\varepsilon}\right)^{\frac{1}{3}}.$$

Not surprisingly, this quantization step is a kind of discrete affine erosion of scale ε . Thus, as we want to minimize its influence on the affine erosion, we must choose $\varepsilon \ll \sigma$, where σ is the scale of the computed affine erosion. This condition forces the second iteration of E_σ to be **non-local** in the sense that the σ -chord sets of the resulting approximate polygon contain many edges (i.e. $k - i \gg 1$ for the valid $H_{i,k}$, see Figure 6.10). In that sense, our algorithm is quite different from a local point evolution scheme, for which the scale quantization step must be small compared to the space quantization step in order to ensure a minimum of stability. *Here, the inverse phenomenon happens* : the scale quantization step (σ) is much larger than the space quantization step (ε). An important consequence is that we can effectively iterate only a few times (i.e. with large scale steps) the affine erosion to compute the affine scale space. Indeed, we do not loose accuracy since ε can remain small and the affine erosion remains near its tangent operator (the Affine Scale Space) even for rather large scales, as we noticed in Section 2.4.

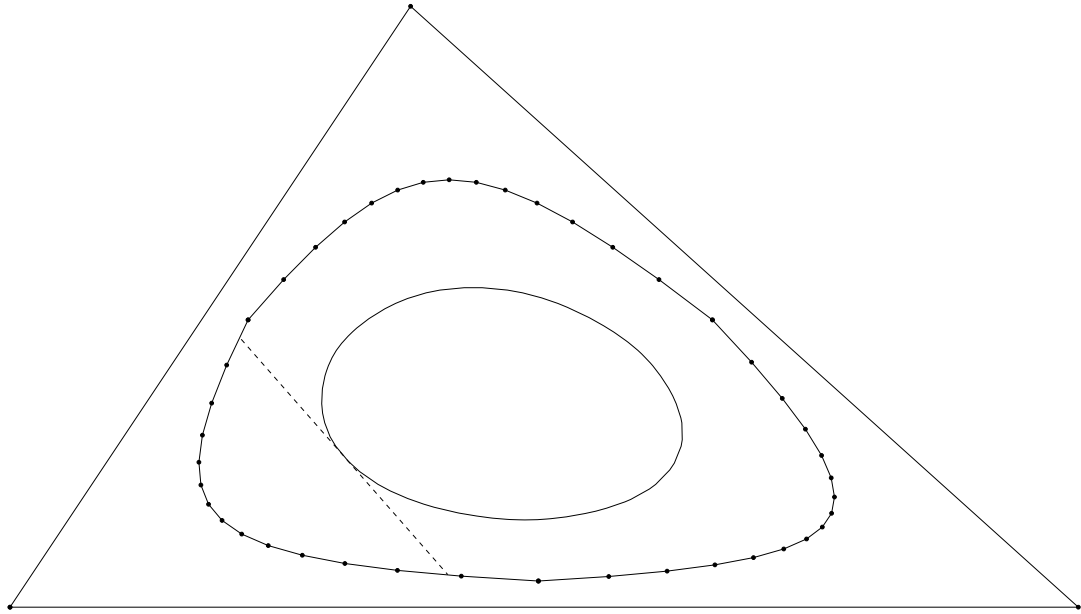


Figure 6.10: Two iterations of the affine erosion on a triangle. The second iteration is non-local with respect to the quantization, since each piece of the second iteration curve depends on many points of the first iteration one.

6.4 A simplified algorithm

Another way to implement the affine scale space is to iterate a pseudo affine erosion, written E'_σ , which processes separately the convex components of a given piecewise convex closed curve.

6.4.1 Pseudo affine erosion

If we want to define a kind of affine erosion for a non semi-closed curve c — that is, a curve with two endpoints —, we must choose a boundary condition. Our approach will be to fix these endpoints : in practice, these endpoints will correspond to inflexion points of a larger curve, and we know that these points do not move at order 1 since the curvature of the curve vanishes at them. How can we define the affine erosion of c ? We shall not investigate the problem in general, but one can see easily that for small scales, no external occlusions appear and c itself is included in the boundary of

$$c_\sigma = \bigcup_{S \in K_\sigma(c)} S,$$

so that it makes sense to define $E_\sigma(c)$ by

$$\partial c_\sigma = c \sqcup E_\sigma(c),$$

the symbol \sqcup meaning a disjoint union (see Figure 6.11).

Let us call $\sigma_m(c)$ the maximum scale for which we can compute the affine erosion of c as described previously. If no external occlusion appear at any scale (i.e. if the two endpoints of c

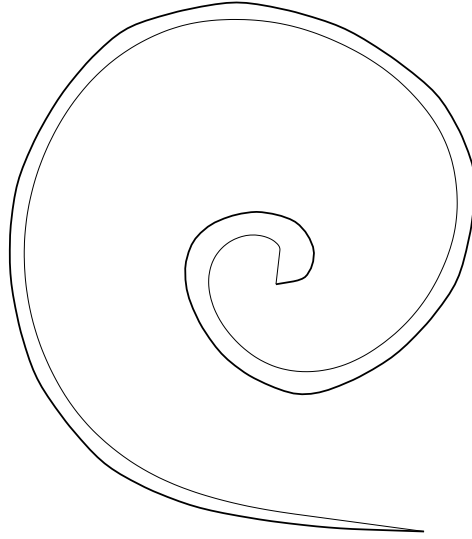


Figure 6.11: Affine erosion of a non semi-closed curve

are a non-zero chord of c), we restrain $\sigma_m(c)$ to the area of c (defined as the area of the chord set associated to the extremal points of c).

Given a piecewise convex closed curve \mathcal{C} , we consider the canonical decomposition $\mathcal{C} = c_1 c_2 \dots c_n$, the curves c_i being defined as the convex (or concave) curves extracted from \mathcal{C} between two successive junctions (see Chapter 3 and Figure 6.12). For any $\sigma < \sigma_m(\mathcal{C}) = \min_i \sigma_m(c_i)$, we can define the pseudo affine erosion of c by

$$E'_\sigma(\mathcal{C}) = E_\sigma(c_1) E_\sigma(c_2) \dots E_\sigma(c_n).$$

As for the affine erosion, one can prove that the pseudo affine erosion of a curve cannot have any double junction.

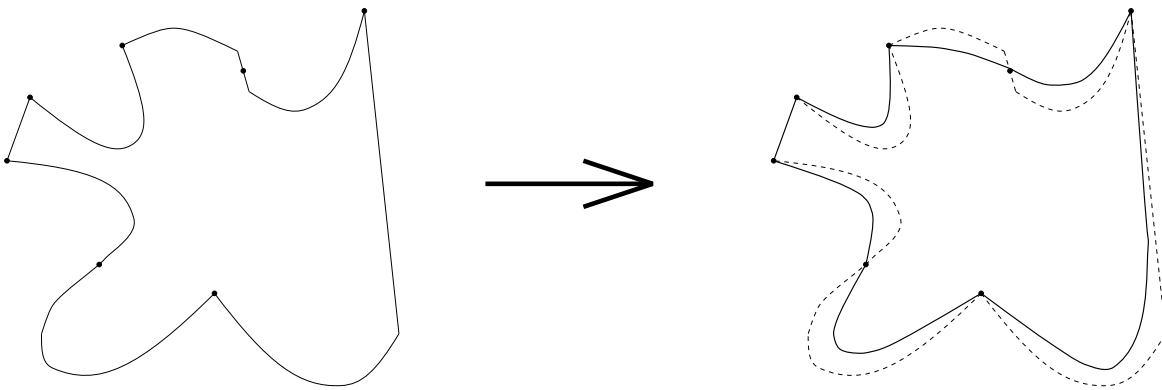


Figure 6.12: Pseudo affine erosion of a closed curve

6.4.2 Algorithm

The algorithm to compute $E'_\sigma(\mathcal{C})$ when \mathcal{C} is a polygon is easy to devise. First, we remark that a polygon has no double junctions, and that its simple junctions are the middle of “inflexion” edges. Then, the algorithm to compute the affine erosion of each convex component of \mathcal{C} is exactly the one we described previously for convex polygons. Hence, computing $E'_\sigma(\mathcal{C})$ is simpler and faster than computing $D_\sigma \circ E_\sigma(\mathcal{C})$, since it does not require to compute intersections in general (unless non-regular chords happen, which is very rare for small scales).

It is clear that E'_σ is consistent with the affine scale space. However, the inclusion property is only satisfied for small scales, because if \mathcal{C} and \mathcal{C}' are two piecewise convex closed curves, we only have

$$\mathcal{I}(\mathcal{C}) \subset \mathcal{I}(\mathcal{C}') \Rightarrow \forall \sigma \leq \min(\sigma_m(\mathcal{C}), \sigma_m(\mathcal{C}')), \mathcal{I}(E'_\sigma(\mathcal{C})) \subset \mathcal{I}(E'_\sigma(\mathcal{C}')).$$

Another drawback of this simplified algorithm is that if the curve \mathcal{C} is very irregular, $\sigma_m(\mathcal{C})$ may be very small and a lot of iterations are required to compute the affine scale space of \mathcal{C} at a large scale. This happens because only a few inflexion points disappear at each iteration.

In practice, the simplified algorithm based on the pseudo affine erosion is faster and simpler. We checked on experiments (see next chapter) that it produces similar results compared to the exact three-steps algorithm we described previously, *provided that the scale steps are chosen small enough*.

